INVESTIGATION OF CORE CLOSEOUTS IN FIBER-REINFORCED SANDWICH LAMINATES

by

Russell Lee Evertz

A thesis submitted in partial fulfillment
of the requirements for the degree

of

Master of Science

in

Mechanical Engineering

MONTANA STATE UNIVERSITY – BOZEMAN
Bozeman, Montana

September 2000

APPROVAL

of a thesis submitted by

Russell Lee Evertz

This thesis has been read by each member of the thesis committee and has been found to be satisfactory regarding content, English usage, format, citations, bibliographic style, and consistency, and is ready for submission to the College of Graduate Studies.

Dr. Douglas Cairns _____ _____

(Signature) Date

Approved for the Department of Mechanical Engineering

Dr. Vic Cundy _____ _____

(Signature) Date

Approved for the College of Graduate Studies

Dr. Bruce McLeod _____ _____

(Signature) Date

STATEMENT OF PERMISSION TO USE

In presenting this thesis in partial fulfillment of the requirements for a master's degree at Montana State University-Bozeman, I agree that the Library shall make it available to borrowers under rules of the Library.

If I have indicated my intention to copyright this thesis by including a copyright notice page, copying is allowable only for scholarly purposes, consistent with "fair use" as prescribed in the U.S. Copyright Law. Requests for permission for extended quotation from or reproduction of this thesis in whole or in parts may be granted only by the copyright holder.

Signature_____

Date_____

ACKNOWLEDGEMENTS

I would like to express gratitude to all of my friends and family for all of the support and motivation they have given me over the past two years. Many thanks to the members of the Composites Group and Engineering Department who extended a helping hand in my direction.

This work was supported under DOE and the State of Montana funding for improved wind turbine blades (MSU Contract Numbers 428173 and 428174). Funding was also provided by Sandia National Laboratories under MSU Contract Numbers 429801.

TABLE OF CONTENTS

LIST OF FIGURES

LIST OF FIGURES

LIST OF TABLES

ABSTRACT

Wind is an environmentally friendly renewable energy source that becomes more attractive when composite materials technology is applied; particularly technology associated with fiber reinforced plastics. This technology allows the design of lighter wind turbine blades, which may increase the efficiency of wind turbines, making wind generated electric power less costly. The application of sandwich panel construction can stiffen the blades while keeping overall blade weights low. Due to manufacturing and design parameters, the sandwich panel configuration is only employed in certain areas of the blade, where additional buckling resistance is needed. Although initially thought to be of little importance, the effect that the transition between fiberglass/balsa sandwich panel and the fiberglass laminate may have on the performance of the blade is not trivial.

This research is an investigation of balsa core sandwich panels, thin laminates (which were the facesheets for the sandwich panel), and transitions from sandwich panels to thick and thin laminates. Sandwich panels were tested in tension, resulting in strengths slightly above the thin laminate without the balsa core in place.

A sandwich panel to thin laminate transition can reduce static tensile strength by up to a factor of six when using a 30 degree fillet transition, as discovered in this research through finite element models and experimental tests. Transitions were tested with fillet angles ranging from 5 to 30 degrees. The 5 degree specimens with a transition to a thin laminate reduced strength by only 7 percent, well above the performance of the 10 degree transition, which lowered strength by 48 percent. Finite element models were created for use as a design tool to evaluate the transition behavior, and were validated using experimental data.

A transition from a sandwich panel to a thick laminate was also investigated. Specimens tested included angles of balsa termination of 5, 10, and 90 degrees. The 5 degree termination performed the best, failing at a value that was only 23 percent less than that for a sandwich panel. The 90 degree specimens delaminated at a stress as much as 55 percent less than the sandwich panel alone.

Fatigue performance of the thin laminate, the sandwich panel, and the sandwich to thin laminate transition were investigated. The sandwich panel had fatigue strengths only 1.1 times lower than the baseline thin laminate at one million cycles. The transition had poor fatigue performance, 3.4 times lower than the thin laminate at a million cycles due to delamination in the transition region.

Design and manufacturing guidelines were made based on the results of experiments and models completed through this research. Recommendations for finite element modeling to be used as a design tool were also made.

CHAPTER 1

INTRODUCTION

Environmentally friendly, renewable energy alternatives have been investigated for decades [Cheremisinoff (1978)]. In the past ten years, there has been a substantial increase in the interest in wind power as an ecologically sound and renewable energy source. The growing interest can easily be seen in Europe where the wind power industry is flourishing [Gipe (1995)].

Wind power becomes more attractive when composite materials technology is applied, particularly with fiber reinforced plastics. Composites are a combination of reinforcement, such as glass or carbon fibers, and a binder or matrix [Dostal, (1989)]. This technology allows the design of lighter wind turbine blades, which may increase the efficiency of wind turbines, making wind generated electric power less costly. Increases in efficiency includes decreased cost of blade manufacturing and the additional power gained as the mass of the turbine is reduced while the wind gathered remains the same. A popular composite material among wind turbine blade producers is fiberglass-reinforced polyester. As turbines increase in size, blades need increased stiffness and durability. While early, small turbine blades used randomly oriented fiber mats, larger blades use aligned fiber fabrics in their construction [Mayer (1996)].

To make wind turbines more efficient, blades are designed to be as light as possible. Minimizing weight and maintaining blade performance is an ongoing

challenge to the designer. The inclusion of sandwich panel construction to resist buckling in blade designs allows designers to reduce weight without sacrificing blade performance. Sandwich construction has been developed for decades, and used as early as the mid 1800's [Allen (1969)]. It consists of three or more layers of material. The outer facesheets or skins are strong, stiff materials, such as fiber reinforced plastics, while the center layer or core is lightweight. The facesheets carry the load, while the core separates the facesheets and carries shear stresses, preventing buckling. Sandwich panel construction is illustrated in Figure 1.1.

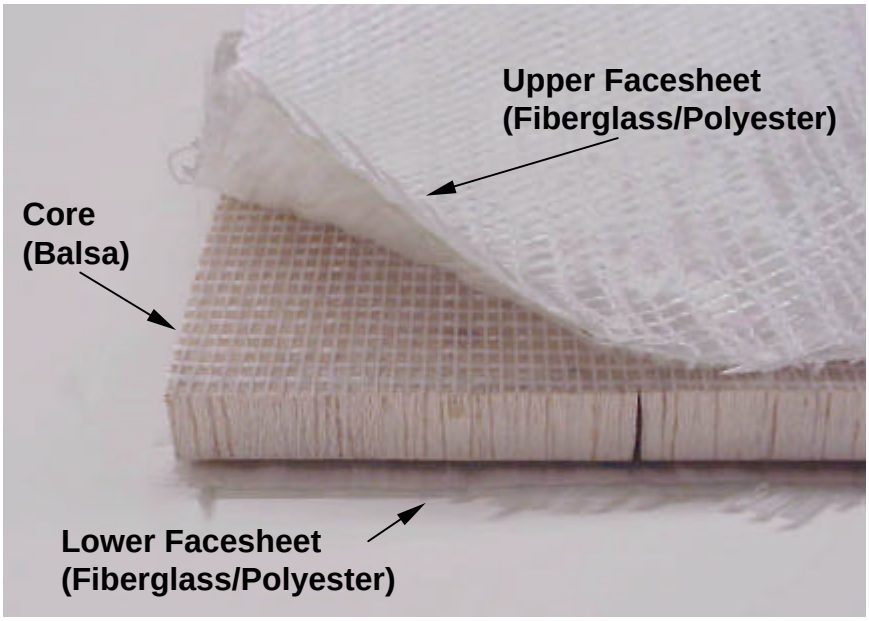

Figure 1.1 Sandwich panel construction (polyester matrix has been omitted for clarity.)

The application of sandwich construction can increase local buckling resistance by at least an order of magnitude with little increase in weight [Gere &

Timoshenko (1990)]. Since sandwich panel construction is only employed in local areas of the blade, the termination of the sandwich panel into a thin laminate is inevitable in an efficient design. Insert info about load introduction

A discontinuity in any composite system should be examined carefully to ensure it does not substantially reduce the overall strength of the design. Several design details that introduce discontinuities are discussed by Mandell et al. (1998). Although initially overlooked, the transition between a fiberglass/balsa sandwich panel and the fiberglass laminate may be significant after reviewing the stress concentrations of other structural details such as ply drops, surface indentations, and locally high fiber contents.

The main objective of this research was to investigate the transition zone between the fiberglass/balsa sandwich panel and the fiberglass laminate. The parameters of interest are the static and fatigue strengths of the transition area, compared with the strengths of thin laminates as well as sandwich panels. The study has evaluated a variety of transition region parameters, using both experiments (after extensive test development) and finite element models. The results were used to develop design and manufacturing guidelines for designers to use when developing turbine blades containing fiberglass/balsa sandwich panel construction.

CHAPTER 2

BACKGROUND

Motivation

A wind turbine blade design has been developed as part of the Montana State University Wind Program for the AOC 15/50 wind turbine [McKittrick et al. (1999)]. The blade design consists of two skins separated by a spar. A diagram of the blade is shown in Figure 2.1. The top and bottom sections are secondary bonded to the spar; they are also secondary bonded at the leading and trailing edges. Secondary bonds are accomplished with high strength adhesive, joining parts manufactured in two or more pieces.

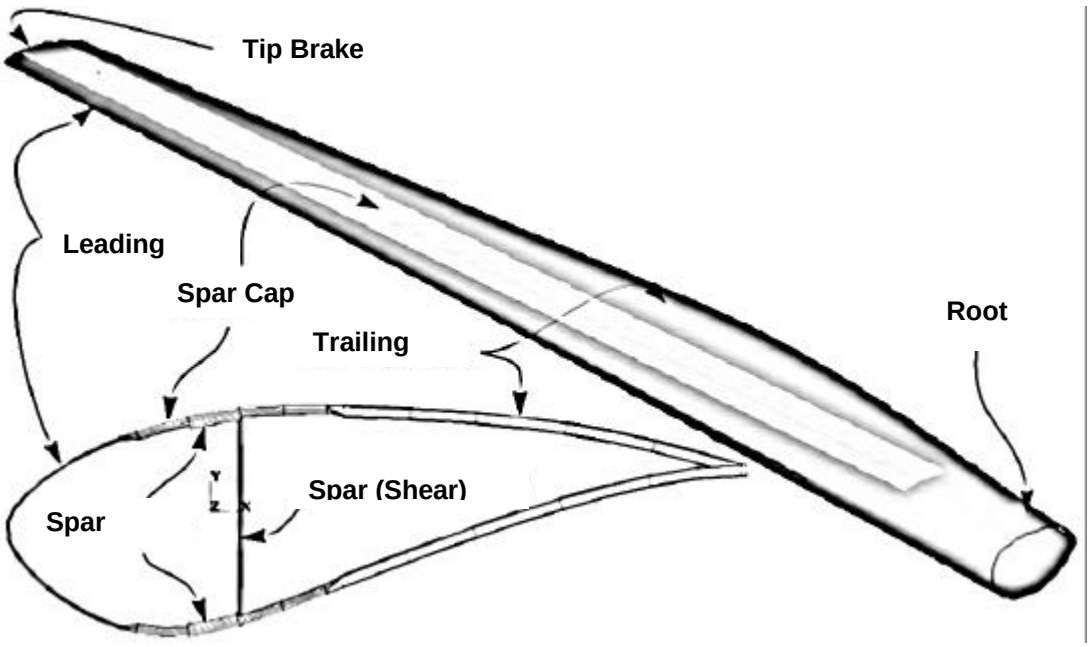

Figure 2.1 Diagram of blade design for the AOC 15/50.

The thin, relatively flat areas of the trailing edge could potentially buckle from compression loads during operation. To increase buckling resistance without adding significant weight, sandwich panel construction is used for most of the trailing edge airfoil area. The blade section photograph in Figure 2.2 shows the sandwich panel construction used in these areas. Materials for the blade consists of oriented fiberglass fabrics, polyester resin, and balsa core.

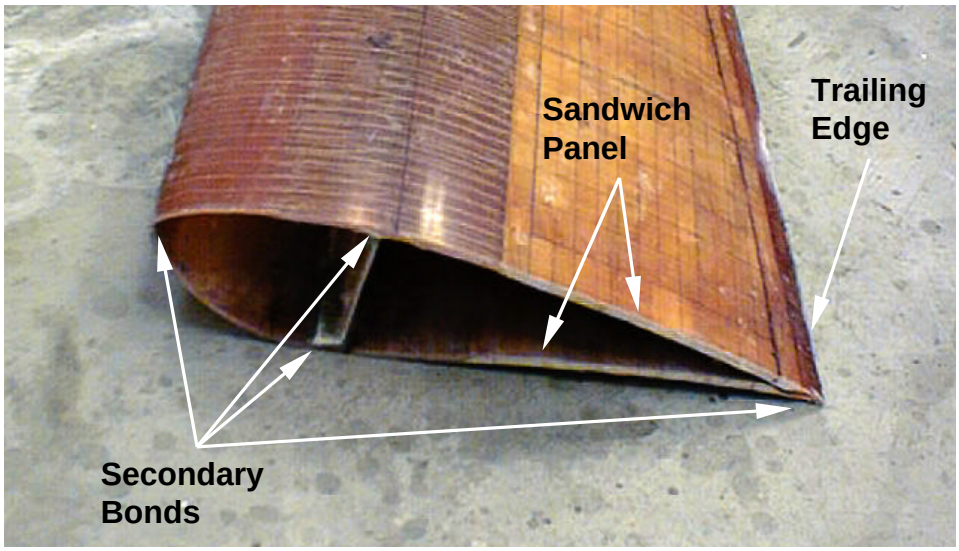

Figure 2.2 Section view of wind turbine blade showing sandwich construction in trailing edge.

At the start of this research project, a section of a prototype blade was examined for manufacturing defects and design details that could be areas of concern. This was examined at Headwaters Composites where the prototype blade section was manufactured. Headwaters Composites owner, Charles Hedley (1999) offered suggestions and insight to a few potential problems.

Several defects and details were found. Poor fabric quality was one concern that could affect blade performance. This included fabric manufacturing problems such as fiber waviness, fiber misalignment, additional tow (bundle of several fibers) sewn onto fabric, discontinuous fibers, and missing tows. Other possible details were noted such as resin rich regions caused by score marks in the flexible balsa core, ply drops, balsa core termination (longitudinal and transverse), balsa to fabric delamination, secondary bond failure, and the small radius curved laminate in the spar. A few of these details have been investigated and their knock-down factors are displayed in Figure 2.3 [Mandell et. al (1998)]; the knock-down factor indicates how much lower the detail will perform with a lifetime of one million cycles compared to a simple coupon with the same lifetime.

The focus of the research presented in this paper will be on the longitudinal sandwich core termination detail, which has not previously been investigated. Sandwich panel transitions are labeled on a blade segment shown in Figure 2.4.

The longitudinal transition consists of a fiberglass/balsa sandwich panel that is terminated into a thin laminate consisting of the two fiberglass facesheets. The transverse sandwich termination consists of a fiberglass/balsa sandwich panel termination into a thick fiberglass laminate. This termination can be abrupt, cutting the core at a right angle, or distributed over a distance, by tapering the core. The highest loads on the longitudinal transition are perpendicular to the balsa tip, but parallel in the transverse transition.

Detail	Sketch		F
Simple Coupon (Straight Material)			1.0
Bonded Stiffener (Beam - Web)	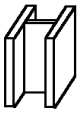		1.2
Cracked Transverse 90^{o} Patch	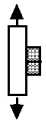		1.0
Single Interior 0^{o} Ply Drop		$V_F < 0.4$	1.2
		$V_F > 0.4$	- - -
Double Interior 0^{o} Ply Drop		$V_F < 0.4$	1.6
		$V_F > 0.4$	1.0
Locally Higher Fiber Content D155 / DB120 Fabrics (2 - 90^{o} plies in center)	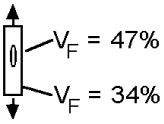		1.4
Surface Indentation A130 / DB120 Fabrics (V_f increased, thickness reduced by 25%)	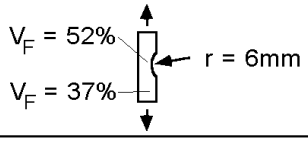		1.8
Surface Indentation D155 / DB120 Fabrics (V_f increased, thickness reduced by 25%)	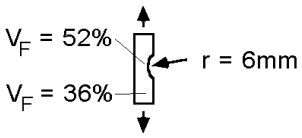		2.5

$$10^{6}\,\text{Cycle Strain} = \frac{(\text{Coupon } 10^{6}\,\text{Cycle Strain})}{F}$$

Figure 2.3 Preliminary tensile fatigue knock-down factors for selected structural details relative to simple $[0,\pm45, 0]_s$ fiberglass/polyester coupons (From Mandell et al. (1998)).

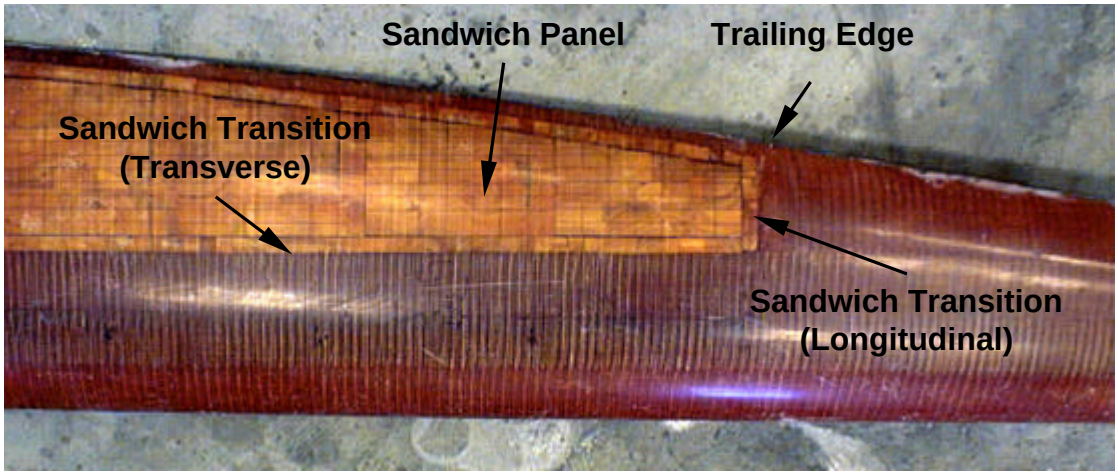

Figure 2.4 Wind turbine blade segment

It was assumed that the longitudinal case would cause a larger knockdown in strength because it is the primary loading direction and because the thickness changes by such a large amount, causing geometric as well as material discontinuities.

The average strains imposed on the transition regions will be the same as on the adjoining structural components such as the spar. Thus, the transition must be capable of withstanding the same strains as the surrounding areas. Often, detail regions contain stress concentrations, as a consquence, knockdown factors are used to lower the allowables in these regions.

Detailed photographs of the sandwich terminations are shown in Figure 2.5. The importance of a smooth, uninterrupted aerodynamic surface requires the core to be tapered on only one side. Unfortunately, this creates a local asymmetric loading that puts the transition in local bending due to the global tension and compression stresses from the blade bending moments. The

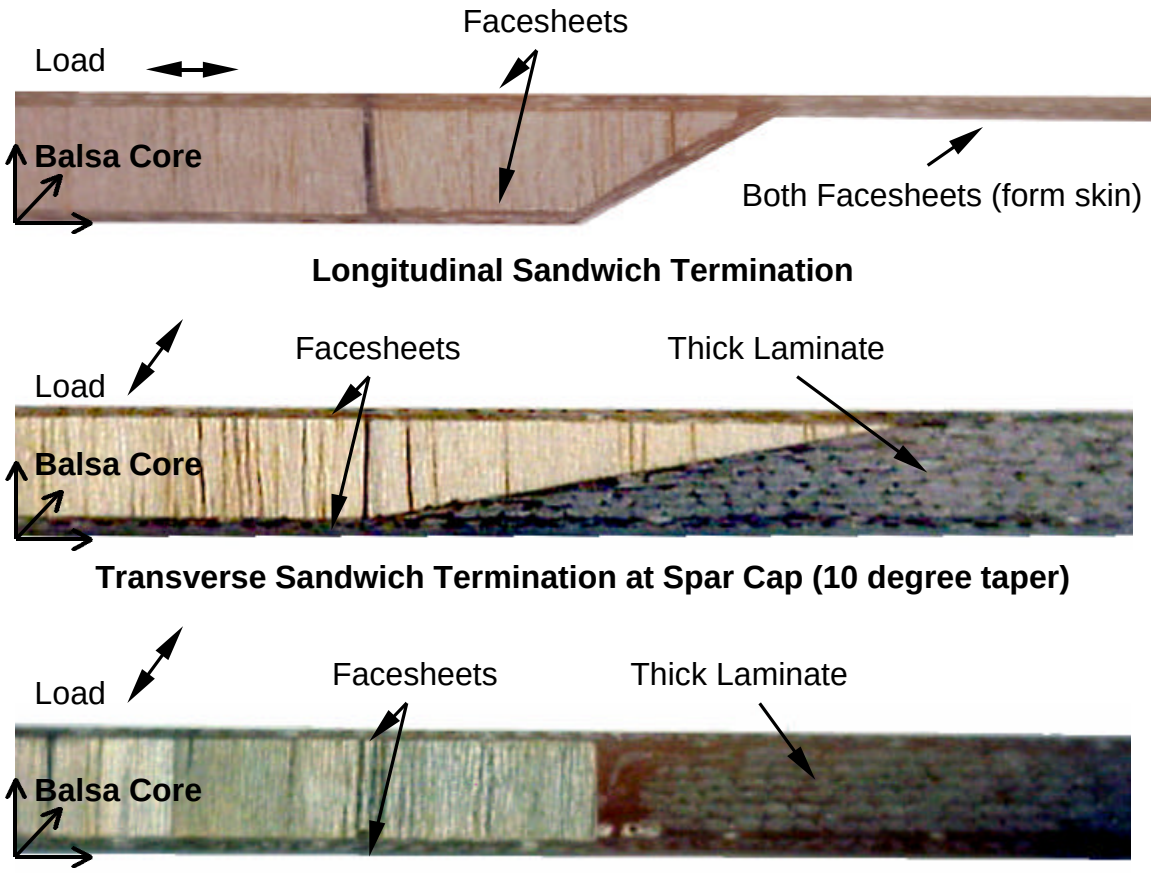

Figure 2.5 Local detail regions of sandwich terminations

asymmetry compounds the material discontinuity present at the transition. Another inherent disadvantage of the transition has is that as the balsa separates the two facesheets, there may be a strong dependence on the transverse laminate properties; these properties are much lower than the longitudinal (fiber dominated) properties. Finally, the local change in modulus may invoke a local stress concentration. These are some of the reasons the sandwich to laminate transition was thought to be of some concern.

Sandwich Theory

As noted in the introduction, sandwich construction consists of three or more layers of materials. The outer facesheets or skins are constructed from strong, stiff materials such as oriented fiber-reinforced plastics. The facesheets carry all axial load. The core is a low density material that serves several functions. Some common core materials are corrugated paper or metal, foam, honeycomb, and balsa. The core must keep the facesheets separated and have shear resistance to generate bending stiffness, which increases buckling resistance.

The analytical treatment of sandwich panels typically assumes that the axial and bending stiffness of the core material is negligible because the facesheets are usually much stiffer than the core material. Based on this assumption, the core has a constant shear stress throughout its thickness.

Previous Work

Very little work has been reported on sandwich panel terminations in the literature. One paper was found pertaining to work done by Gin-Boay, Leong-Keey, and Lee-Soon (1999) on a sandwich panel with aluminum facesheets and a honeycomb core. Through correspondence with the authors, it was learned that they had not found any other information on such a detail either. Unfortunately, the work they did was on a nonsymmetric sandwich panel with facesheet thicknesses differing by a factor of four. The test geometry used was

not as continuos as the blade application due to a doubler which was 1.5 times the thickness of the thick facesheet. A diagram of the specimen is displayed in Figure 2.6. A similar investigation was done on a specimen with no doubler present. These are both applications common to helicopter construction [Gin-Boay et al. (1999)].

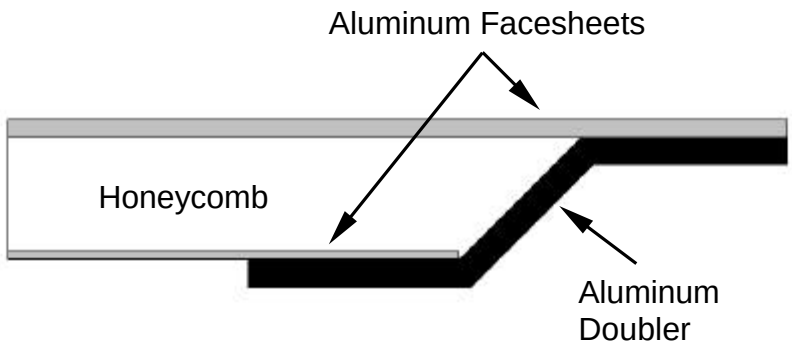

Figure 2.6 Diagram of Gin-Boay et. al. (1999) specimen

Gin-Boay et al. formulated models for the specimen with and without the doubler. The specimen without the double was investigated first. The variables used in their formulation are as follows:

E_a Elastic modulus of top skin
t_a Thickness of top skin
E_b Elastic modulus of bottom skin
t_b Thickness of bottom skin
E_k Elastic modulus of doubler
t_k Thickness of doubler
h Distance between centers of facesheets
G Shear modulus of core material
L Length of bottom skin to line of symmetry
z Distance from end of bottom skin (z=L at line of symmetry)
P Load carried by sandwich panel
P_a Load carried by top skin
P_b Load carried by bottom skin
q Shear stress in the core

The governing equations used to solve for facesheet load distributions were:

$$\frac{\partial P_a}{\partial z} = -q \tag{2.1a}$$

$$\frac{\partial P_b}{\partial z} = q \tag{2.1b}$$

$$P_a + P_b = P \tag{2.2}$$

Assuming that transverse strains were negligible, the following solutions were found using a shear lag model.

$$P_a(z) := \frac{P}{t_a \cdot E_a + t_b \cdot E_b} \left(t_a \cdot E_a + t_b \cdot E_b \cdot \frac{\cosh(\lambda(L - z))}{\cosh(\lambda \cdot L)} \right) \tag{2.3a}$$

$$P_b(z) := \frac{P \cdot t_b \cdot E_b}{t_a \cdot E_a + t_b \cdot E_b} \left(1 - \frac{\cosh(\lambda(L - z))}{\cosh(\lambda \cdot L)} \right) \tag{2.3b}$$

$$q(z) := \frac{\lambda \cdot P \cdot t_b \cdot E_b}{t_a \cdot E_a + t_b \cdot E_b} \cdot \frac{\sinh(\lambda(L - z))}{\cosh(\lambda \cdot L)} \tag{2.4}$$

where

$$\lambda := \frac{G}{h} \cdot \left(\frac{1}{t_a \cdot E_a} + \frac{1}{t_b \cdot E_b} \right) \tag{2.5}$$

Additional work was done to model the specimen that included the doubler. The geometry was much more complex so additional terms were needed. A schematic of the model used by Gin-Boay et al. (1999) is shown in Figure 2.7. It was assumed that the model with the doubler could be cut at the beginning of the taper of the core, and superposition could be used to add the doubler model to the original shear lag solution.

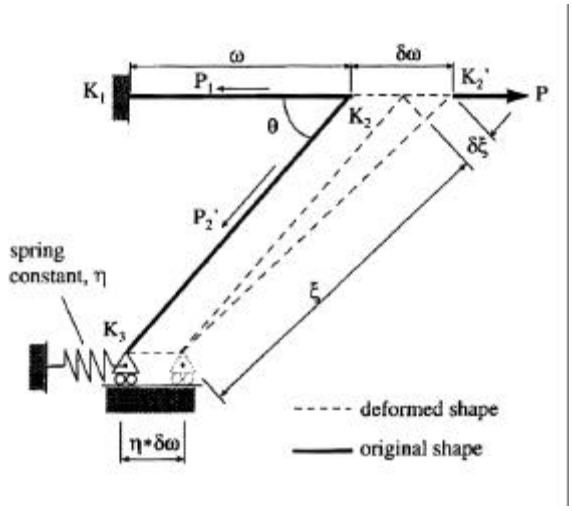

Figure 2.7 Diagram of model containing doubler developed by Gin-Boay et. al. (1999).

Some additional variables are defined as follows.

P_1 Load carried by top skin on doubler section
P_2 Load carried by doubler
η Ratio of t_aE_a to t_kE_k

Once this was completed, the following solution was developed.

$$P_c(z) := \frac{P_2 \cdot t_a \cdot E_a}{t_a \cdot E_a + t_b \cdot E_b}\left(1 - \frac{\cosh(\lambda(L - z))}{\cosh(\lambda \cdot L)}\right) + \frac{P_1}{t_a \cdot E_a + t_b \cdot E_b}\left(t_a \cdot E_a + t_b \cdot E_b \cdot \frac{\cosh(\lambda(L - z))}{\cosh(\lambda \cdot L)}\right) \quad (2.5a)$$

$$P_d(z) := \frac{P_1 \cdot t_b \cdot E_b}{t_a \cdot E_a + t_b \cdot E_b} \cdot \left(1 - \frac{\cosh(\lambda(L - z))}{\cosh(\lambda \cdot L)}\right) + \frac{P_2}{t_a \cdot E_a + t_b \cdot E_b} \cdot \left(t_b \cdot E_b + t_a \cdot E_a \cdot \frac{\cosh(\lambda(L - z))}{\cosh(\lambda \cdot L)}\right) \quad (2.5b)$$

$$q(z) := \frac{\lambda \cdot \left(P_1 \cdot t_b \cdot E_b - P_2 \cdot t_a \cdot E_a\right)}{t_a \cdot E_a + t_b \cdot E_b} \cdot \frac{\sinh(\lambda(L - z))}{\cosh(\lambda \cdot L)} \quad (2.6)$$

It was reported that experimental data collected validated the theoretical model. The current theoretical model omits bending, but this may be added later.

Previous work has also been done on the properties of balsa used in sandwich panels. This work has conclusively showed that balsa supplier's nominal shear strength data may be over stated and other available data suggest shear strengths that vary by as much as a factor of two [Kilbourn (2000)] [Wienhold, Lennon, Roberts, Rooney, Kercher, Nagle, Sorathia (2000)]. Other results presented in these same papers indicated that ASTM C 273-94(Shear Properties of Sandwich Core Materials) was more conservative than ASTM C 393-94 (Flexural Properties of Sandwich Construction) in determining core shear strength. These ASTM standards will be talked about in more detail later in the paper. Kilbourn suggests that thickness affects the shear strength, which is not typically taken into account.

Design Detail To Be Investigated

The longitudinal sandwich core termination, pictured at the top of Figure 2.5, is the detail of greatest interest in this research. It was assumed that the longitudinal case would cause a larger knockdown in strength due to the loading direction and the fact that the thickness changes by such a large amount, causing geometric as well as a material discontinuity.

The load transfers in the longitudinal transition pictured at the top of Figure 2.5 are illustrated in Figure 2.8. The stress states at several locations of the fillet region are also included in the figure. The stresses away from the transition are pure tension in the thin laminate and the sandwich panel as illustrated in element 7 in Figure 2.8. The longitudinal tensile load in the straight facesheet rises rapidly as one moves to the left along its length from point 7d to 6. The rise in stress is an effect of the drop in stress at point 3 when the fillet facesheet fibers become less effective as they move out of plane. From this point forward, as one moves along the fillet towards the sandwich end, the stress in the straight facesheet decreases while the stress in the fillet or upper facesheet rises.

The shear stress jumps rapidly at the fillet tip, but begins to dwindle as an equal far-field stress is reached in each facesheet in the sandwich panel end. The shear stress in the core transfers the higher load of the straight facesheet to the fillet facesheet, which has a lower load throughout the fillet region. There are transverse stresses that arise from the fibers moving in and out of plane at the fillet start and end. The transverse stress at 3 and 6 is a tensile stress, which

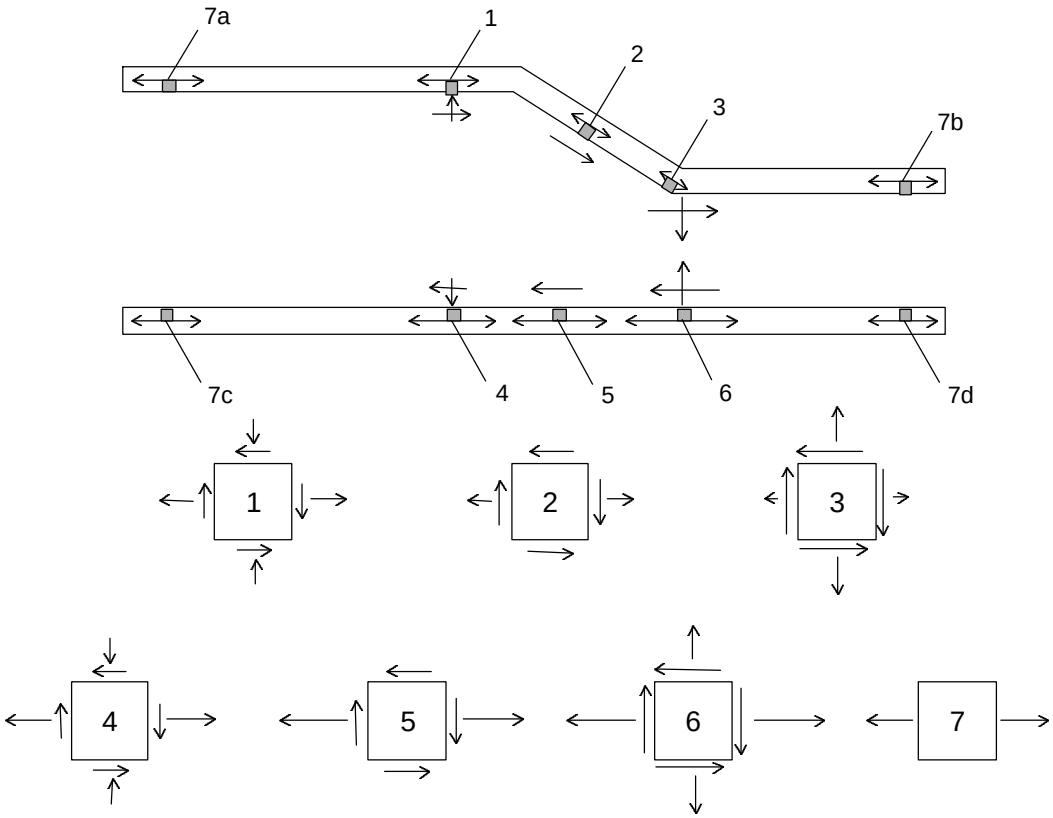

Figure 2.8 Illustration of load transfer in a sandwich to thin laminate transition loaded in tension, including stress states at several locations (Length of arrows represent relative magnitudes).

can initiate delamination; while the transverse stress at 1 and 4 is compressive, which merely compresses the core.

The sandwich to thick laminate transition was also a concern, but was investigated in less detail. Problems with this transition stem from the material discontinuity present when the core transitions from balsa to a solid fiberglass laminate.

Testing a large blade section presents many challenges that would have overshadowed the investigation of the sandwich panel termination. For this

reason, sub-scale coupons were used to test only the termination, without other details of the blade which have been the subject of other studies [Haugen (19), Sears (1999), Morehead (2000)].

All investigations in this study focus on tensile tests of the transition. Tension tests were chosen to alleviate the difficulty associated with compression testing. Although compression performance is important, this was left as future work. The information gained from the small-scale tests can be applied to the blade by using a strength knock-down factor in the regions of the transition.

CHAPTER 3

EXPERIMENTAL METHODS AND TEST DEVELOPMENT

Several experiments were performed throughout the course of this research. However, most of them used similar materials and manufacturing techniques. For instance, the ply configuration of the composites tested was the same in all experiments. The configuration was taken from the MSU AOC 15/50 blade design. Thin laminates used a layup of [±45, 0, 0, ±45], while sandwich panels used [±45, 0, balsa, 0, ±45]. Both of these layups are found in the trailing edge of the blade. The fabric reinforcement and matrix were also chosen due to their inclusion in the blade design.

Materials

The fabric used for the zero degree or longitudinal direction was A130 supplied by Owens Corning. The fabric is named for its areal weight of 13.0 ounces per square yard, which is equivalent to 441 grams per square meter. This is a woven fabric made by weaving fiberglass tows around a thermoplastic bead. Unfortunately, due to its weave, laminates made from this fabric have relatively poor compression strength. However, unlike stitched fabrics with straight fibers, which provide excellent baseline compression strength, design details, such as those shown in Figure 2.3, have less effect on the A130 fabric

[Samborsky D. D., Mandell, J. F., and Cairns, D. S. (1999)]. Tensile properties are the same for both, A130 and straight fiber, stitched fabric.

The ±45 degree plies are a bias stitched ±45 fabric, DB120, supplied by Owens Corning. As before, the name indicates an areal weight of 12.0 ounces per square yard or 407 grams per square meter. This fabric is difficult to work with because it deforms very easily during handling, and care has to be taken to be sure fibers remain straight. Unfortunately, the fabric manufacturing process has variables, so the fibers can be misaligned by five or more degrees from the nominal ±45 degrees. Another important point about layups including the DB120 fabric is that parts are not truly symmetric. When laying up the part, as the first DB120 is laid down, the outer ply is plus 45 degrees from the longitudinal axis. When the last DB120 is placed on the opposing surface, the fabric is not reversed, so outer ply is minus 45 degrees from the longitudinal axis. This asymmetry is noticeable by a small amount of warping, but is typically neglected. Photographs of these fabrics can be seen in Figure 3.1.

The resin used in this project is the resin specified in the blade design, CoRezyn 63-AX-051, an unsaturated orthothalic polyester resin, obtained from Interplastic Corporation. According to the *DOE, MSU composite material fatigue database: Test methods, material, and analysis* [Mandell, J. F., Samborsky, D. D., (1997)], this is a typical resin type used in the wind turbine blade industry. The resin was catalyzed using Methyl Ethyl Ketone Peroxide (MEKP). The amount of catalyst varied according to the time needed before it gelled. If two

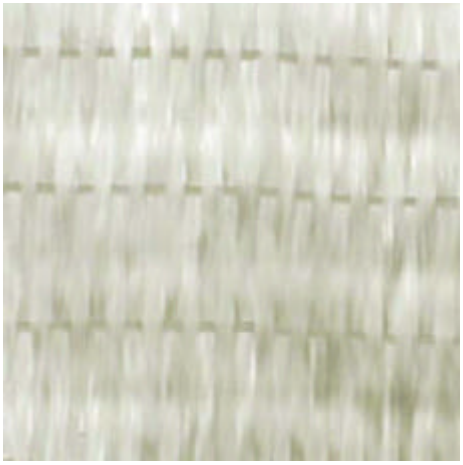

A130

DB120

DB400

Type 31300 (with edge view)

Figure 3.1 Fiberglass fabrics used to prepare test specimens.

percent by volume of the catalyst was used, gel times were around thirty minutes. A gel time of 90 minutes was obtainable with 1.5 percent MEKP.

Once again, core materials were specified by the blade design. This was a balsa core manufactured by Baltek Corporation. The core chosen for the blade design and the project at hand was Contourkore CK-100 AL-600/10 with a

nominal thickness of 3/8 inch or 9.5 mm. The core is scored into one inch by two inch or 25 by 50 mm sections and bonded to a lightweight fiberglass scrim. The scrim holds the sections together and gives the core its flexibility and name. This allows the core to drape into complex curves. A photograph of the Contourkore as well as a piece of sandwich panel is in Figure 3.2. The sandwich panel in Figure 3.2 clearly shows the score marks which fill with resin during manufacturing. AL600/10 is Baltek's proprietary chemical treatment that reduces porosity and increases bond strength. Resin absorption into the balsa is reduced or eliminated by the treatment; this produces parts with less parasitic weight. The designation CK-100 refers to the density of the balsa core. Baltek specifies the density of CK-100 as 150 kg/m^3. In order to accommodate core terminations, Baltek manufactures a transitional strip called a "Flexible Fillet Strip." This is a small strip of balsa manufactured to the same thickness of the core. The fillet strip has an edge tapered at 30 degrees to facilitate core termination. The fillet strip is not treated with AL600/10 and does not have a density specified by

Figure 3.2 Sandwich panel, Contourkore (scored side), and Contourkore (scrim side).

Baltek. The fillet is scored and bonded to a paper strip to give it flexibility [Baltek Corporation (1999)]. Other fillets used in this research were manufactured from Contourkore at MSU. These details will be discussed later in this chapter.

Fabrication Methods

Test specimens were all prepared at MSU by similar methods. All were made using a modified hand layup technique. A base mold or plate was used for the bottom surface. The base mold was different for each type of specimen, described later. Frekote 700-NC by the Dexter Corporation was used as a mold release in all cases, applied at least twice and allowed to dry for at least five minutes. This proved to be sufficient drying time and the parts released well every time.

The following is an account of how a sandwich panel containing a transition was produced. A series of photographs illustrating this process called Modified Hand Layup can be seen in Figure 3.3. Fabrication was done in a well-ventilated room with personnel wearing a cartridge respirator and latex gloves. Once the mold surface was prepped (Figure 3.3a) and fabric and core material were cut, a panel could be made. The first piece of dry DB120 fabric was placed in the mold (Figure 3.3b). Applying the first pool of resin liberally allowed the fabric to wet out without working it too much by hand. The layer was wet out while spreading resin with a plastic scraper (Figure 3.3c) and working with a hand layup roller (Figure 3.3d). When DB120 layers are worked, a little distortion can be seen in the fiber orientation, so overworking these layers was avoided.

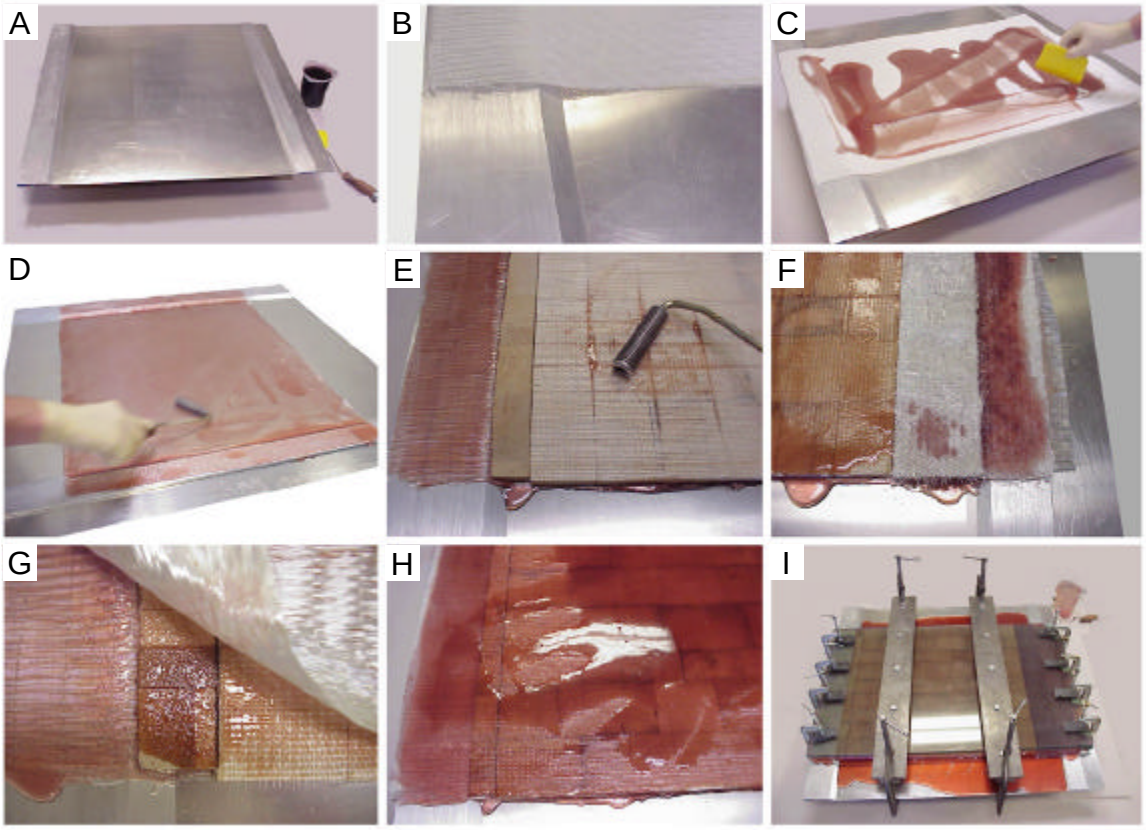

Figure 3.3 Series of fabrication photographs for sandwich panel with transition to thin laminate. A) Mold surface with fillets B) DB120 fabric on mold C) Spread resin over first layer of fabric D) Use roller to remove air entrained in resin and fabric E) Resin coming through balsa score marks as it is rolled F) Solid core built up for grip G) First layer of straight facesheet H) Resin pool before clamping to reduce porosity in straight facesheet I) Glass placed over sandwich panel; clamped to remove excess resin

Next, a resin pool was spread on the wet out DB120, and a layer of A130 was laid down. Resin was applied and rolled until it was thoroughly wet out. Another liberal coat of resin was spread over the A130 layer to ensure that the next layer, the balsa core, was entirely wet out through the thickness. The balsa and balsa fillet were laid down at same time, with the fiberglass scrim on top. In order to keep these together, the two pieces were stapled together every 25 cm.

Although this introduced a foreign object into the part, part quality was better because it limited the size of the gap between the fillet strip and the core. The effect of the staple is negligible and is something that might be found in a large scale manufacturing process. Care was taken to ensure that the fillet strip was positioned at the start of the taper. The layer of balsa was rolled with higher pressure, to force the resin through the scores in the core. The balsa was well saturated if resin was forced from the bottom up through the score marks (Figure 3.3e). To ensure that saturation was thorough, resin was pooled on top of the balsa and spread until all of the scrim was saturated. The next step was to build up a solid laminate at the end of the balsa core that could be gripped with high pressure during mechanical testing.

Building the core up was done two different ways. Some samples had a solid core built up using nine layers of DB400, a heavy ±45 fabric with an areal weight of 40.0 ounces per square yard or 1356 grams per square meter supplied by Owens Corning. Other samples were built up using five layers of Type 31300 fabric with an areal weight of 780 grams per square meter, supplied by Ahlstrom. The latter fabric was chosen due to its high permeability, ease of wetting out, and high bulk. It consists of two chopped strand mats bonded to the surfaces of a resin flow layer. Both of these fabrics are included in Figure 3.1. The method used to build up the core will be discussed in more detail later.

Once all of balsa core was wet out and the solid grip end was built up as a solid laminate, the next layer of A130 was added (Figure 3.3g). This was covered with resin and rolled until the entire layer was wetted out. Again, resin

was pooled and the final DB120 was added and rolled cautiously to reduce fiber movement. After the entire layer of DB120 was wetted out, a large resin pool was spread over the entire part a thickness of one to three millimeters, deepest in the center (Figure 3.3h). A piece of, 12 mm thick, tempered glass, which was previously treated with Freekote, was placed over the entire part. This was doubled with a second piece of 12 mm thick tempered glass. Finally, two pieces of steel were positioned over the glass in the center and clamps were tightened by hand. Additionally, four clamps with small steel pads were tightened on each end (Figure 3.3i). These were tightened periodically as resin flowed out of the part over the next thirty minutes.

The finished parts were allowed to cure for at least eight hours before they were removed from the mold. After the part was removed from the mold it was post cured in a convection oven at 65 degrees Celsius for two hours. The parts were then laid out, sanded for strain gages and cut to their final size using a wet saw fitted with a diamond blade. An extended fence was adapted to the saw to ensure parts were cut straight and parallel.

These are the general methods used to manufacture many of the panels for testing. Some panels used different methods, which will be noted as specimens from that panel are discussed.

Experiments to Establish Material Properties

Several experiments were executed to establish material properties for use in finite element modeling. These were all done as simply as possible to

isolate the unknown property. The properties of the individual plies have been evaluated in the past and were not investigated in detail in this study. This information was taken from the DOE/MSU Composite Material Fatigue Database [Mandell, J. F., Samborsky, D. D., (1997)]. Initially, the balsa properties were not well known, so several balsa tests were conducted.

The shear modulus and strength of the balsa core was initially investigated using a sandwich panel with stiff facesheets. This method gave poor results, so a test method based on ASTM C-273-94 Standard Test Method for Shear Properties of Sandwich Core Materials (1997) was used. A tension fixture was constructed by the author in the MSU Machine Shop using specifications from ASTM C-273-94. A photograph of the fixture with a specimen is shown in Figure 3.4. The backing plates were bonded to 9.5 mm thick aluminum plates using Hysol EA 9309.2NA adhesive supplied by the Dexter Corporation. Aluminum was chosen over steel because of its compatibility with the Hysol adhesive. The balsa samples were 50 mm by 150 mm by 9.33 mm thick. They were oriented so that there were fewer score marks in the load direction. Using removable tabs that were machined in the machine shop, an extensometer was used to measure the longitudinal displacement of the backing plates. This provided greater accuracy than simply using the actuator displacement from the testing machine.

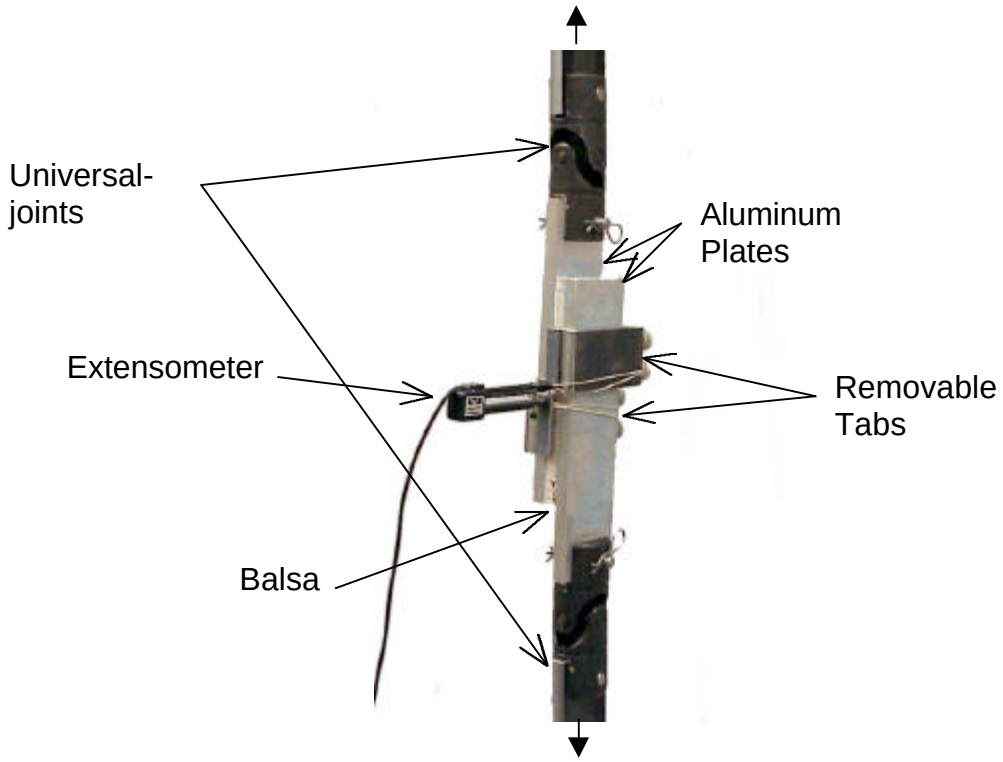

Figure 3.4 Balsa shear test per ASTM C-273

The experiment was performed using the Instron 8562 screw machine. A Hewlett Packard 34970A data acquisition system was used for the experiment. All of the static tests were performed using this machine and data acquisition arrangement. The first set of shear tests was not accurate because the adhesive bond failed against the aluminum. The aluminum surfaces were not roughened enough to allow for good adhesion. For all subsequent tests, the aluminum plates were sanded thoroughly and then cleaned with acetone, preparing the surface for a good bond with adhesive to the balsa.

The extensional modulus and strength were needed for the balsa, in addition to shear properties. These tests were performed with two specimen sizes. Baltek Corporation scores most of the balsa into 25mm by 50 mm pieces. However, there is one strip along the edge which is 50 mm by 50 mm. Both of these sizes were used in the extensional modulus tests. The use of both sizes was to eliminate concerns of Poissonic effects during the test. If there are significant Poissonic effects, samples with different aspect ratios should have different results. In order to keep the tests similar with regard to load and test duration, two 25 mm by 50 mm samples were tested side by side as one specimen, having the same nominal test dimensions as the 50 mm by 50 mm tests. The specimens were carefully chosen from a sheet of Contourkore using several stipulations. The specimens had to include balsa originating from only one tree. This was easily seen by the growth rings of each tree in the sheet of ContourKore, as displayed in Figure 3.5. For the side by side specimens, each side was from the same tree. This would eliminate variations from tree to tree within each specimen. The same specimens were used to find the local density of the balsa core. Another important specification is that the growth rings could not be parallel or perpendicular to the longitudinal axis of the test. Care was taken to find samples that had growth rings at approximately 45 degrees to the longitudinal axis. This ensured that neither the radial or tangential modulus of the balsa tree would dominate.

The same fixture that was used in the balsa shear modulus test was used to determine the extensional modulus. All scrim material was removed and the

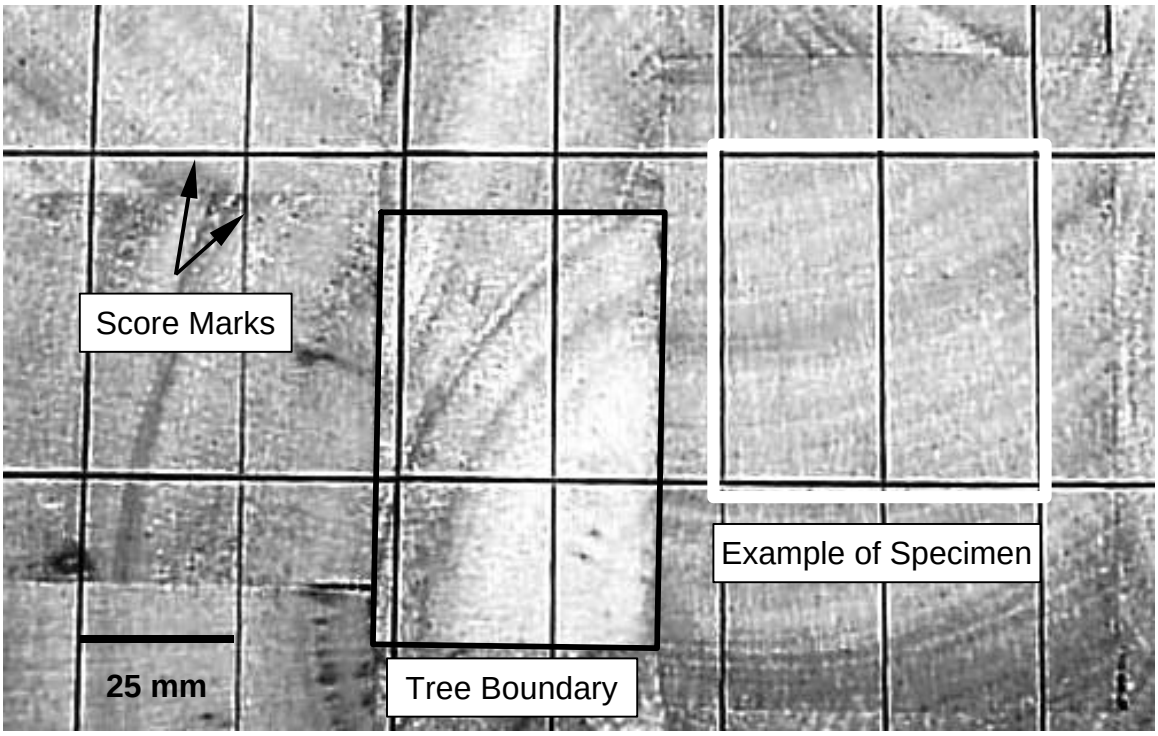

Figure 3.5 Baltek ContourKore view showing score marks and growth rings of tree sections used.

edges of the balsa specimen were sanded to right angles because the scoring process leaves them slightly angulated. The ends of the samples were then bonded to 9.5 mm aluminum barstock. This method was chosen over other methods, such as gripping the balsa directly, because the size of balsa specimens obtainable from the Contourkore was so small between the score marks. The barstock had holes to mate with the u-joint fixtures. The u-joints were used to eliminate any moments that may have been induced by clamping the barstock directly in the testing machine. Again, the removable tabs were used with the extensometer to calculate local extension. Photographs of the

fixture as well as two specimens are included in Figure 3.6. Notice the growth rings marked on the specimens.

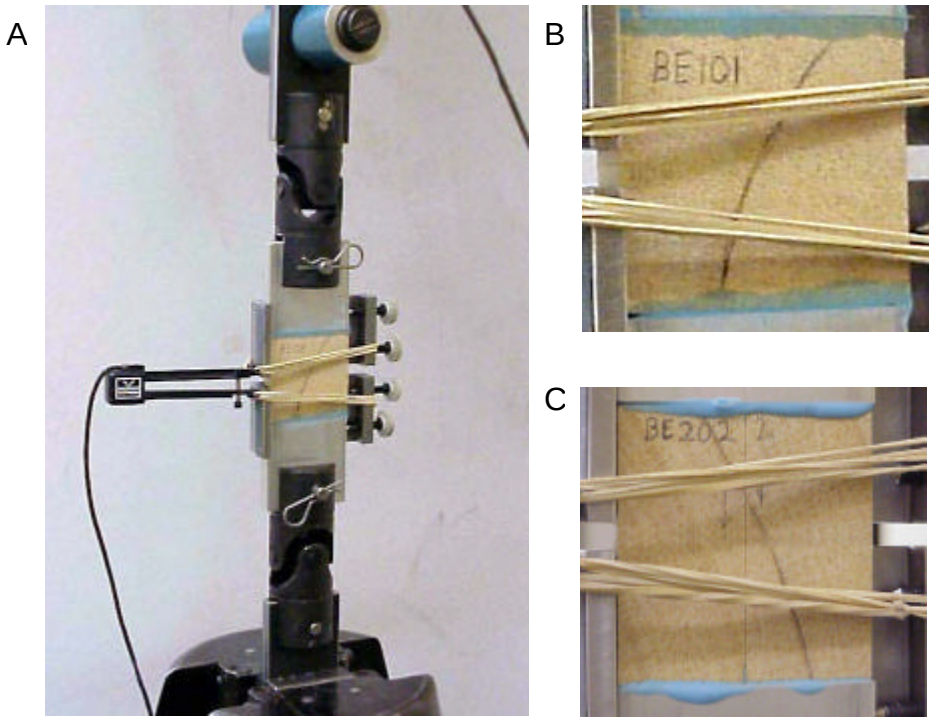

Figure 3.6 Balsa Extensional Modulus Test; A) Test Setup, B) 50 mm by 50 mm specimen, C) Two 25 mm by 50 mm specimens bonded side by side with edges free.

An additional test was performed to validate material properties in the finite element model for a simple geometry in bending. This test was a sandwich panel flexural test. This test was carried out following specifications listed in ASTM C 393-94 Standard Test Method for Flexural Properties of Sandwich Core Materials (1997). The test chosen was a “Long Beam—Midspan Loading” test because it captured the bending in a sandwich panel, and fixtures existed to carry out the test without acquiring or manufacturing more costly equipment. The

material used was actually a sandwich panel cut from parts made for other tests. A span of 238 mm was used in three point bending with a specimen width of 50 mm, the width of the grips. The width was chosen as large as the grips allowed to reduce any edge effects. A piece of 9.5 mm barstock cut at a right angle was used as a loading nose. This gave the center nose a 9.5 mm wide distributed load, reducing local effects of a single point load.

The end supports were 19 mm diameter rollers. This setup can be seen in Figure 3.7. A dial indicator was used to check the actuator displacement readings for accuracy. Since the actuator displacement was within one percent of the dial indicator, actuator displacement was used for all specimens.

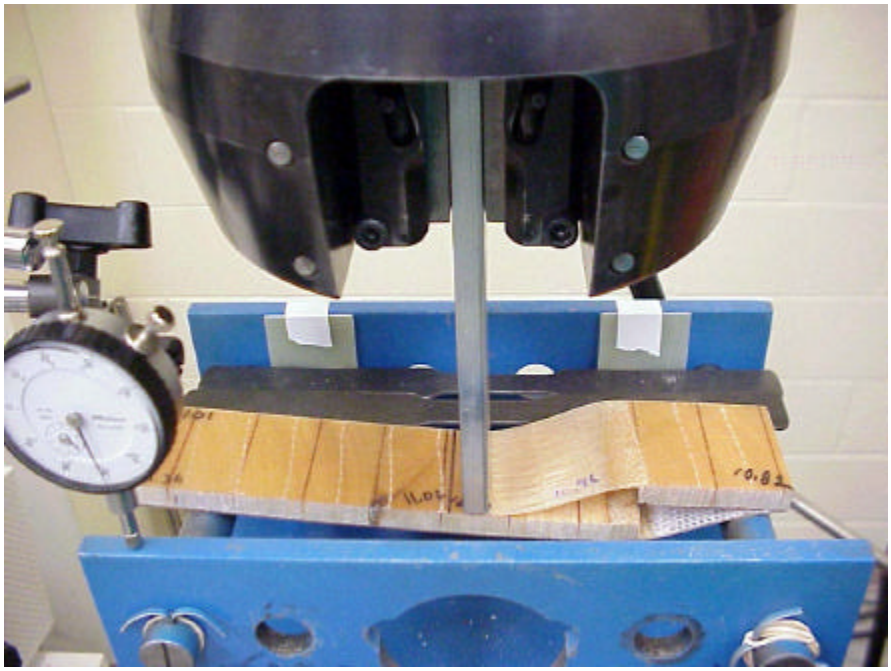

Figure 3.7 Photograph of Sandwich Panel Flexural Property Test—Long Beam—Midspan Loading.

These were the primary experiments perfomed to establish basic material properties. The most important were the balsa properties because little was known about balsa at the start of this project. The sandwich panel flexural test served as a benchmark for comparison to a finite element model.

Experiments to Establish Baseline Strengths

Two basic configurations are on either side of the sandwich panel transition. These are the sandwich panel, composed of fiberglass facesheets and balsa core, and the thin laminate, consisting of both facesheets co-cured together. The experiments described in this section were carried out to establish the baseline strength of each of these laminates without the transition affecting their performance.

The facesheet control material was manufactured in a similar manner to the other parts, except the core was omitted. Another manufacturing difference is that when the facesheet material was clamped, spacers were put into the mold before clamping to ensure that the facesheet had a constant or near constant thickness. This would fix the fiber volume fraction and, hopefully, produce better results. Two tests were executed with this material, one with a straight gage section and one with a dogboned gage section. The straight specimen had a width of 25 mm and a gage length of 74 mm, while the dogboned specimen had a gage length of 127 mm, a width at the grip of 36 mm, a minimum width in the gage section of 23 mm and a radius of 280 mm forming the dogbone shape. Both specimens were tabbed for a length of 25 mm on each end using a G-10

laminate bonded with Hysol to prevent grip failures. Both of these specimens are shown in Figure 3.8.

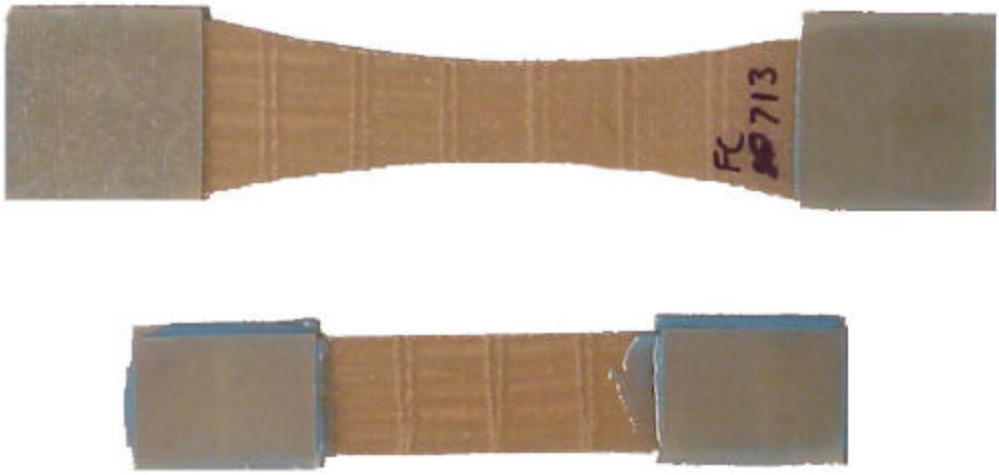

Figure 3.8 Facesheet control specimens—Dogbone and straight specimen.

These specimens were tested in tension, using a constant displacement rate ramp at 30 mm per second. Strain gages were used at the center of the gage section. Strain gages from BLH Electronics were used exclusively throughout this research. Gages were 120 ohms with a gage factor of 2.01 and dimensions of 6.35 mm long by 3.1 mm wide. An extensometer was used at the center of the gage region as well, in case the strain gages failed. The strain gages were used to get a direct comparison to data from more complicated tests where the extensometer was not usable.

Another baseline material was the sandwich panel. This was investigated to see if there was any noticeable change in strength due to the presence of a

balsa core, relative to the two facesheets alone. The sandwich panel test specimens were prepared using methods discussed earlier, except the sandwich panel specimens had a solid core on each end. This allowed high pressure gripping on each end during the tensile tests. Five layers of Type 31300 fabric were used for the solid core on each end.

These tests had several problems at the start. A satisfactory test method had not been developed previously at MSU. Several test variations were tried before a usable test geometry was found. The final tests produced reliable gage section failures, and yielded results representative of a sandwich panel without stress concentrations. The final dogboned test geometry is pictured in Figure 3.9.

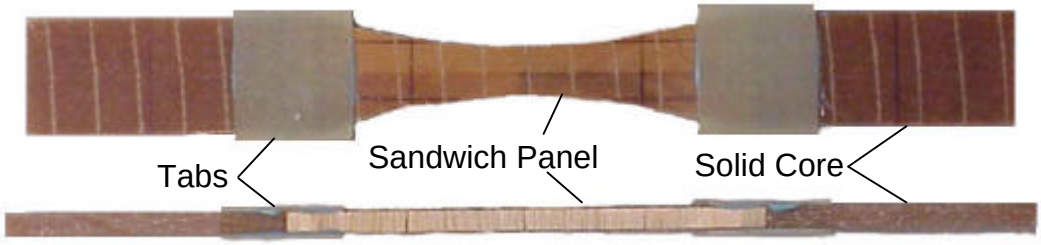

Figure 3.9 Sandwich panel control specimen—Front and edge view.

The specimen had to be tabbed to prevent failure at the core material change. This was a large stress concentration that was not overcome by the dogbone alone. Tabs were terminated before the grip area because the grips could not accommodate the full thickness of the sandwich panel plus the

thickness of the G-10 tab material. The specimens had a maximum width at the grip of 50 mm, a minimum gage section width of 22 mm, a sidecut radius of 280 mm on each side, and a gage length of 151 mm between 50 mm long tabs. The tabs were important to alleviate the potential stress concentrations associated with balsa core to solid core transition. Once again, strain gages were used at the center of the gage section as well as the extensometer. There was a little difficulty using the extensometer because it is not designed for specimens of with this thickness (10.75 mm). This was overcome by attaching the extensometer on at an angle to the edge, contacting only the corner, rather than having it contact the entire thickness. This produced good results compared to strain gages until major cracking developed, in which case the extensometer would slip and the strain gage could still provide good readings.

The facesheet and sandwich panel tests provided baseline composite strength and modulus values. These baseline values were used to calculate knockdown factors for stress and strain at failure with specimens containing the transition region.

Sandwich Termination Effects

Preliminary Specimen and Mold Development

The following describes experiments that contain sandwich panel terminations into thin laminates, the typical case of interest shown in Figure 2.5 as the longitudinal termination. Initial investigation of the termination was done with small symmetric parts prepared using standard hand layup procedures.

These tests gave interesting results but the specimens were of poor quality, so parts with higher quality were manufactured using a sheet metal mold. The next step was to make a sheet metal mold for a nonsymmetric part with a longer gage section. After testing, this specimen still appeared too short to transfer adequate shear loads to reach far-field conditions where each facesheet had the same strain. Therefore, a longer specimen was developed to test far-field results.

Finally, it appeared that an adequate specimen had been developed to test the sandwich termination. To reduce variability from part to part, a more precise mold was manufactured. A modified hand layup technique was employed using this mold to provide high quality parts that had little variation. Although these parts would not be totally representative of the hand layup techniques used on the wind turbine blade, a better understanding could be developed because part variation was reduced. A better understanding could then be applied to the actual wind turbine blade.

Hand Lay-up Sandwich Transition

The first parts were manufactured using hand layup techniques as mentioned earlier. These parts contained a small length of sandwich panel. A picture of two hand layup parts bonded together can be seen in Figure 3.10. These parts were symmetric along the length about the center of the gage section. The panel contained two Baltek fillet strips, and was laid up on a flat aluminum plate with the last two layers of fiberglass draped over the two fillet strips. Small glass plates were put over the thin laminate section to ensure a flat

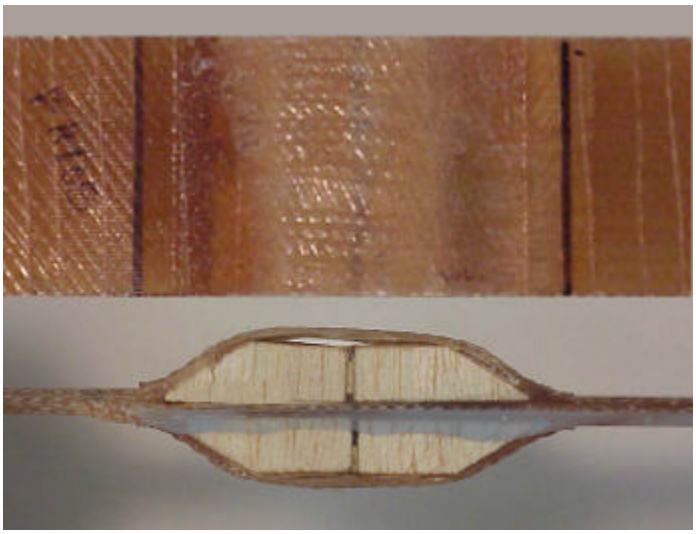

Figure 3.10 Two hand layup parts secondary bonded together to produce a symmetric specimen –void can be seen as a light area in front and edge views.

and parallel section to clamp against. The poor quality of these parts stemmed from the fact that the fabric would not drape to the 30 degree fillet angle.

Two types of tests were done with these parts, including a single specimen, which included bending due to eccentric loading and asymmetric geometry. Bending may not be present in the wind turbine blade because the blade cross-section is curved, so out of plane bending may be restricted by hoop stresses. A symmetric test that incorporated two parts bonded back to back was performed as well. This specimen, pictured in Figure 3.10, resulted in a test that had no bending present.

The poor quality of these parts can be seen in Figure 3.10; the void regions are present where the facesheet does not contact the core. The problem

exists because the fabric does not drape onto the bends contained in the part and is worsened because there is such a short section between the angles.

Fillet Mold Sandwich Transition

To increase quality, it was decided that a mold must be built to force the fabric onto the contour created by the fillet strips. A sheet metal mold was bent to match the dimensions of the part. A photo of the mold and a Fillet Mold specimen is shown in Figure 3.11. The edges of the mold were supported and

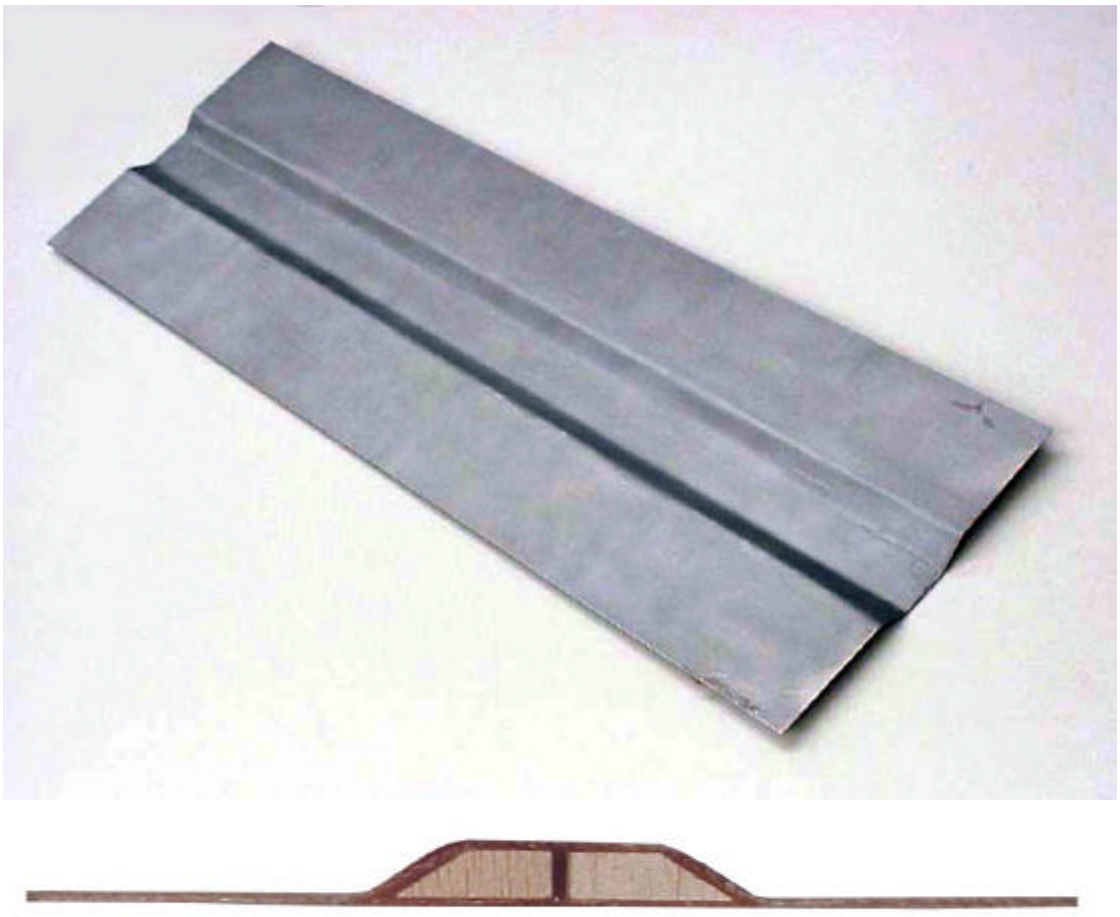

Figure 3.11 Sheet metal mold for double fillet specimen with edge view of specimen maunufactured in mold using modified hand layup technique.

the specimen was laid up using the modified hand layup technique described earlier. The quality of the parts was increased dramatically. These specimens were tested using strain gages at the center of the gage section and the extensometer at the same location on the straight side of the specimen. The parts were tested both individually (asymmetric) and bonded back to back (symmetric).

The tests showed that there was a large strength difference caused by the geometric discontinuity. As previously stated, a coupon with a longer section of sandwich panel and a single fillet to provide more shear transfer to the fillet surface was utilized.

Fillet Single Sandwich Transition

Another specimen was designed to contain only a fillet at one end and to have a longer sandwich section with 155 mm of balsa and a gage section of 290 mm. Another sheet metal mold was manufactured due to the satisfactory performance of the first mold. The mold was supported on one side and a modified hand layup method was used once again. This time a solid core was needed for gripping. This was accomplished by cutting a thick laminate to the same thickness as the balsa core and replacing it as the core for the last 25 mm of the sample. It should be noted that this procedure differed from the fabrication procedures explained earlier. A piece of thick laminate was cut and bonded using Hysol to the thin laminate end of the specimen. This put the load during testing through the centerline of the sandwich panel, parallel to the straight

facesheet to eliminate geometric differences of the centerlines of the sandwich panel and the thin laminate. Photographs of the mold and a Fillet Single specimen are shown in Figure 3.12. One of these specimens was tested nondestructively at low loads to find a strain distribution along each facesheet. An extensometer was positioned at several intervals along the each facesheet. For each position the specimen was loaded to two loads below where any damage would occur. This showed that a converged farfield strain was unattainable in a test with this gage length because the strain in each facesheet was different even at the end of the sandwich panel. A longer specimen was needed to achieve farfield results.

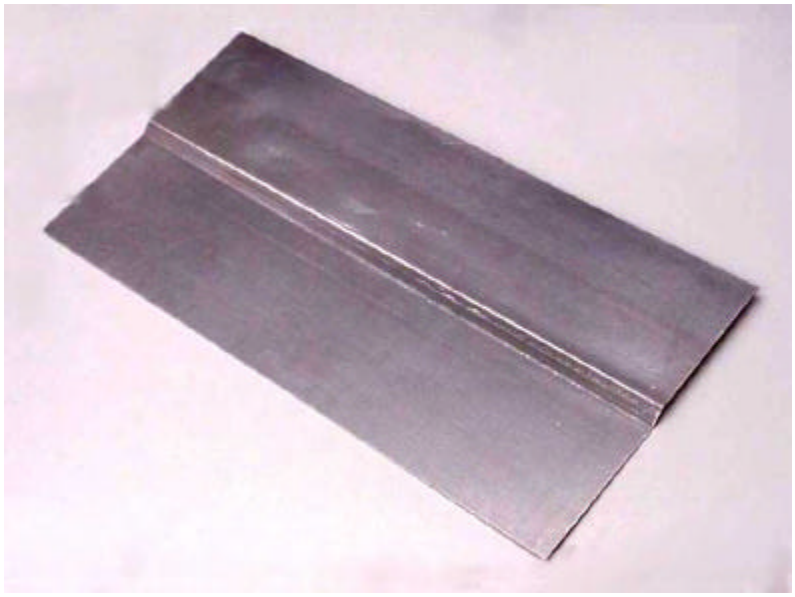

Figure 3.12 Single fillet sheet metal mold used with modified hand layup techniques.—Fillet Single specimen manufactured with mold.

Fillet Long Sandwich Transition

An extension was added to the existing sheet metal mold by simply joining a piece of sheet metal of the same thickness using tape to create a mold for a longer specimen. Again, a modified hand layup method was used to create parts with a gage length of 842 mm with 767 mm of balsa. These were tested in the same manner as the previous specimen, by using the extensometer at several locations on each facesheet to capture strain at two nondestructive loads. This showed that the strain in each facesheet converged to nearly the same value. Another test was run by placing a dial indicator at several locations and loading the specimen, checking out of plane displacement at each location. A photograph of each of these tests is shown in Figure 3.13.

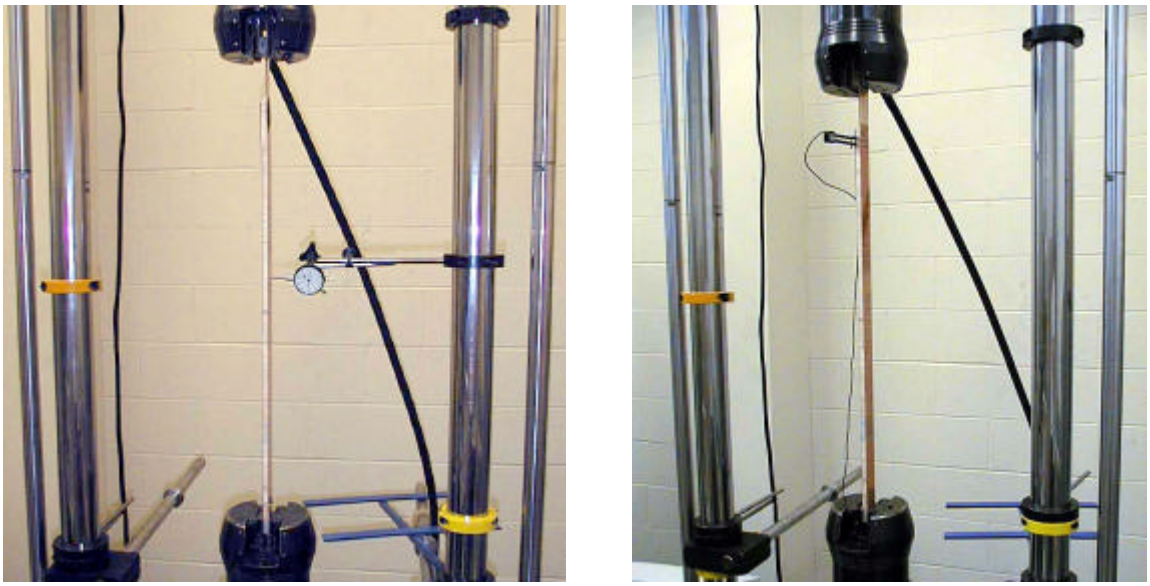

Figure 3.13 Displacement and strain mapping on Fillet Long specimen.

Symmetric tests with these specimen bonded back to back were also performed. The maximum thickness the grips would accept was 13 mm, so a specimen which was stepped down in thickness was required. A shear joint was used to bond a composite attachment stepped down in thickness from 22 mm to 12 mm. This proved to have only limited success and necessitated a redesign that could accommodate symmetric tests.

Final Fillet Sandwich Transitions

The previous specimen showed that a converged farfield strain was achievable through shear transfer in that length of specimen. Thus, the specimen reflected the in-situ performance in a blade. The specimens made using the sheet metal mold had some variation in the fillet or transition region. This included resin rich areas in several different spots: at the tip of the balsa, above and below the balsa fillet strip, and along the angled section of the fillet strip. Pictures of these variations are displayed in Figure 3.14. The cause of this problem was that the sheet metal mold pictured in Figure 3.12 was not manufactured to tight tolerances. It was anticipated that the resin rich areas and the changing local fiber contents could influence the performance of the fillet region. This prompted the design of another mold with tighter tolerances.

A final mold was manufactured from aluminum bar stock, the same thickness as the core material, which had an edge milled to a 30 degree bevel, identical to the fillet angle. This was bonded to a 3 mm thick sheet of aluminum, creating a high tolerance mold. This ensured constant fiber content throughout

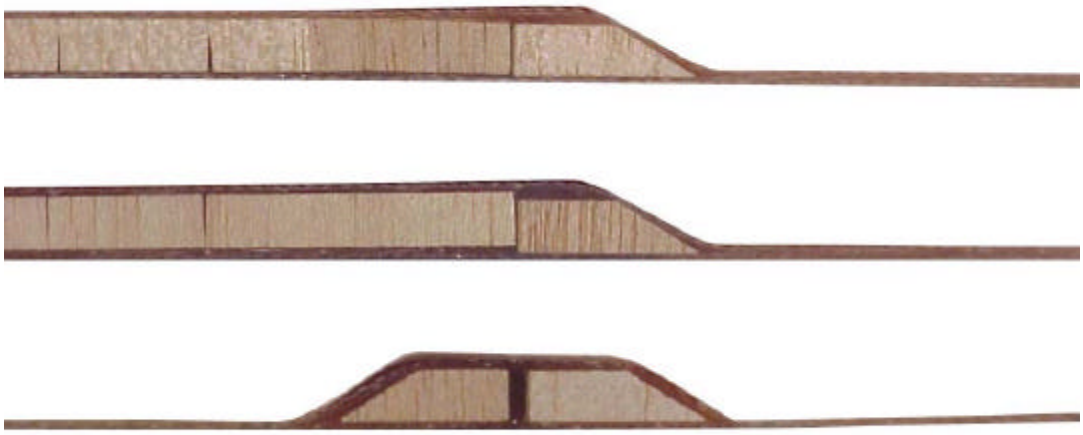

Figure 3.14 Variation and quality problems using the sheet metal molds.

the part, reducing resin rich regions. The entire mold was 900 mm by 900 mm, which was suppoted by a 20 mm thick aluminum plate. The glass plates available for the surface clamping were 600 by 900 mm. Matching the largest dimension allowed the mold to be used in either orientation, increasing its versatility.

The difficulty in performing the symmetric tests needed to be addressed as well. To achieve the necessary strength and the 12 mm thickness at the grip, a thickness reduction was incorporated into solid core section of the specimen. This was done while keeping the fibers in the facesheets continuous throughout the entire length of the specimen. The mold incorporated the thickness reduction with another piece of aluminum bar stock; this time a thickness of 6mm was used. As before, the edge was milled to a 30 degree bevel.

A 30 degree angle would allow the continuous fibers to transfer load without moving them too far out of the loading plane. This was also the shallowest angled cutter readily available. This piece of aluminum was simply taped in place, which provided freedom to change the geometry of the mold quickly and easily. The tape provided a good seal at the tip of the bevel and had only a small effect on the part.

Type 31300 fabric was used in the solid end. Two continuous layers of 31300 fabric were used near the outer layers to continue through the thickness change, and three additional layers were used to fill the thick section of the solid core. This fabric was easier to use than the DB400 because it wet out easily and could compress easily to differing thicknesses.

A solid core length of 70 mm provided enough shear transfer that the thickness change at the end of the balsa core had no significant effects. To use the specimen for the single asymmetric tests, a solid laminate was bonded to the thin end, and the end with the reduced thickness was cut off. A photograph of the mold can be seen in Figure 3.3a, and the specimens are shown in Figure 3.15. The parts were made using the modified hand layup method. A change was made when clamping the solid core end. In order to produce a constant thickness at the end of the specimen where the laminate was compressible, spacers of appropriate thickness were used.

This specimen provided good results for both, single (asymmetric) and back to back (symmetric) tests. This specimen is hereafter referred to as ‘Fillet

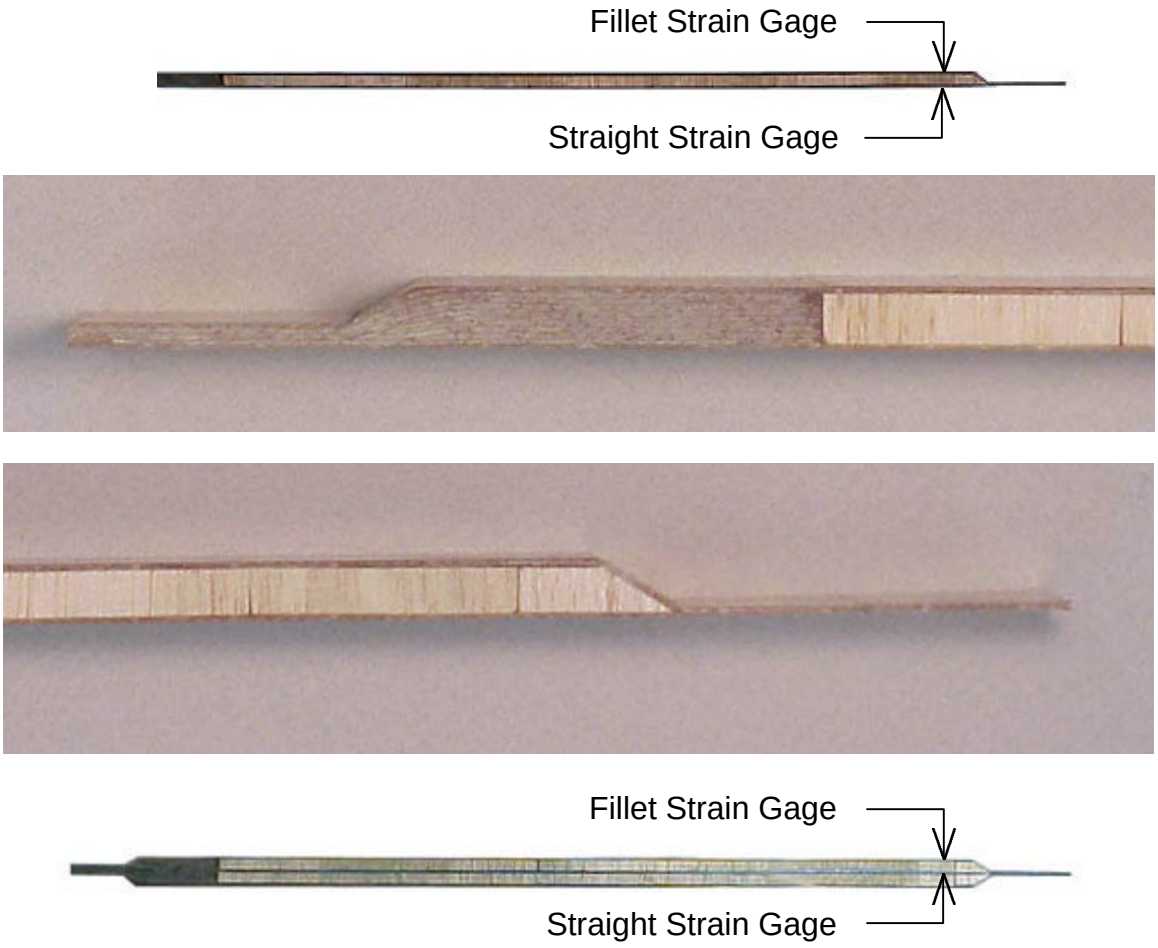

Figure 3.15 Fillet Normal specimen, close-up of solid core tapered for gripping, close-up of sandwich transition, and two parts secondary bonded together to form one symmetric specimen.

Normal' for its use of the typical Baltek termination fillet strip. Strain gages were used to record strain on each surface of the sandwich panel.

The strain gages were located 35 mm from the thin laminate as shown in Figure 5.15. The point at which the thin laminate ends and the core begins is taken as zero coordinate throughout this project. The 35 mm distance was determined after some preliminary finite element runs that indicated no local

spikes in the strain field at that point. For symmetric tests, strain gages were mounted on both sides of one part, then the parts were bonded back to back with the leads protruding out of the bond. The strain gages were protected with tape to avoid direct Hysol to strain gage contact. This created an embedded strain gage that could give strain readings for the straight facesheet in the center of the specimen. The extensometer was used on every test to provide more data from each test. Actuator displacement and load were recorded during each test as well.

An additional Fillet Normal test was performed using asymmetric specimens cut to 25 mm wide, half the width of all other fillet tests. This was to ensure that there was no reduction in strength due to edge effects introduced by narrow (50 mm wide) specimens.

Fillet Modifications

The Fillet Normal tests provided surprising results that stirred interest in developing a stronger fillet design. First, a stronger material was investigated for the fillet area to increase initial shear transfer. A laminate made of 9 DB400 fabric layers was used for the fillet region in place of the Baltek fillet strip. The fillet laminate was prefabricated and cut using the diamond saw to the same thickness and bevel as the Baltek fillet. A nominal length of 25 mm was chosen because it was close to the Baltek fillet length of 29 mm.

The same techniques were used to manufacture these parts as the Fillet Normal parts except that a rigid fillet was inserted in place of the balsa fillet strip.

These specimens were identified as ‘Fillet Rigid,’ for parts containing a rigid fillet. A detail at the fillet end is shown in Figure 3.16. These were tested in the same manner as the Fillet Normal specimens.

Figure 3.16 Detail of Fillet Rigid showing solid DB400 laminate fillet.

Next, effects of the fillet geometry were investigated using different fillet angles. Fillet angles of 20 degrees and 10 degrees were studied first, termed ‘Fillet 20 degree’ and ‘Fillet 10 degree’. Later another geometry was added which included a 5 degree fillet termed ‘Fillet 5 degree.’ All of these specimens were manufactured in a similar manner as described in the fabrication section.

The fillet strips were not available commercially for any angle other than 30 degrees. A manufacturing method was developed. A table saw worked best to cut the fillets to the different angles. A strip of Contourkore was temporarily bonded to a 100 mm by 100 mm wooden member using spray contact adhesive to attach the scrim side of the core. The blade in the saw was oriented to the appropriate angle off of vertical and the assembly was cut, ripping the balsa core to the correct angle. Due to the size of the blade, the 5 degree fillet had to be cut

from both, the top and bottom. All fillets produced in this manner were of good quality. The various fillets can be seen in Figure 3.17.

Figure 3.17 Balsa fillet strips for various tests—5 degree, 10 degree, 20 degree, and Baltek 30 degree.

The Fillet Normal mold was redesigned to accommodate the different angles. To reduce the cost of the fillet section of the mold, strips of G-10 were cut to precisely the right dimensions and used to build up a piece of “barstock” beveled to the appropriate angles. The 10 and 20 degree “barstocks” had their leading edge beveled to a point at the corresponding angle. This was simple for the 20 degree part, but rather difficult for the shallow bevel of 10 degrees. The beveled edges were taped to a flat aluminum plate using tape.

The leading edge of the 5 degree mold could not be beveled to a point. Instead, the 5 degree “barstock” tip was left at the full G-10 thickness, and was

butted-up and taped to a piece of G-10 creating a seamless mold. As before, the 6mm aluminum was used at the solid end. Each “barstock” is displayed in Figure 3.18.

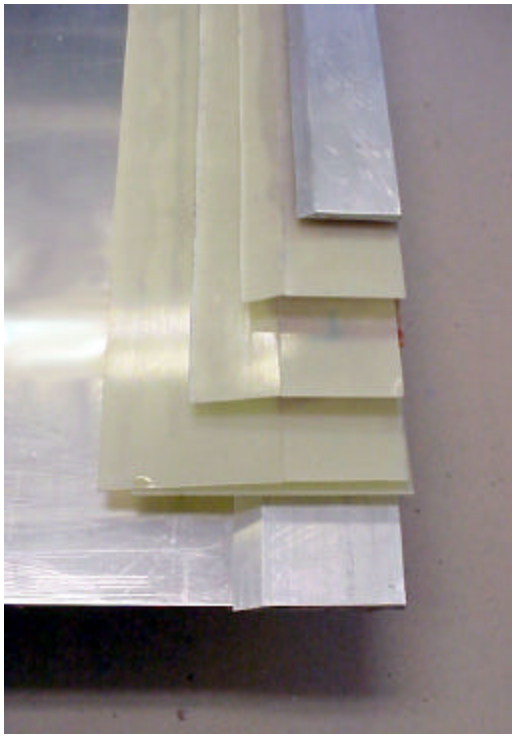

Figure 3.18 Sections used for mold—30 degree for solid core taper (6 mm aluminum), 20 degree, 10 degree, 5 degree, and aluminum 30 degree with sheet aluminum for fillet molds.

Modified Fillet Fabrication and Testing

All of the test panels were laid up using the modified hand layup process described earlier. Type 31300 fabric was used as before in the solid core region. A photograph of each of these specimens is given in Figure 3.19.

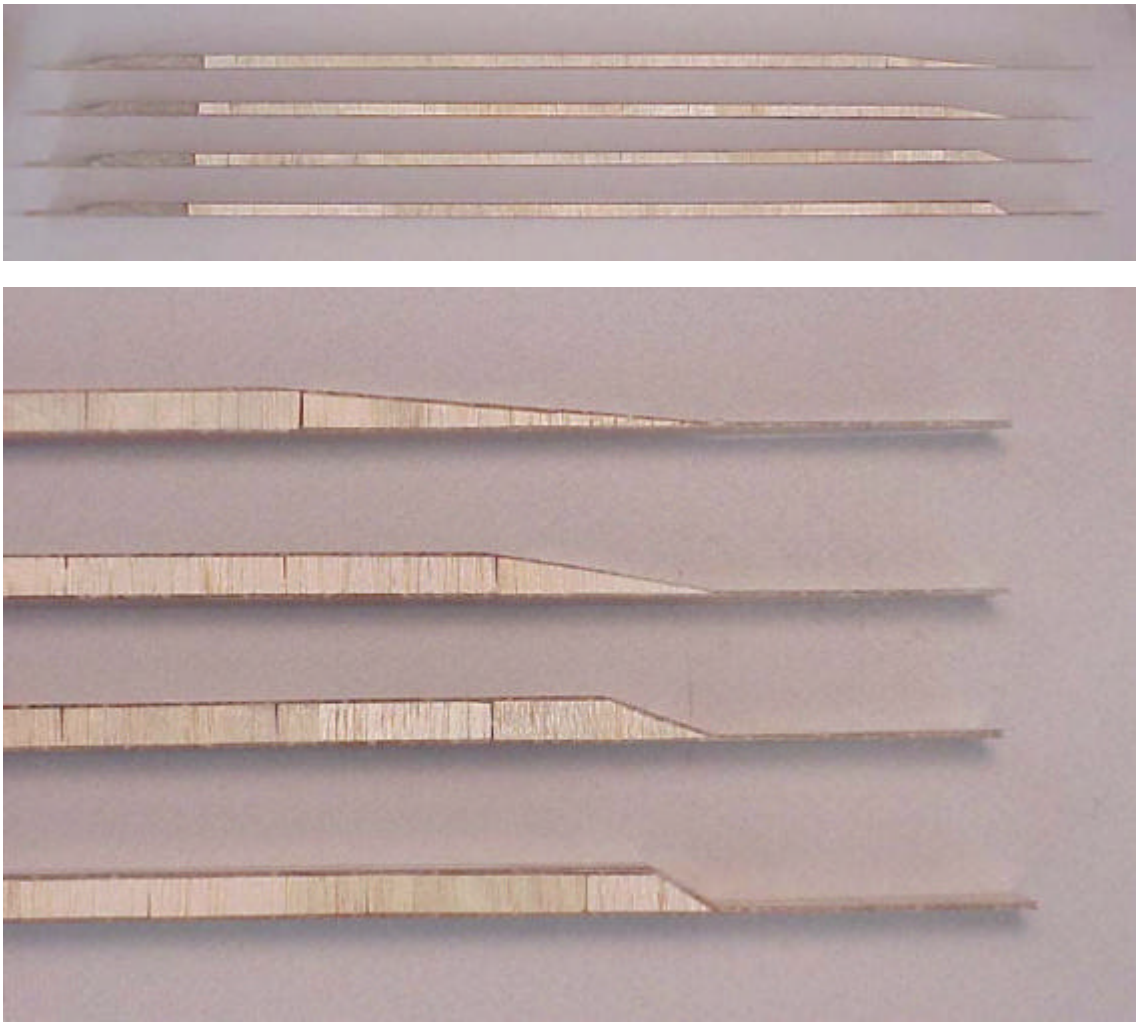

Figure 3.19 Fillet samples—full specimen with terminations of 5 degree, 10 degree, 20 degree and 30 degree, close-up of sandwich transition end for each specimen (same order).

Test procedures were the same as for the Fillet Normal tests except for the position of the strain gages, which changed slightly for each specimen. The 10 and 20 degree tests were run without problems, but difficulty was encountered with the Fillet 5 tests at the end opposite of the fillet. Prior to testing the Fillet 5

specimens, tabs were added as in the Sandwich Panel tests to ensure adequate strength at the balsa to solid core transition. The tabs did not provide enough reinforcement and the specimen failed at the balsa to solid core laminate transition before the fillet was damaged at all due to the high strength of the 5 degree fillet.

This prompted the use of longer tabs with more compliance and the ends tapered to reduce the abrupt change in modulus. This was once again unsuccessful. Finally, the coupons were tabbed at the balsa to solid core transition using the same tabs as the sandwich panel tests, and a section including the fillet was reduced in width from 50 mm to a width of 35 mm. The reduction in width was done as shown in Figure 3.20, by routering a 280 mm radius dogbone shape away from the fillet. These tests were satisfactory in that failure occurred at the fillet end before occurring at the solid core end, but failure at the farfield end was not far behind failure at the fillet. During all of the tests, the fillet failed first, but did not always delaminate prior to fiber failure.

Figure 3.20 Front view of Fillet 5 degree specimen showing reduction in width.

Experiments with Sandwich Termination into a Thick Laminate

Previous sections have considered sandwich panel terminations into thin laminate. However, another situation in wind turbine design could be to start the balsa core at an area composed of a thick laminate near the root. This was illustrated earlier (Figure 2.5) as a transverse termination into the spar, but this termination could be longitudinal as well. In some blade areas, the balsa may be unnecessary for buckling purposes, but the continuation of the balsa to the thicker root section might reduce the required knockdown factor. This would keep both facesheets straight, so load could be transferred easily. However, this case also produces a material discontinuity at the end of the balsa core.

The first test designed to explore the termination was done with 90 degree termination of the balsa. These specimens were termed ‘Sandwich Termination’ specimens. Other tests were balsa terminated with a 10 degree and 5 degree taper named ‘Sandwich 10’ and ‘Sandwich 5’ respectively. All of the specimens were made symmetric about the center of the gage section. This allowed the specimen to break at either end and still be a valid test. The problem of shear transfer is reduced or even eliminated compared to other tests because each facesheet remains planar and carries nearly the same load. A photo of each of these terminations is shown in Figure 3.21.

The specimens used 9 layers of DB400 fabric as the solid core and the facesheets were kept continuous over the entire length of the part. DB400 was chosen because it is relatively thick, requiring less layers, yet it still has

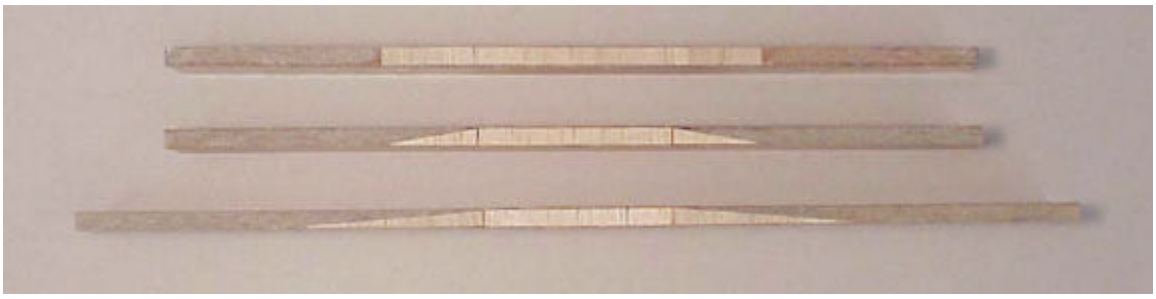

Figure 3.21 Thick termination specimens—90 degree, 10 degree, and 5 degree.

characteristics of blade fabrics, unlike the Type 31300 fabric. The 90 degree termination used a Contourkore core 200 mm long. The 10 and 5 degree tapers were cut from Contourkore as described earlier. The Sandwich 10 and Sandwich 5 specimens had a 100 mm length of constant thickness core. The end of each layer of DB400 was evenly staggered in the angled terminations to reduce resin rich regions as much as possible. All of these parts have some unavoidable areas of pure resin. As with many other parts, a modified hand layup method was used for manufacturing, but spacers were used at each clamp to keep the thick laminate from compressing.

Instrumentation was carried out with strain gages and the extensometer, both at the center of the gage section. The extensometer was used primarily as a backup just as in most other tests. Only one strain gage was used on the 90 degree tests due to symmetry, while two were used on the 10 and 5 degree tests. This was done to capture any differences in the facesheet strains.

Fatigue Specimens and Test Procedure

Facesheet, sandwich panel without fillets, and 30 degree sandwich panel transition to thin laminate specimen were tested in fatigue. The dogboned facesheet and sandwich panel specimen used for the fatigue tests were the same as the specimens decribed for the static tests. Unfortunately, the 30 degree fillet fatigue tests could not be performed on the specimen used for static tests because the specimens were too long for fatigue testing at reasonable frequencies (too much actuator movement required).

To run fillet tests in fatigue, a shorter specimen was developed for the 30 degree Fillet Normal case, termed 'Fillet Fatigue,' with a gage length of 222 mm, on the order of the lengths of the sandwich panel and the single fillet specimens. A photograph of this specimen is shown in Figure 3.22.

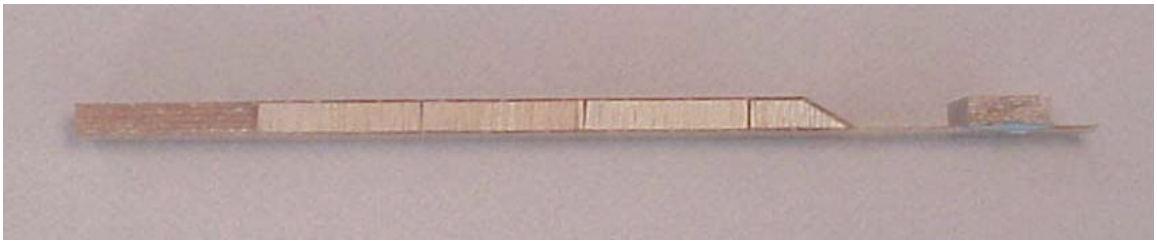

Figure 3.22 Fillet Fatigue specimen with spacer secondary bonded to make loading parallel to facesheets.

To ensure that the specimen would be representative of the Fillet Normal tests, static tests were performed. All testing procedures were the same as described earlier except the gage length, which was reduced to match the fatigue

specimen dimensions. Only the asymmetric tests were performed in fatigue. Three tests were performed at each load level, with four different load levels corresponding to different percentages of the average static ultimate strength.

All of the fatigue tests were performed with the MTS 880 with Instron electronics at speeds near the machine capacity of around 3 to 4 hertz using a sine waveform in load control, at an R ratio (minimum load/maximum load) of 0.1. This speed did not produce any measurable hysteritic heating and was only limited by the speed of the actuator. Tests were run to the range of one million cycles, which allowed test durations to range from less than a minute to as long as 8 days.

The facesheet and sandwich panel tests were simply cycled until fiber failure, and the number of cycles was recorded. The Fillet Fatigue tests were cycled under close supervision to see the number of cycles when delamination was initiated, when delamination reached across the width of the specimen, and when delamination reached the grip. The thin laminate end of the Fillet Fatigue specimen was 35 mm long, and would delaminate completely (to the grip); the number of cycles was recorded when any part of the delamination reached the grip. The number of cycles when the delamination hit the grip can be used as an inspection allowable because a delamination 35 mm long should be easily seen during inspection (in unpainted parts).

Overall Test Matrix

A test matrix including all tests performed is given in Table 4.1. Three asymmetric specimens as well as three back to back symmetric specimens were tested for each fillet geometry. Three specimens were tested in all other tests as well.

Table 3.1 Experimental test matrix

Test Description	**Test**	**Motivation**	**Geometry**
Balsa Extensional BE1	Balsa extensional modulus	Obtain an extensional modulus and strength for use in finite element models	50x50x9mm balsa specimen with aluminum tabs glued to end and loaded with u-joints
Balsa Extensional BE2			Two 25x50x9mm balsa specimen with aluminum tabs bonded to end and loaded with u-joints (to check the influence of Poisson effects).
Balsa Shear BS	Balsa Shear Test (ASTM C-273)	Obtain shear modulus and strength of balsa	Aluminum facesheets 9.5mm thick were bonded to 100 mm by 300 mm balsa specimen with fixture manufactured for ASTM C-273
Sandwich Flexural SF	Sandwich Flexural Modulus (ASTM C-393)	Determine overall bending stiffness to compare to finite element model	Three-point bend test with 238 mm span using sandwich panel specimen
Facesheet Control FC1	Facesheet Control	Strength of both facesheets without balsa	Rectangular gage section of top and bottom facesheets manufactured as one laminate; gage length 74 mm
Facesheet Control FC2			Dogbone specimen of top and bottom facesheets manufactured as one laminate; gage length 127 mm
Sandwich Panel SP	Sandwich Panel control test	Nominal strength of balsa sandwich panel	Dogbone specimen with solid grip section incorporated at time of fabrication; gage length 151 mm

Test Description	Test	Motivation	Geometry
Fillet Hand-Layup (30 Degree) FH	Fillet test with two fillets—hand-layup	Preliminary test to establish reduction In strength due to presence of fillet using hand-layup similar to blade manufacture process.	Picked double fillet to reduce details associated with asymmetry. Some specimens were bonded back to back (60 mm core length).
Fillet Mold (30 Degree) FM	Fillet test with two fillets—sheet-metal mold	Establish reduction in strength with parts of reproducible quality	Double fillet to reduce details associated with asymmetry. Some specimens were bonded back to back (60 mm core length).
Fillet Single (30 Degree) FS	Intermediate length single fillet test-sheet metal mold	Eliminate the interaction between the fillets on each end	To study farfield features and show shear load transfer of balsa (155 mm core length)
Fillet Long (30 Degree) FL	Long single fillet test—sheet-metal mold	Increase length of shear transfer in core	Test has more farfield features and shows more shear load transfer of balsa better(767 mm core length)
Fillet Normal (30 Degree) FN	Long Single Fillet Test--Final mold	Good quality parts to investigate Baltek fillet strip effects	Core length of 639 with 30 degree fillet transition to thin laminate-Asymmetric and back to back symmetric tests
Fillet Normal Narrow (30 Degree) FNN	Long Single Fillet Test--Final mold	See if edge effects influence results of Fillet Normal test	Core length of 639 with 30 degree fillet transition to thin laminate; 25 mm wide (half the width of Fillet Normal)- Asymmetric and back to back symmetric tests
Fillet Rigid (30 Degree) FR	Long single rigid fillet (±45 laminate) test--Final mold	Check increased shear transfer of rigid(±45 laminate) fillet to balance facesheet loads sooner	Used Fillet Normal geom. with a solid(±45 laminate) fillet substituted for the balsa fillet Asymmetric and back to back symmetric tests
Fillet 20 Degree F20	Long single 20 degree fillet test--Final mold	Find effect of 20 degree balsa fillet termination	Core length of 632 with 20 degree fillet transition to thin laminate-Asymmetric and back to back symmetric tests
Fillet 10 Degree F10	Long single 10 degree fillet test--Final mold	Find effect of 10 degree balsa fillet termination	Core length of 632 with 10 degree fillet transition to thin laminate-Asymmetric and back to back symmetric tests
Fillet 5 Degree F5	Long single 5 degree fillet test--Final mold	Find effect of 5 degree balsa fillet termination to see if it approches SP results	Core length of 632 with 5 degree fillet transition to thin laminate; specimen width reduced on fillet end-Asymmetric and back to back symmetric tests

Test Description	Test	Motivation	Geometry
Sandwich Termination (90 Degree) ST	Sandwich termination into thick laminate	Find effect of 90 deg. termination of sand. panel into thick laminate	Each end is a thick laminate with a perpendicular termination to a center section of 200 mm long of balsa sandwich panel-facesheets are continuous
Sandwich 10 Degree S10	Sandwich 10 degree Termination into thick laminate	Find effect of 10 deg. termination of sand. panel into thick laminate	Each end is a thick laminate with a 10 degree transition to a center section of 100 mm of sandwich panel-facesheets are continuous
Sandwich 5 Degree S5	Sandwich 5 degree termination into thick laminate	Find effect of 5 deg. termination of sand. panel into thick laminate	Each end is a thick laminate with a 5 degree transition to a center section of 100 mm of sandwich panel-facesheets are continuous
Fillet Fatigue (30 Degree) FF	Fillet Fatigue specimen--Final mold	Test specimen to compare its strength to FN specimen	Core length of 187 with 30 degree fillet transition to thin laminate-Asymmetric and back to back symmetric tests

CHAPTER 4

NUMERICAL METHODS

The major focus of this chapter is to document the methodology and details used to create finite element models used for this research. The primary purposes of these models were to understand the mechanisms of failure and to predict failure. Ultimately, the FEA models would serve as a predictive tool when designing structures containing sandwich to thin laminate transitions. Each model was constructed to match a corresponding experimental test. This allows direct validation and gives more confidence in these types of models, as well as a methodology for fillet design without experiments.

Modeling Details

All finite element modeling was performed using Ansys 5.5 and 5.6 (1999). Macros were used exclusively to construct and solve all models. A macro is a subroutine written including all of the geometry, loads, and solution information for a given model. They make it possible to run the same model several times with only a single command to start the subroutine each time. Some post-processing was included in the macros but most was done using the Graphical User Interface.

The first macro built was a model of the Fillet Normal specimen. All subsequent models were derived from this model. For each model, the entire

Fillet Normal geometry was created and then parts that did not pertain to the model at hand were deleted. This sacrificed a small amount of efficiency, but ensured that all models had the same foundation. It was also convenient because many models had the same commands, so little modification was necessary.

All modeling was done using Plane13 elements. Plane13 is a two-dimensional, Coupled-Field element. Two-dimensional elements were sufficient because there is little change along the width for any tests beyond the non-critical free edge stresses. There are three main reasons this element was chosen. The element allows two-dimensional models, which is a feature common to all models developed in this research. Plane13 allows the element coordinate system to be aligned using the edges of the element rather than local coordinate systems. Finally, the element allows for anisotropic plasticity in the model. The importance of these last two features will be discussed later. A linear element had to be used because a quadrilateral element with these features was not available.

A Fillet Normal specimen was tested to failure with the addition of a transverse strain gage. The transverse strain was -0.49 percent, which was on the same order as the longitudinal strain of 1.26 percent. A Fillet 20 degree specimen was tested in a similar manner, with transverse strain at failure of -0.87 compared to the longitudinal strain of 1.81 percent. Both of these tests showed considerable transverse, out of plane strain, so the specimens were clearly not

plane strain. Consequently, the Plane 13 element was used with the plane stress option, to match experimental investigation.

Fixed displacement was used for boundary conditions, while loading was done using nodal forces. Force loading was used rather than displacement loading because global stresses could be calculated and plotted easily. The models included only the area between the grips. To account for the moments that could be supported by the grips, the nodes at the ends of the specimen were coupled in the longitudinal direction so they could not rotate and remained planar.

Mapped meshing was done whenever possible, while free meshing was done in areas with difficult geometry. To obtain more control over the mesh, all lines in the models contained mesh seeds to force a known mesh density on all area boundaries. Near the fillet tip, weighted line divisions were used to change mesh density along a single line. All layers of fabric contained three elements through the thickness and had an aspect ratio of less than two in areas of interest. The aspect ratio was usually pushed up to three in farfield areas. As the models were being developed, some areas were split into several parts. This allowed more control on mesh density in areas of concern. All meshing was done with quadrilateral elements except for a few unavoidable triangle elements. These were at the union of the two facesheets in the fillet region. Meshing will be illustrated and discussed in more detail as each individual model is described.

Material Properties Used for Finite Element Models

Material properties were gathered from several sources to use in the models. Some properties, which were either unknown or questionable, were later found from tests as described in the Experimental Methods chapter.

Fabric properties were the most important. These were taken from the MSU Database. Properties for all three axes were not included in the database for the A130 and DB120 fabrics used in this research. To solve this dilemma, the available three dimensional properties (MSU Database) of D155 fabric were analyzed. This is a 0 degree stitched fabric supplied by Owens Corning. It has an areal weight in the same range as A130 and DB120.

Unknown properties were Poisson's ratios and mechanical properties through the thickness. Ratios were calculated between the D155 in-plane transverse properties and the out of plane properties at two different fiber contents. The two ratios were averaged and applied to the known properties of A130 and DB120 to approximate all other material properties.

A complete set of fiber properties was obtained in this manner for one fiber content. The next step was to change the properties to match fiber contents in the model. The modulus values and Poisson ratios were adjusted using approximations from Halpin and Tsai presented in the MSU Database. Ultimate strengths in the fiber direction were calculated using a direct ratio of fiber volume fractions. Other values were left the same, being matrix dominated properties. This yielded a complete set of properties for the two fabrics of interest.

The properties for the DB120 fabric are only for one 45 degree layer oriented in the 0 degree direction. These properties are difficult to use in a two-dimensional model because the fibers go out of the plane that is modeled. To solve this problem, the DB120 properties as a ±45 degree fabric were found using Laminate Analysis [Minguet(1992)]. This program uses classical lamination theory to rotate fiber coordinates into laminate coordinates. This produced a set of properties that lined up with the coordinates of the model.

Laminate Analysis was used to construct a predicted stress-strain plot of the DB120 fabric, which is displayed in Figure 4.1. It is important to note the point of matrix failure on the graph, this causes a softening in the DB120 and was modeled as an elastic-plastic behavior. The zero degree fibers will fail at strains below three percent. This allowed the use of a bilinear elastic-plastic model to

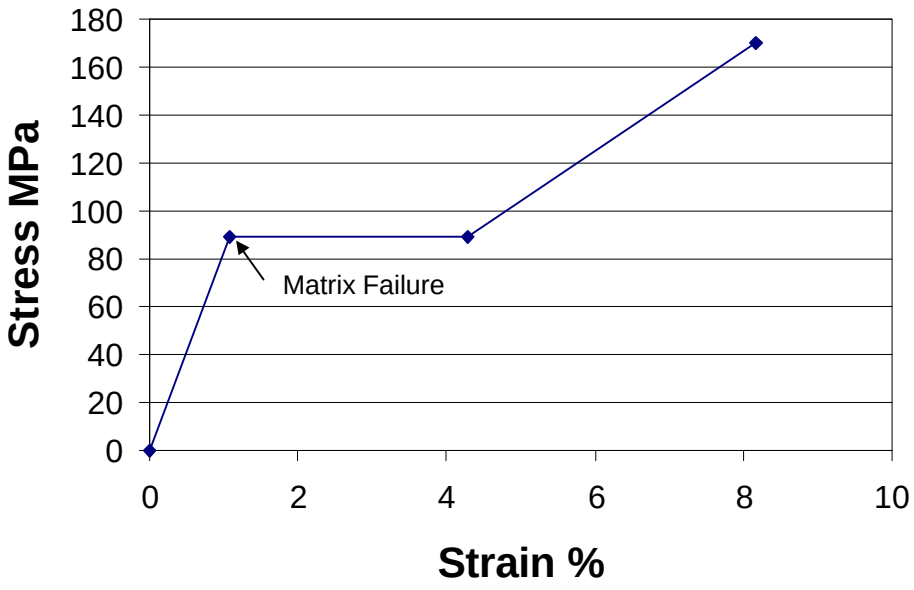

Figure 4.1 Theoretical plot of DB120 ±45 fabric found using Laminate Analysis.

represent the DB120 fabric, which is one of the primary reasons the Plane13 element was used. The element allowed yield stresses for each coordinate and a corresponding tangent modulus could be used after yielding had occurred in that direction.

The local fiber volume fractions of each layer were calculated using data and a technique developed with Scott Rossell (2000). The main hypothesis behind this is that fabric has a fixed volume of fiberglass per unit area. This volume of fiberglass per unit area can also be thought of as a relative thickness of only the glass in a layer. One can simply take the actual thickness of a layer and use the relative thickness of the fiberglass to calculate a fiber volume fraction. Rossell has shown that this technique is acceptable after being compared to data for fiber volume fractions found from matrix burnoff tests.

Each model was constructed with layers of equal thickness because it was initially thought that the thickness of A130 and DB120 in a laminate were the same. Rossell also did work on compressibility of fabrics and found that the same compressive force on DB120 and A130 will actually produce different local fiber volume fractions within each layer. Although the equal thickness assumption made modeling easier, it was later discovered that local fiber volume fractions were different in each ply.

The model was originally constructed to match a matrix burnoff test of a Facesheet Control sample with a fiber volume fraction of 0.328. The actual fiber content in the model ended up being 0.363 for the A130 layer and 0.292 for the DB120 layer. These fractions were used to calculate the correct material

properties. Using the correct fiber volume fraction in a model is critical. It would be more convenient if properties could be entered as 'force per ply,' this would take the strong dependence on fiber volume fraction introduced by 'force per area' material properties.

Resin properties were necessary because there is a small resin rich region at the tip of the balsa fillet, shown in Figure 4.2. These properties were taken from Orozco (1999). There is some uncertainty as to whether the ultimate strength of a neat resin sample reported by Orozco is representative of the small resin rich area in the fillet models.

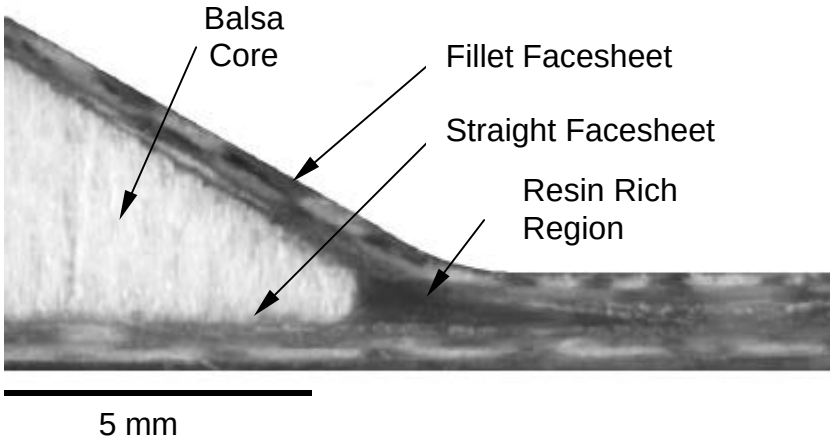

Figure 4.2 Resin rich region in Fillet Normal part.

Properties of the balsa core were difficult to establish. For initial values, Baltek, the balsa supplier, gave specifications of the balsa. These included only a few select properties. Baltek also provided a data sheet that was compiled from several references. These included all properties as a function of density,

but properties were given in coordinates of a tree, with a grain axis, a radial growth ring axis and an axis tangential to the growth ring. Contourkore is made of randomly oriented balsa sections. Therefore, these coordinates were not truly representative of Contourkore and there were inconsistencies in the data sheet supplied by Baltek as well. A photograph of Contourkore is given in Figure 3.2; notice the varying orientation of the growth rings. This creates mixed tangential and radial properties in the sheet longitudinal direction. Literature reviews also raised suspicions, as they concluded that there were large variations in reported balsa properties, as mentioned in the Background Chapter. This led to the balsa extensional and shear tests described in the experimental methods chapter.

Table 4.1 includes all materials and their respective properties used in finite element models.

Table 4.1 Material properties and failure parameters for all materials used in finite element models.

		Ultimate Strengths (MPa)					**Ultimate Strains (%)**			
*	V_f	Utl	Ucl	Utt	Uct	Shear	Utl	Ucl	Utt	Uct
A130	0.36	701	-270	34	-93	87	2.53	-0.92	0.39	-1.05
DB120	0.29	89	-170	89	-170		1.06	-2.03	1.06	-2.03
Balsa (Baltek)		13	4			3				
Resin		54		54			2.00		2.00	

Utl= Ultimate tensile stress in longitudinal direction
Utt= Ultimate tensile stress in transverse direction
Ucl= Ultimate compressive stress in longitudinal direction
Uct= Ultimate compressive stress in transverse direction
*Properties in coordinates of fabric roll, 0° for A130 and ±45° for DB120

Table 4.1 cont.

		Elastic Modulus (GPa)			Poisson Ratios			Shear Modulus (GPa)		
****	V_f	Ex	Ey	Ez	vxy	vxz	vyz**	Gxy	Gxz	Gyz
A130	0.36	29.96	7.10	7.43	0.35	0.33	0.44	2.43	2.86	1.65
DB120	0.29	8.35	5.96	8.35	0.37	0.44	0.27	1.99	5.03	5.03
DB120***	0.29	2.08	1.39	2.08	0.13	0.80	0.08	0.40	4.62	4.62
Balsa (Baltek)		0.053	2.51	0.053	0.11	0.34	0.36	0.16	0.16	0.16
Resin		3.18	3.18	3.18	0.35	0.35	0.35	1.18	1.18	1.18

**Switched vzy to vyz using $\frac{Vxy}{Ex} = \frac{Vyx}{Ey}$

***found using Laminate Analysis after matrix cracked

****Properties in coordinates of finite element models

Fillet Normal Model

This was an important macro because all other models were mere modifications. The macro was parametric in some areas in order to allow changes to be made quickly and efficiently. The geometry of the fillet area was not done parametrically. The fillet area contained curves, local coordinates, and an angle section, which would have made parametric construction difficult. Figure 4.3 contains a local view of the Fillet Normal model at the transition region as well as an actual part that the model is representing. This figure shows all areas used to create the geometry. Each material type is a different shade in the model.

In order to represent the geometry as accurately as possible a CAD drawing was used with dimensions at each line end. These dimensions were used to define keypoint coordinates from which the model would be generated.

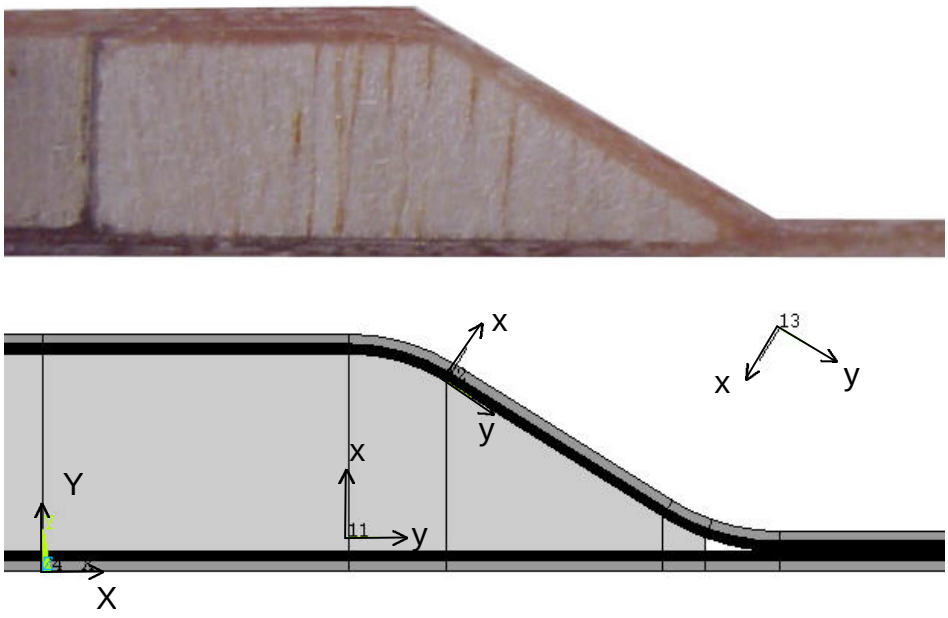

Figure 4.3 Close-up photograph of Fillet Normal specimen; Close-up of Fillet Normal model with areas outlined, material properties shaded, and local and global coordinate systems shown.

As the geometry was created, each area was made without common boundaries. By creating areas without common sides, elements along boundaries were created with different nodes. This required all nodes to be merged before the model was solved, but allowed discrete damage to be included in the model along any area boundary quickly and easily.

The difficulty in modeling this part came in the reversal of the two local polar coordinates (12 and 13) used to define the beginning and end of the taper. If these local coordinates were used to define element coordinates, the positive direction of the coordinate would be reversed in moving from one radius to the next. This was overcome by using a feature in Plane13, which aligns the

element coordinate system with the element boundaries, namely, the first two boundaries of the element. When elements are created, they align the first two sides with the first two sides of the area with which they are associated. Special attention was required when creating the areas to ensure that all element coordinate systems would be continuous along a ply.

Coordinates of elements not included in the upper or fillet facesheet were simply defined using global coordinates. This was adequate for all other parts of the model because the material coordinates did not stray from the global coordinates. This was also necessary because in the areas that were free meshed, the first two element boundaries were not always orthogonal and would have created discontinuous material properties.

Attempts were made to systematically reduce mesh density away from the filet region. This was important because the aspect ratio of the ply thickness to the model length was very large. As mentioned earlier, the mesh in each ply contained three elements through the thickness. This was reduced to one or two elements through the thickness, but large jumps in the strain field resulted, probably due to the fact that the elements were linear and several triangle elements had to be used to reduce the mesh density. Consequently, in the final model, mesh density through the thickness of the fabric was not changed along the length.

Conversely, the mesh density was changed to a degree in the balsa core without noticeable effects. This allowed a small reduction in the number of elements but even the size of the balsa elements was constrained by aspect ratio

problems associated with such a small ply thickness. Figure 4.4 contains a plot of the Fillet Normal mesh in the region where mesh density is changed.

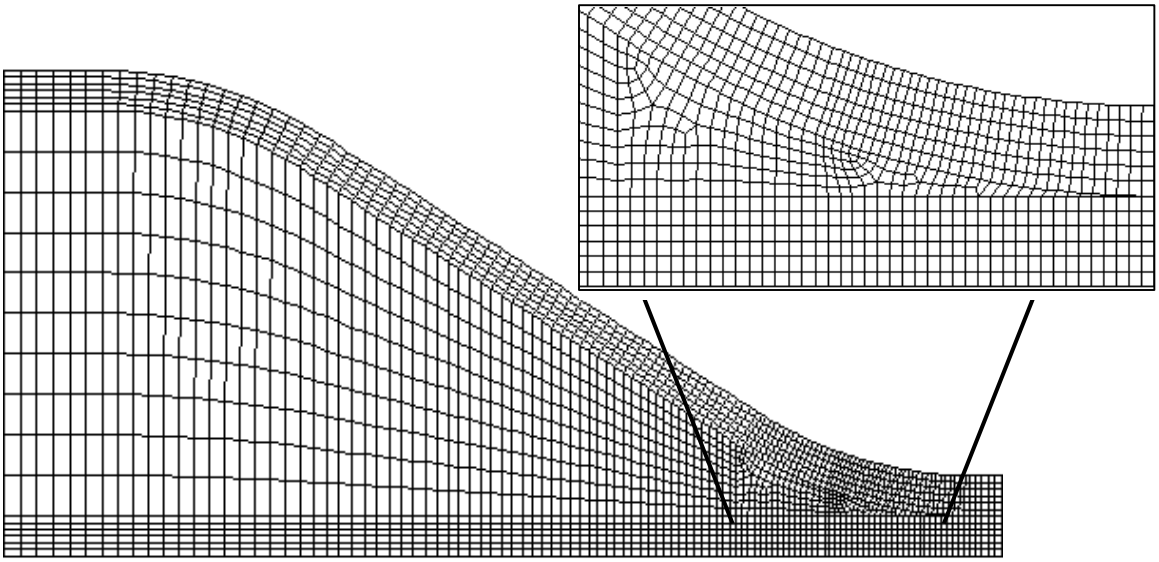

Figure 4.4 Mesh of Fillet Normal model; Detail of fillet region.

The Fillet Normal specimen was only modeled in the region between the grips as mentioned previously. The farfield sandwich core end was fixed using displacement constraints in the longitudinal and transverse directions. This constrained rotation, which was also constrained in the experiment by the grips. All nodes in the thin end were constrained in the transverse direction and coupled in the longitudinal direction. These nodes were counted and a force was divided and distributed to each node.

The load was applied using a ramp function to a value slightly above experimental failure. This was done using the auto time-stepping function in

Ansys (5.6). Initial, maximum, and minimum time steps were input and subsequent step sizes were automatically determined. This resulted in less than ten load sub-steps even with elastic plastic material behavior in place.

The nonlinear geometry option was used during the solution of the model due to the out of plane bending caused by the eccentric loading. Several components were formed to allow post-processing to be done more efficiently. Most components simply contained all elements from one material type. Finally, output was created to compare the model to the experiment. A stress-strain plot was constructed for the nodes corresponding to the strain gage locations during the experiment. This provided a direct means of comparison between experimental and numerical results.

Other Models Containing Sandwich To Thin Laminate Transition

The following is a brief description of each model and the associated experiment. These will not be discussed in as much detail because they were similar to the Fillet Normal model in several ways.

A macro was written for the Fillet Rigid experiment. This was a simple model to develop because the specimen still had the 30 degree taper, so much of the geometry was the same. Differences were in the length and material property of the fillet strip. To ease modeling, the fillet strip was modeled with the same properties as the DB120 fabric. The fillet was actually made from DB400, another $\pm$45 degree fabric. It was decided that the properties of the DB120 fabric would be very similar to those of the DB400 fabric, and that fiber properties in

this region were not going to dominate the results of the model. A close-up of the model areas including different material properties is shown in Figure 4.5.

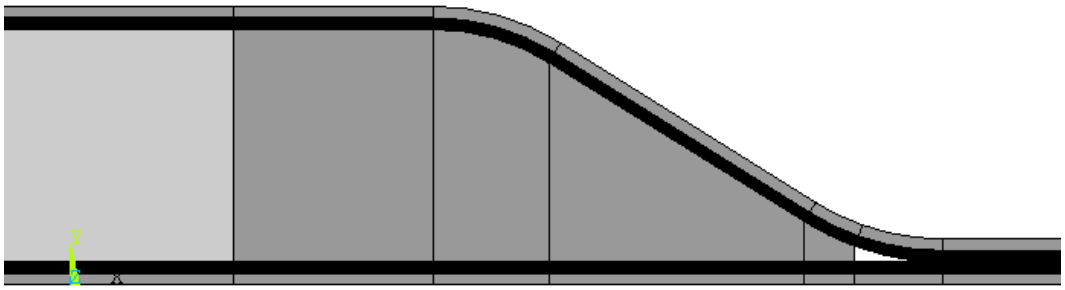

Figure 4.5 Fillet Rigid model close-up with dissimilar materials having different shades.

The model contained the same boundary and loading conditions and mesh as the Fillet Normal test. Again nodes were selected at the strain gage locations and stress-strain plots were constructed to compare to the experimental results.

Next, was the Fillet 20 model containing the 20 degree balsa fillet. Due to the different fillet angle, the geometry was redrawn in a CAD program and the new keypoint locations entered in the fillet area. Even with the changes in geometry, there was still a lot of the Fillet Normal macro used. A few details of meshing were changed to get good aspect ratios and as few triangle elements as possible. This included the use of weighted line divisions to improve mesh quality. A local view of the mesh is shown in Figure 4.6. Mesh not included in the local view is continued with the same density. All of the same boundary and

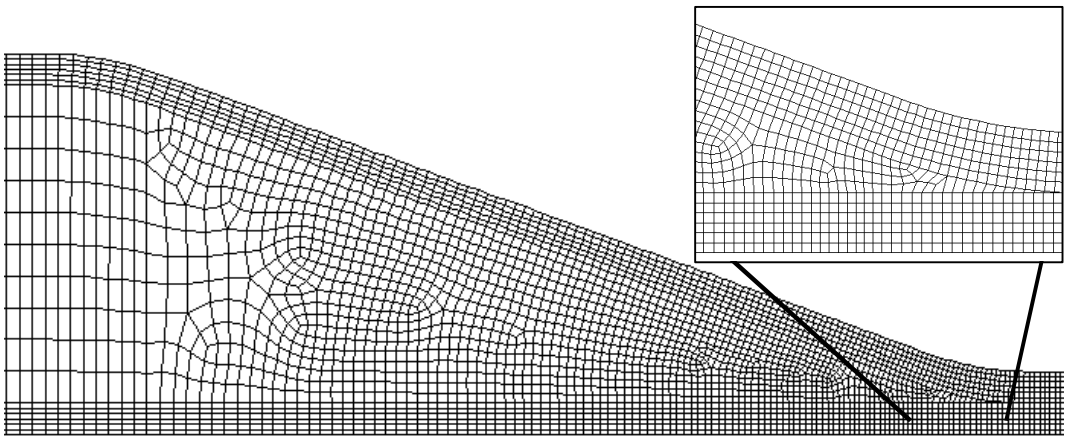

Figure 4.6 Close-up of Fillet 20 model including detail region at fillet.

loading conditions were used once again. Stress-strain plots were drawn just as before for comparison with experimental data.

The Fillet 10 model with the 10 degree transition was done next. This was done just as the Fillet 20 model, by redrawing the specimen and correcting the keypoints in the region of the fillet. A detail of the mesh in the fillet region is displayed in Figure 4.7. This model provided a greater challenge when it came to meshing because of the long fillet region. This was handled easier by using the weighted line division in Ansys where divisions of a line for mesh seeds can be smaller on one end than the other. All loading and boundary conditions were done the same way. Similarly, the stress-strain plot was compared to the Fillet 10 experiment.

A model was then designed for the Fillet 5 degree specimen. This was done in the same manner as the other fillet models. Just as with other models,

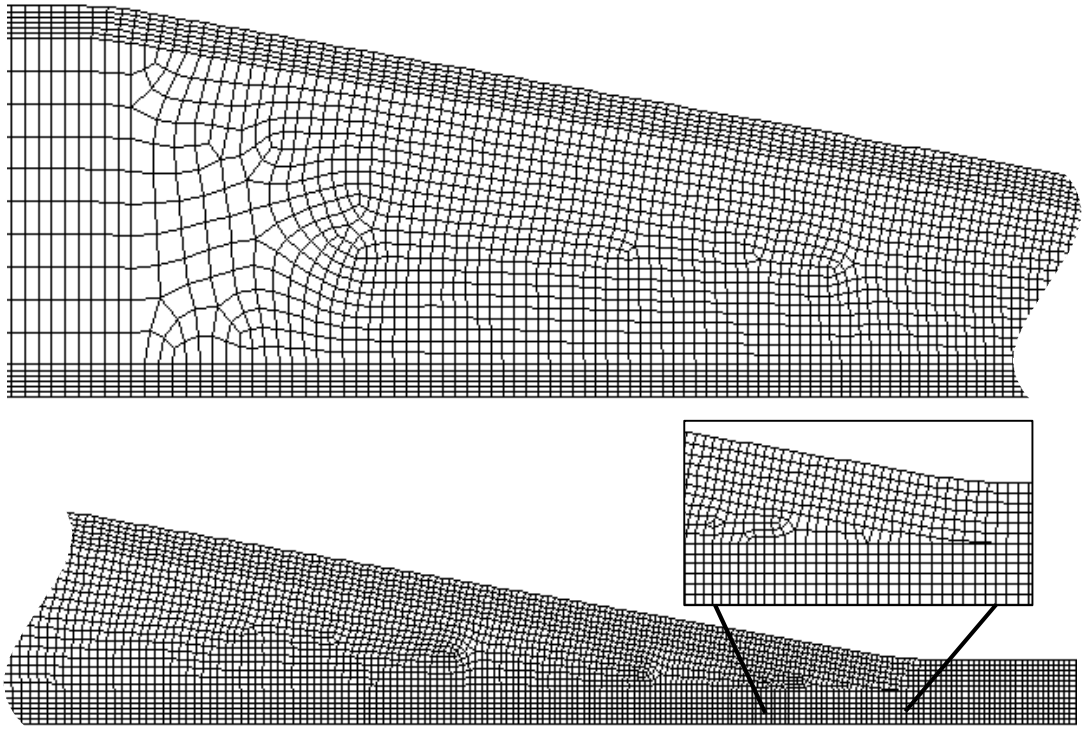

Figure 4.7 Close-up of Fillet 10 mesh with detail of fillet region.

the Fillet B model contained the resin rich region, sized by looking at several experimental specimens. The mesh in the fillet region can be seen in Figure 4.8. The resin region can be recognized in the detail inset because it is the only section that is free meshed rather than using the mapped mesh option. The length of the model was not as easily matched to the experiment. This is because the specimen had a tapered width. Models with the entire balsa length and the length of the constant width section were solved. Output included stress strain curves for comparison to the experimental tests.

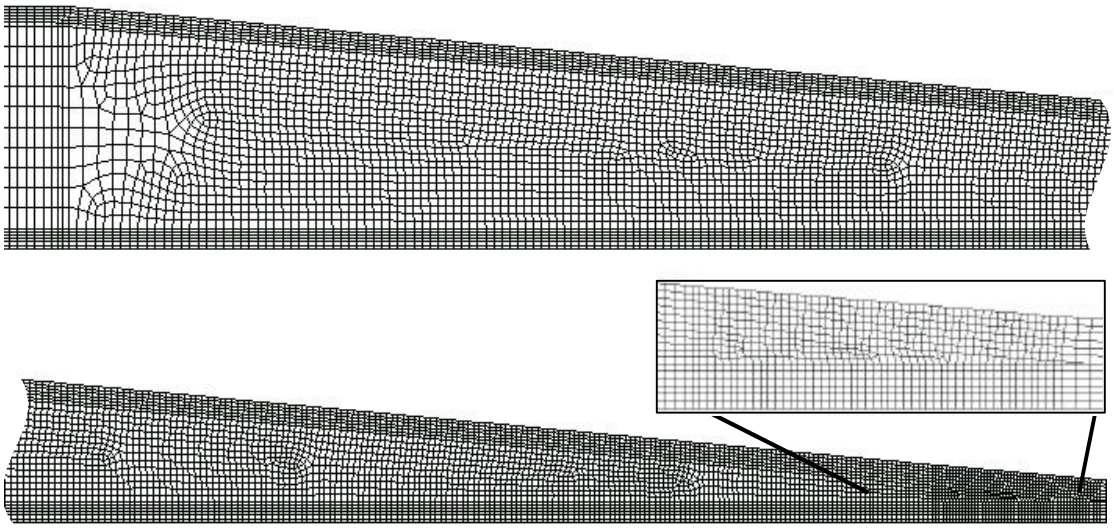

Figure 4.8 Local Fillet 5 mesh including a detail of the fillet region.

Models of Simple Geometry for Material Property Validation

Three models were made to check the material properties on simple geometry. These models were built using the Facesheet Control, Sandwich Panel, and Sandwich Flexural experiment specimens.

The Facesheet Control model was built using the macro developed for the Fillet Normal test. This ensured that there were no gross differences in how the models were created, as mentioned earlier in the chapter. The entire Fillet Normal geometry was built in the macro and then all the areas were deleted except the areas corresponding to the thin laminate section. The length of the model was matched to the Facesheet Control by changing one parametric variable.

Displacement boundary conditions of zero (in the longitudinal and transverse direction) were used on the left end of the sample to model the grips. The left end of the sample had a force load distributed over a coupled plane of nodes. As before, the coupling prevented any rotation and ensured that the nodes at the edge of the grips stayed planar. Only the rectangle specimen could be modeled because of the limitation of two-dimensional elements, which requires all elements to have a constant depth. The local effects of the grips were ignored in evaluating the solution because the stress concentrations that the grips imposed during experimental testing were taken care of by the tabs. A stress-strain plot of a node at the center of the model was compared to the experimental results.

The Sandwich Panel model was constructed in a manner similar to that of the Facesheet Control model. The Fillet Normal geometry was created and all but the Sandwich section was deleted. The model was reduced to the length of the experimental specimen and meshed using mapped meshing. The model was once again limited to a rectangle since it was two-dimensional. Again, the grip effects were ignored because the gripped area was wider in the experiments, so stress concentrations at the grips could be easily mitigated. Stress-strain information was used to compare the numerical and experimental models.

The final model was the Sandwich Flexural model. This was similar to the Sandwich Panel model in its geometry and meshing. The areas and boundary conditions for the Sandwich Flexural model is shown in Figure 4.9. The boundary conditions were modeled by fixing a node at one support in both the

vertical and horizontal directions while the other support was fixed in only the vertical direction. The load was applied to the top facesheet by selecting nodes included in a 10 mm loading width, and evenly distributing the total load over these nodes. Unlike other tests, this experiment did not use strain gages for instrumentation. Instead, a load versus displacement plot was generated to compare to the experimental output.

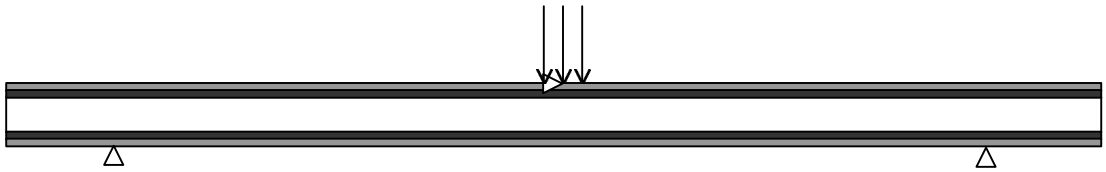

Figure 4.9 Areas and boundary conditions of Sandwich Flexural model.

Overall Numerical Model Matrix

All of these models were used as a direct comparison of experimental results to finite element models. This was to establish higher confidence in finite element modeling for the designer in the Fillet series models. The other models were used as tools to verify material properties and validate general material behavior in a model as compared to an experiment. A matrix of all numerical models is included as Table 4.2.

Table 4.2 Numerical model matrix.

Model Name	Experimental Test modeled	Motivation	Explanation Of Geometry
Facesheet Control FC1	Facesheet Control	Validate the strength and modulus of pure facesheet without balsa present.	Rectangular specimen was modeled to allow the use of plane stress, which was verified experimentally.
Sandwich Panel SP	Sandwich Panel control test	Validate modulus of sandwich panel and predict tensile failure.	Rectangular specimen was modeled (although specimen was dogboned) to allow the use of plane stress.
Sandwich Flexural SF	Sandwich Flexural Modulus (ASTM C-393)	Validate overall bending stiffness using a load displacement curve.	Test was modeled with same geometry excluding thickness. The thickness of each specimen varied 1 mm, so the model was constructed with an average thickness.
Fillet Normal (30 Degree) FN	Long single fillet test--Final mold	Validate strain field, strain just after fillet in balsa section, and predict delamination failure. Also predict final failure stress.	Geometry was modeled asymmetrically to validate FN1XX test. Thickness measurements were taken from a few specimens, averaged, and used for all models.
Fillet Rigid (30 Degree) FR	Long single rigid fillet(±45 laminate) test--Final mold	Validate strain field, strain just after fillet in balsa section, and predict delamination failure. Also predict final failure stress even though delamination will not be modeled.	Geometry was modeled after asymmetric experimental specimen.
Fillet 20 Degree F20	Long single 20 degree fillet test--Final mold	Validate strain field, strain just after fillet in balsa section, and predict delamination failure. Also predict final failure stress even though delamination will not be modeled	Geometry was modeled after asymmetric experimental specimen.
Fillet 10 Degree F10	Long single 10 degree fillet test--Final mold	Validate strain field, strain just after fillet in balsa section, and predict delamination failure. Also predict final failure stress even though delamination will not be modeled	Geometry was modeled after asymmetric experimental specimen.
Fillet 5 Degree F5	Long single 5 degree fillet test--Final mold	Validate strain field, strain just after fillet in balsa section, and predict delamination failure. Also predict final failure stress even though delamination will not be modeled	Geometry was modeled after asymmetric experimental specimen.

CHAPTER 5

EXPERIMENTAL RESULTS

Several tests were performed throughout the course of this research. The following will explain the results of these tests, which were useful in understanding the sandwich panel to laminate transition. The tests are divided into sub-categories; tests will be compared within and between each category.

Experiments to Establish Material Properties

Material property experiments were performed to establish more confidence or to narrow the range of material properties presented in the literature.

Balsa Extensional Modulus Experiment

The extensional modulus test specimens were weighed and their density calculated to compare to the nominal density reported by Baltek. It was expected that the density may be slightly higher because of the AL600/10 coating added to the balsa. This hypothesis was not supported by the data, which is displayed in Figure 5.1. The 100 series were one piece, while the 200 series were two pieces as described in the experimental methods section. The scrim was removed to insure that neither its weight nor thickness would affect the density results. It is surprising that there is such a large variation in the density throughout the sheet;

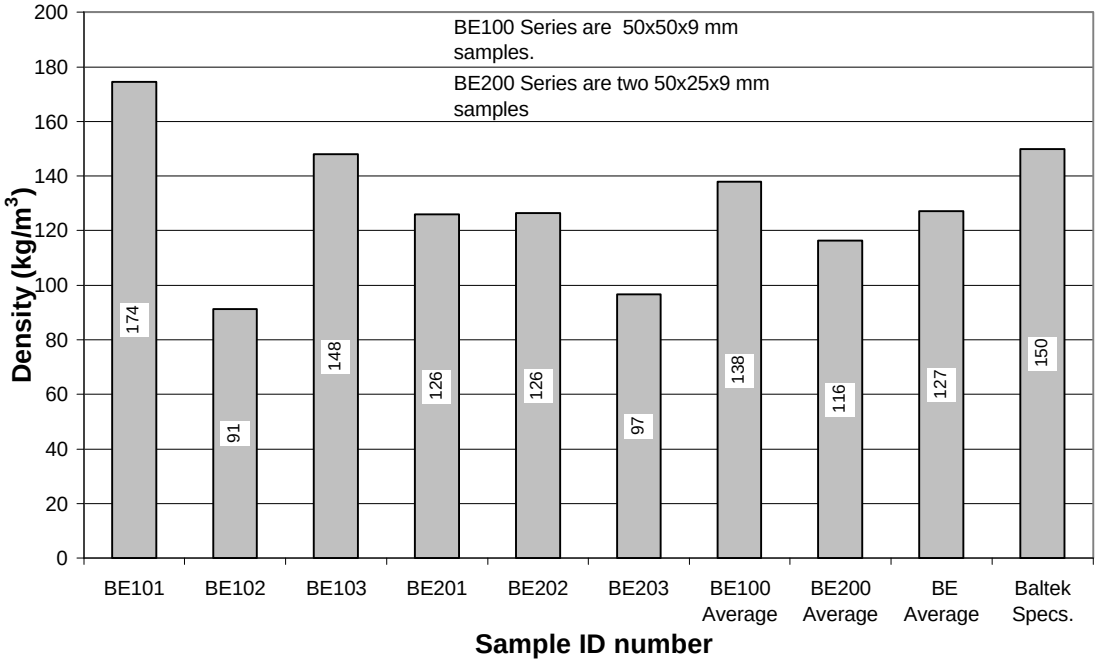

Figure 5.1 Density of Baltek ContourKore material (with scrim removed).

the minimum density was 52% of the maximum value. The average of 127 kg/m^3 is low compared to the nominal density of 150 kg/m^3 reported by Baltek. This may be due to the relatively small number of samples used; the experimental density may be closer to nominal density if a larger batch was measured.

Finally, the specimens were tested for modulus as described in the experimental methods chapter. The modulus had a large variation as did the density. This was expected though, as it was mentioned in the reference by Feichtinger, K. A. (1986). Feichtinger reported that the tensile modulus was a linear function of density. To account for this, the experimental modulus was divided by the density to see if the data looked more consistent. There is a notable drop in variation when viewing the two values in Figure 5.2. There is less

variation in the Modulus/Density values, which becomes more apparent when comparing the Coefficients of Variation (COV) in Table 5.1. It does appear that the ratio of modulus and density proposed by Feichtinger is a bit off of the current experimental values as well as other literature values.

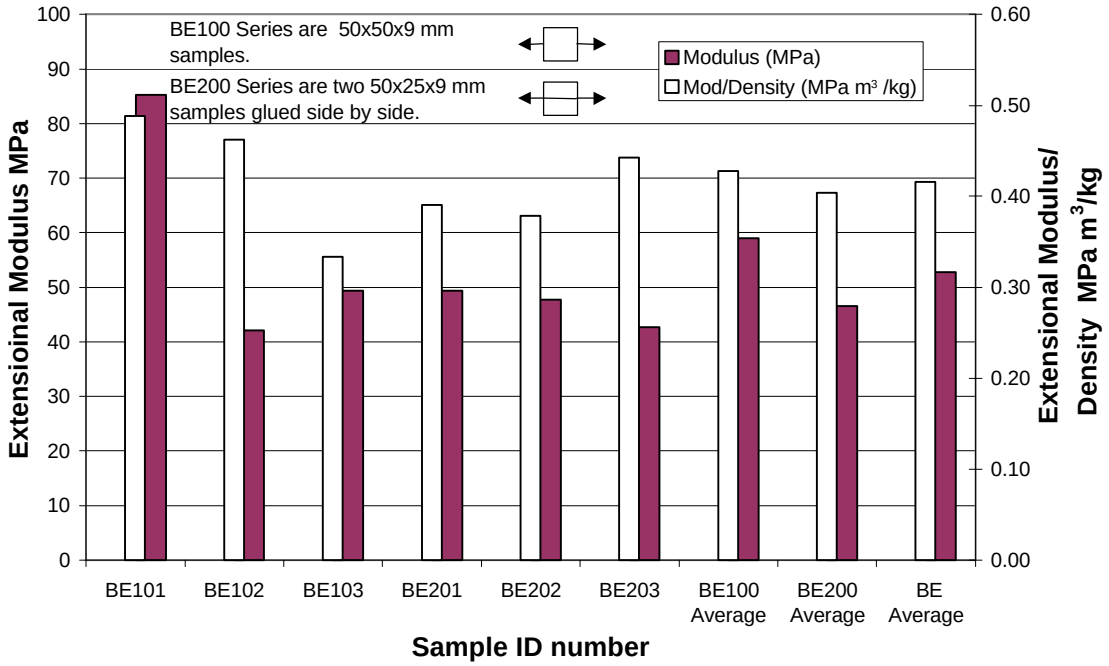

Figure 5.2 Extensional modulus of balsa perpendicular to the grain.

The values reported as Wood Handbook [Forest Products Laboratory (1987)] values were actually calculated using ratios, which were given for balsa with a specific density of .13 instead of .15, to the grain modulus. This was used as the closest approximation found and would probably not have too much bearing on the final results because they are presented as ratios rather than discrete values. The initial modulus in the grain direction was taken from Baltek which matched data from Feichtinger as a compression grain modulus. This was

scaled down by 17%, a value from Feichtinger, to get a tension modulus in the grain direction. Other moduli were found using the Wood Handbook ratios.

Table 5.1 Experimental results of balsa extensional modulus tests.

	Balsa Modulus Experiments			Supplier	Literature	
Experimental Result	Avg.	Std Dev	COV(%)	Baltek	Wood Hndbk	Feichtinger
Density (kg/m^3)	127.16	31.29	24.61	150	150	150
Modulus (MPa)	52.79	16.24	30.77	na	53-164*	1015
Mod/density (MPa m^3/kg)	0.42	0.06	14.00	na	0.35-1.09*	6.77
Strength (MPa)	0.73	0.30	41.00	na	1.0**	na
Strength/density (MPa m3/kg)	0.0056	0.0009	17.00	na	na	na

*Calculated using ratios presented in the Wood Handbook.
**From Science and Technology of Wood (density unknown) [Tsoumis, G. (1991)].

The low and high numbers given for the Wood Handbook in Table 5.1 relate to values in tangential and radial directions respectively. Presumably, these values could be averaged in order to be compared to experimental values. However, doing so would result in a larger value than the experimental values. The low experimental values may be related to the size of balsa timbers compared to part size. Kilbourn suggests that tests of small-scale specimens may have lower values, dominated by the tangential direction regardless of the specimen orientation [Kilbourn (2000)]. This explains the lower values found in the experiment, where the specimens were much smaller than a balsa timber.

Strength was also recorded during the Balsa Extensional modulus test. The data are reported in Table 5.1. As before, it appears that the static strength is a function of density after reviewing the coefficients of variation for strength and strength normalized for density. This was not an item investigated by

Feichtinger so a direct comparison cannot be made. The values were low once again, but this may be attributed to the scale of the test, just as Kilbourn stated. A photograph of the tested samples in Figure 5.3 shows the growth ring orientation and the failure plane. It is important to note that all of the growth rings are oriented at nearly 45 degrees as explained earlier.

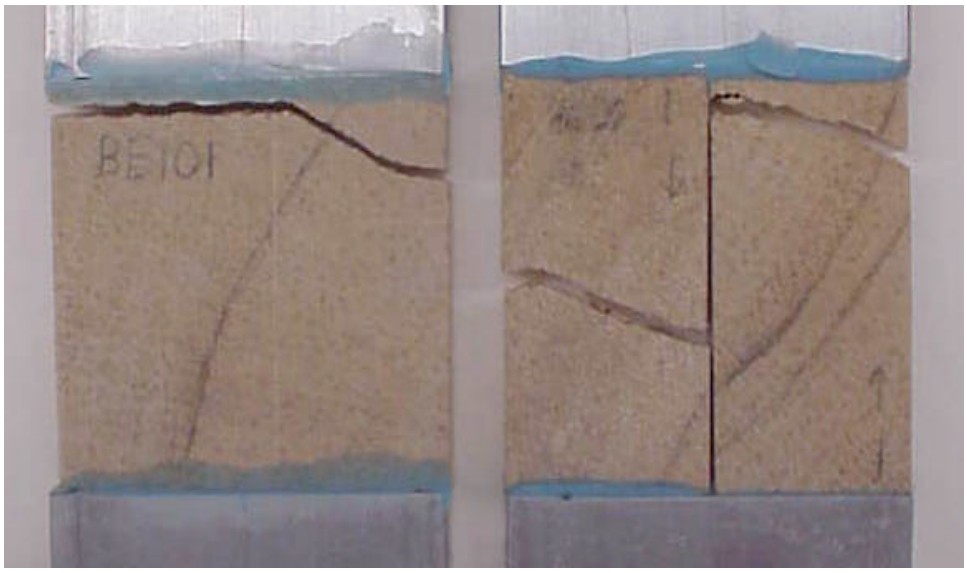

Figure 5.3 Balsa extensional modulus specimens (single, BE100 and double, BE200 specimen)

The results of this test suggested the use of a balsa extensional modulus of 53 MPa, as found in the experiment, for numerical models. Although this does not correspond to literature values exactly, it is representative of the small scale parts which were modeled. The strength value chosen for numerical purposes was 0.73 MPa, the experimental static strength.

Shear Modulus Experiment

The shear modulus was the next unknown property. Baltek reported a value, but literature suggested that tests using specimens with the same thickness as the application might be more accurate [Kilbourn (2000)]. The densities of these specimens were not recorded, so data could not be normalized relative to density. The specimens were tested and data were analyzed as described in ASTM C-273. It was fortunate that the extensometer was used to measure displacement because the actuator displacement was nearly an order of magnitude off of true specimen displacement. A photograph of a tested specimen is shown in Figure 5.4.

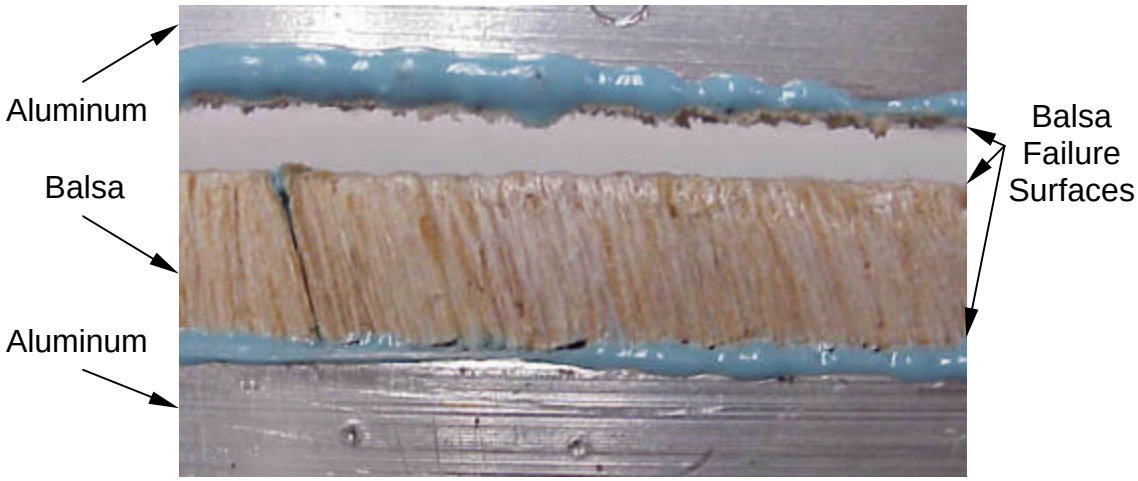

Figure 5.4 Enlarged detail of Balsa Shear modulus test specimen.

All three specimens failed in a similar manner, near the outer surface of the core. Initially it appeared to be an interface failure, but it is actually balsa failure just beyond the interface. One of the specimens failed on both interfaces

at the same time; this confirms that there was nothing forcing failure to one interface or the other.

A chart is included in Figure 5.5 which has shear modulus and shear strength compared to manufacturer's data provided by Baltek. There is quite a bit of variation from sample to sample, which was expected due to density variation. However, unlike the extensional modulus specimens, the shear specimens had multiple tree sections, so each sample was actually an average of these different sections. The experimental values are presented in Table 5.2 along with properties from literature [Baltek (1999), Kilbourn (2000), Mil Handbook 23A (1968), Wienhold et al (2000), Forest Products Lab. (1987)].

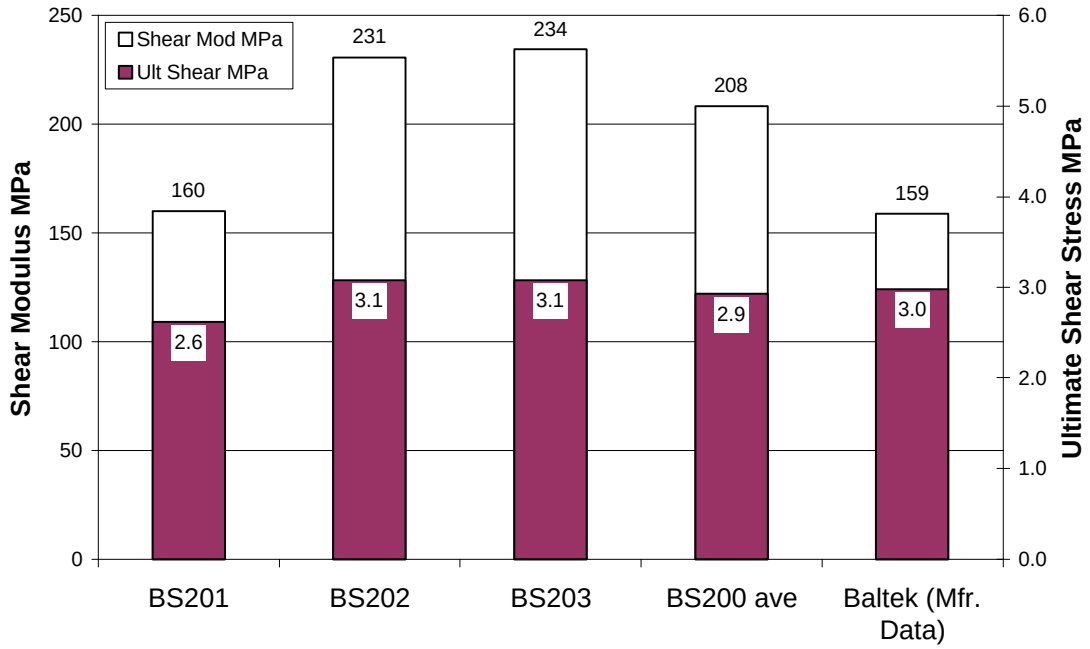

Figure 5.5 Shear modulus and ultimate strength of balsa from ASTM 273.

Table 5.2 Shear modulus and ultimate shear strength of balsa.

	Data Source					
	Experiment	Baltek	Kilbourn	Mil Hdbk 23A	Wienhold et al.	Wood Hndbk
Density	150	150	155	160	152	160
Shear Mod (MPa)	208	159	na	156-235*	na	na
Ult. Shear (MPa)	2.93	2.98	3.00	2.0-2.35*	2.38	2.07

*Range is due to modulus parallel and perpendicular to growth rings.

Differences between the literature and experimental values may be attributed to thickness effects. Kilbourn states that as the thickness of a balsa end-grain shear specimen is reduced, the shear strength will increase. This is also supported by some honeycomb shear tests. Kilbourn's hypothesis is verified when comparing the experiments, done at a thickness of 9.33 mm, with the literature data, which used the ASTM recommended thickness of 12.7 mm, in Table 5.2.

The results of this test showed that the data presented by Baltek were relatively close to the experimental values. The Baltek values of 159 MPa for shear modulus and 2.98 MPa for shear strength were used for numerical modeling and evaluating. These were used because they were close to experimental values and probably had a much broader sample base to provide more confidence in the properties. A table of all balsa properties and their origin is included in Table 5.3.

Table 5.3 Origin of all balsa properties.

Material Property	Value (MPa)	Source		Rational
Ex	52.8	Experiment		Wide range from literature
Ey	2510	Baltek		Given as specification
Ez	52.8	Experiment		Wide range from literature
vxy	0.11	Wood Handbook	Averaged tangential and radial values	Source given by Baltek
vxz	0.34	Wood Handbook		Source given by Baltek
vyz	0.36	Wood Handbook		Source given by Baltek
Gxy	159	Baltek		Given as specification
Gxz	159	Baltek		Given as specification
Gyz	159	Baltek		Given as specification
Utx	13	Feichtinger		Source given by Baltek
Txy	3	Baltek and Exp.		Given as specification

Grain is in direction of y axis
[Baltek Corp. (1999), Feichtinger (1986), Forest Products Laboratory (1987)]

Sandwich Flexural Experiment

The sandwich panel flexural experiment was the final material property validation test performed. This was done, not to find material properties, but to provide a means of validation for material properties used in the numerical models that are important in bending. Each of four specimens was tested to a low level load with load and displacement recorded and then flipped upside down and tested to failure. This was done to eliminate concerns that the facesheets may be slightly different in fiber content and thickness and could cause a nonsymmetric specimen. Both plots were nearly identical, so there was not an appreciable difference due to specimen orientation.

The tests were completed under the specifications of ASTM C-393. A photograph of a failing specimen can be seen in Figure 3.7. All specimens failed in the same manner. Failure was initially a core shear failure and was followed

by rapid delamination. The core remained intact for the most part except where the core was split at one spot parallel to the grain of the balsa. The delamination over the first few millimeters was actually a tensile and shear failure at the core surface where balsa had failed and was still bonded to the facesheets. After a few millimeters, the delamination went to the surface of the balsa where the resin bonding the facesheet and core had failed.

The tests produced good plots of load and displacement, which will be displayed later in the Numerical Results-Baseline Materials section. Core shear strength can also be calculated from this test. However, this is not recommended for use by ASTM but is still used occasionally. Shear strength for this test was calculated as 2.0 MPa with a standard deviation of .11 MPa. This is nearly 32 percent lower than the balsa shear modulus experimental result of 2.93 MPa. The large difference is precisely the reason ASTM does not recommend that the flexural modulus test be used to find core properties. The results of this test are most useful as a comparison to the numerical model using the load versus displacement output.

Experiments to Establish Baseline Strengths

The rest of the tests included in this chapter are on composite laminates. All tests were performed using strain gages at critical locations and an extensometer at various locations to gain a better understanding of the strain field in each type of specimen. For some specimens, the strain gage failed due to severe cracking in surface plies. In this case, the strain was found by using

the increase in strain recorded by the extensometer after the crack occurred. Alternatively, if the other specimens had linear strain plots, the strain was simply extrapolated to the maximum load. If these options did not seem to capture the true strain at failure, the specimen was dropped and only the remaining two were used.

All stresses reported were calculated using a nominal specimen thickness that was found by averaging the thickness of several preliminary specimens. The nominal thickness was important to isolate the effects that geometry and fiber content had on each type of specimen. A thickness was chosen to normalize stresses because it allows the stress of each specimen to be calculated using the area of the fibers regardless of fiber content. All specimens were made with the same fabric so the number of fibers per width is nearly constant in all specimens. In the case of specimens containing balsa core, a thickness including on the facesheets was used. This allowed a direct comparison to facesheet performance with or without the core in the specimen.

The experiments in this section include both the Facesheet Control (composed of both facesheets) and the Sandwich Panel. The Facesheet Control was the first test performed. As described in the methods section, two types of these specimens were tested. The three straight section specimens were tested first and had one failure near the grips while the others failed near the center of the gage section. The influence of the grips was not totally known especially since the specimens were tabbed and this lay-up had not been tested before.

As the test was performed, cracking could be heard and seen in the DB120 layers at about half of the ultimate strain. The extensometer was not helpful for true strains after cracking began because it was usually affected by the discrete cracks that formed between the tows in the outer DB120 layer. Steps were visible in the extensometer plots when cracks popped, but the extensometer still performed well between cracks so it could be used to see changes in strain. In each of the three specimens, the strain gages worked until fiber failure, which is clearly visible in the stress-strain plots. Information gained from this test was laminate static strength as well as laminate modulus. The values can be seen in Table 5.4.

Table 5.4 Baseline laminate property results at failure

		Long. Strength			Long. Strain			Long. Modulus*		
		Avg.	Std Dev	COV	Avg.	Std Dev	COV	Avg.	Std Dev	COV
Specimen		MPa	MPa	%	%	%	%	GPa	GPa	%
Facesheet	Straight	394	6.66	1.69	2.80	0.13	4.64	17.89	0.67	3.75
Control	Dogbone	383	9.61	2.51	2.68	0.09	3.36	18.09	1.23	6.80
Sandwich Panel		409	7.37	1.80	2.64	0.05	1.89	21.13	0.27	1.28

*Modulus calculated for first 10 percent of test

The next test was performed on the dogboned specimens. The specimen geometry resulted in failures of the zero degree plies at least 20 mm away from the grips. These coupons had a small amount of side splitting caused by the shear transfer between tows at the change in specimen width. This can be seen in Figure 5.6. The side splits began when the tests were around 75 percent of

the maximum load. Cracking was seen and heard in the surface DB120 layers at 30 percent of the maximum load. The results of this test are included in Table 5.3.

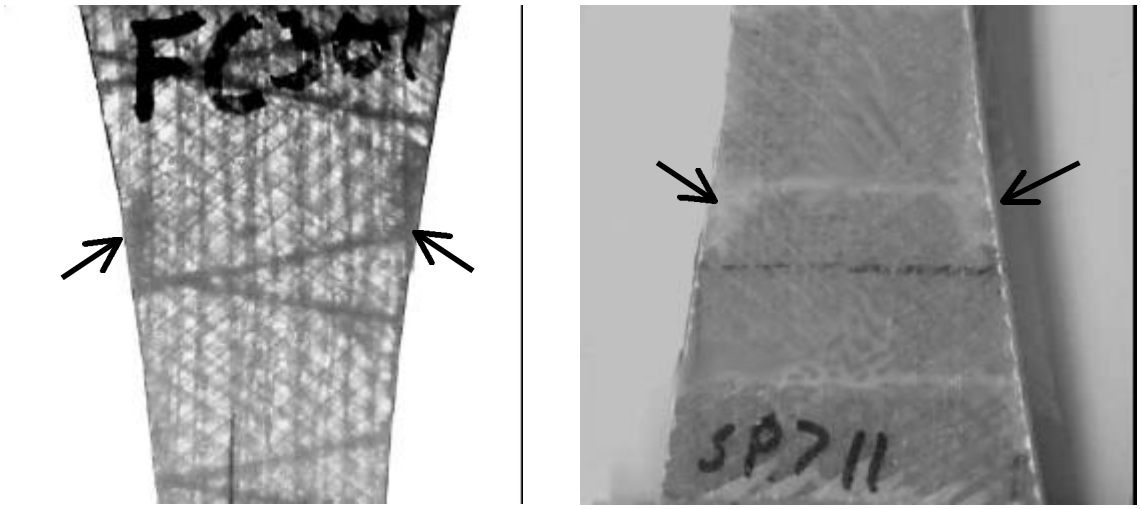

Figure 5.6 Side splits in Fillet Control (lt.) and Sandwich Panel (rt.) specimens.

The straight specimens had a higher average strength than the dogbone specimens. It is typically expected that the dogbone would have a higher strength because the stress concentrations of the grips are alleviated by the increased width. It could be that the side splitting damaged some of the tows in the narrow gage section which lowered the strength. When considering that the test only included three specimens, with the resulting standard deviation, there is probably no statistical difference between the measured strengths of each specimen type.

It was decided that the dogbone specimen strength would be the one used for comparison purposes to sandwich panel and any sandwich to laminate

transition tests. The dogboned geometry was chosen primarily because direct comparisons could be made to the sandwich panel results. Several geometries were used to test the sandwich panels, but the dogbone configuration was the only one that produced reasonable results, with failure in the center of the gage section.

The sandwich panel was tested with a strain gage on only one side due to symmetry. Side splitting began at about 75 percent of total load, just as in the Facesheet Control test. Cracking was heard and seen at 30 percent of ultimate load just as the Facesheet Control tests as well. The sandwich panel specimens all had one facesheet fail in the center of the gage section, and then the other facesheet would fail. The second facesheet would fail immediately or within seconds at the grip. The failure was probably at the grip because the loading went from symmetric to asymmetric in such a short time. A picture of the failed Sandwich Panel and Facesheet Control specimens is displayed in Figure 5.7.

The results of the Sandwich Panel tests are included in Table 5.3. It was not expected that the strength of sandwich panel would exceed that of the facesheets, especially when the axial strength of the core is typically ignored in sandwich panel design. The higher strength can be attributed by the added strength of the balsa core. There were also some theories that the resin rich regions introduced by the score marks in the ContourKore might be stress concentrations which could reduce the sandwich panel strength. After comparing the results, however, it appears that there is not a reduction, but a slight increase in strength due to the presence of the core. The values of the Sandwich Panel

Figure 5.7 Failed Facesheet Control and Sandwich Panel specimen with zero degree fibers failed.

test are so close to those of the Facesheet Control tests that there may not be a statistical difference between them.

The Sandwich Panel and the Facesheet Control tests both provided good failures with important results. These results were used as a baseline to asses numerical model performance. The experimental results were not used to mach numerical and experimental stiffness, but only to validate these values.

Sandwich Termination into Thin Laminate

The first specimens tested were the Fillet Hand-layup specimens. These were of such poor quality that the fillet was not the only detail reducing the specimens strengths. The Fillet Mold specimens were made and tested next,

isolating the fillet detail from the manufacturing problems discussed earlier. The results of both of these specimens are compared to Facesheet Control material in Table 5.5. A large reduction in strength from the Facesheet Control is easily seen when looking at both delamination and ultimate strengths.

Table 5.5 Delamination and failure strength of preliminary 30 degree fillet tests.

		Delam. Strength	Std Dev	COV	Long. Strength	Std Dev	COV
Specimen	#	MPa	MPa	%	MPa	MPa	%
Fillet Control	3	383	9.61	2.51	383	9.61	2.51
Fillet Hand Asym.	3	144	12.20	8.45	182	24.32	13.29
Fillet Double Asym.	3	187	16.21	8.63	238	11.25	4.72

Strain gages were mounted on both facesheets at the center of the gage section for the Fillet Mold specimens. A stress-strain plot of typical asymmetric (100 series) and symmetric (200 series) Fillet Mold tests are shown in Figure 5.8 along with the Facesheet Control plot. Large strain differences are easily seen especially in the asymmetric test. The discontinuities are caused by delamination in the fillet region.

These tests provided information on strength reductions as a result of the sandwich transition. It was unclear with the geometry of the Fillet Hand and Fillet Mold test if the full effect of the fillet was being seen or if the effect was minimized by the compactness of the specimens. The uncertainty moved testing to the larger, Fillet Single specimens as mentioned in the Experimental Methods chapter.

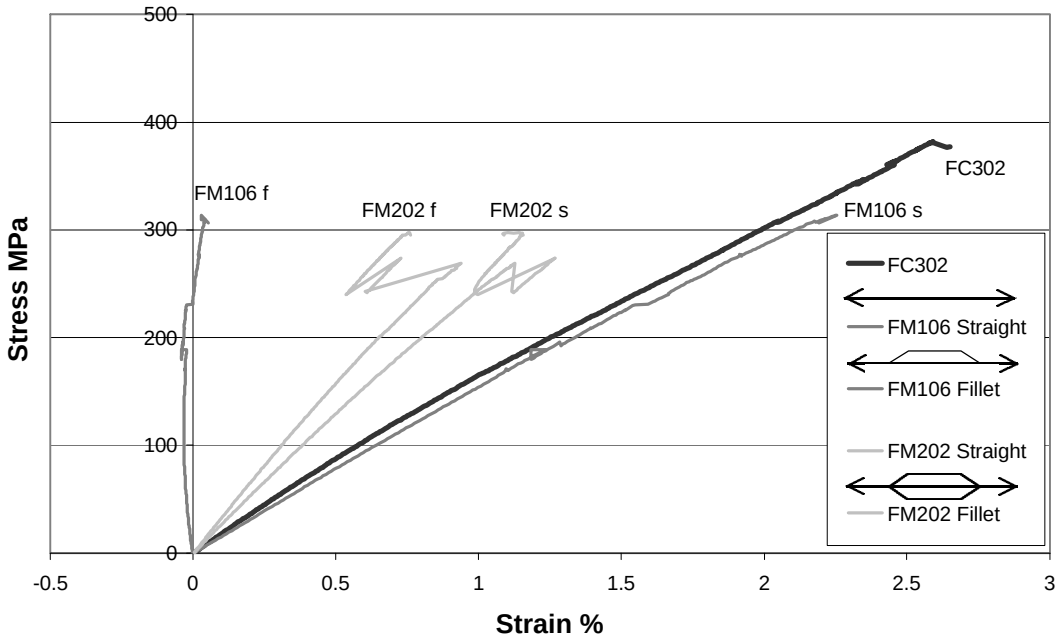

Figure 5.8 Typical stress-strain plots for facesheets of Fillet Mold (FM) and Fillet Control (FC) specimens.

The Fillet Single specimen (FS) is shown in Figure 3.12; it was tested nondestructively in tension using the extensometer as described earlier. The strain along each facesheet is shown in Figure 5.9. The fillet facesheet is the facesheet that bends around the fillet as diagramed in Figure 5.9. There is a large difference in strains at the fillet, as expected. The strain at the end of the Fillet Single specimen is still different in each facesheet. This means that there is not enough shear transfer in the balsa core to equalize the facesheet strains. This was an important parameter that was desired in a test specimen.

The Fillet Long specimen (FL) was tested in the same manner as the Fillet Single specimen. Again, a strain map was constructed for each facesheet. The specimen provided enough shear transfer to equalize strains near the sandwich

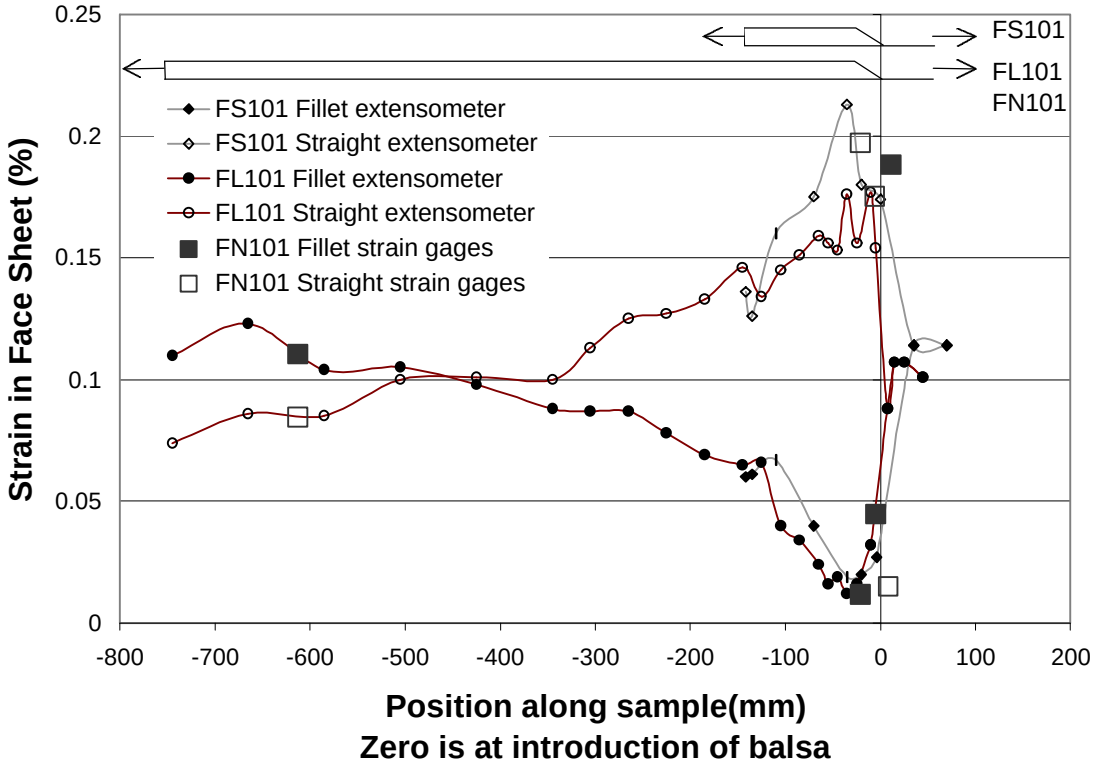

Figure 5.9 Strain in facesheets of Fillet Single, Fillet Long, and Fillet Normal specimens

end. The strains found using the extensometer in the Fillet Long specimen converge and then diverge as shown in Figure 5.9. The divergence of the strains toward the end is a result of bending due to specimen asymmetry. A few strain gages were used on a Fillet Normal specimen (FN) to ensure that the strains found using the extensometer were accurate. As shown in Figure 5.9, there are only two points that do not lie on the same line as the extensometer plots. These points are in the thin laminate where there is a lot of bending present, which the extensometer cannot capture in such a thin cross section.

The geometry of the Fillet Long specimens appeared to have attributes necessary to test the perfomance of the fillet region. However, as mentioned

earlier, the specimen quality and reproducibility was not as high as desired. The Fillet Normal specimens were created with dimensions similar to the Fillet Long specimens but with much better quality.

Fillet Normal Asymmetric Test

The Fillet Normal specimen effectively tested the performance of the Baltek Fillet Strip as it would perform in a full scale part. A stress-strain plot of an asymmetric and a symmetric Fillet Normal test is included in Figure 5.10, with the asymmetric specimen denoted as 100 series and symmetric denoted as 200 series as before. Strain gages were located just before the fillet region, as

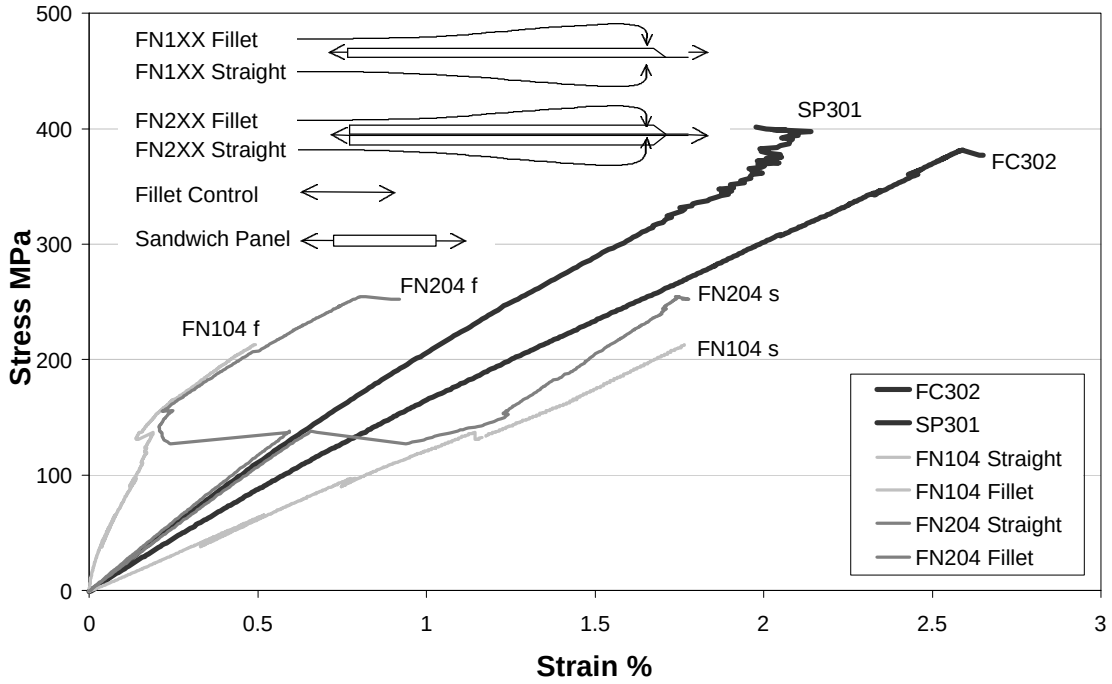

Figure 5.10 Typical stress-strain plots for Fillet Control, Sandwich Panel, and Fillet Normal specimens (Fillet Normal strains are for each facesheet near the fillet on symmetric and asymmetric specimens).

diagramed, to capture high and low strains found during the strain mapping experiments.

The tension tests of the Fillet Normal specimens would delaminate at a much lower load than the sandwich panel failed. Delamination as noted in all tables and plots is the stress or strain during the test when delamination has reached across the entire width of the specimen. The delamination can be seen as discontinuities in the stress-strain plots. A series of photographs in Figure 5.11 illustrates how a delamination is formed. This is typical of about half of all specimens containing fillets, while the other half had instant delaminations, where delamination initiated and propagated across the entire width of the

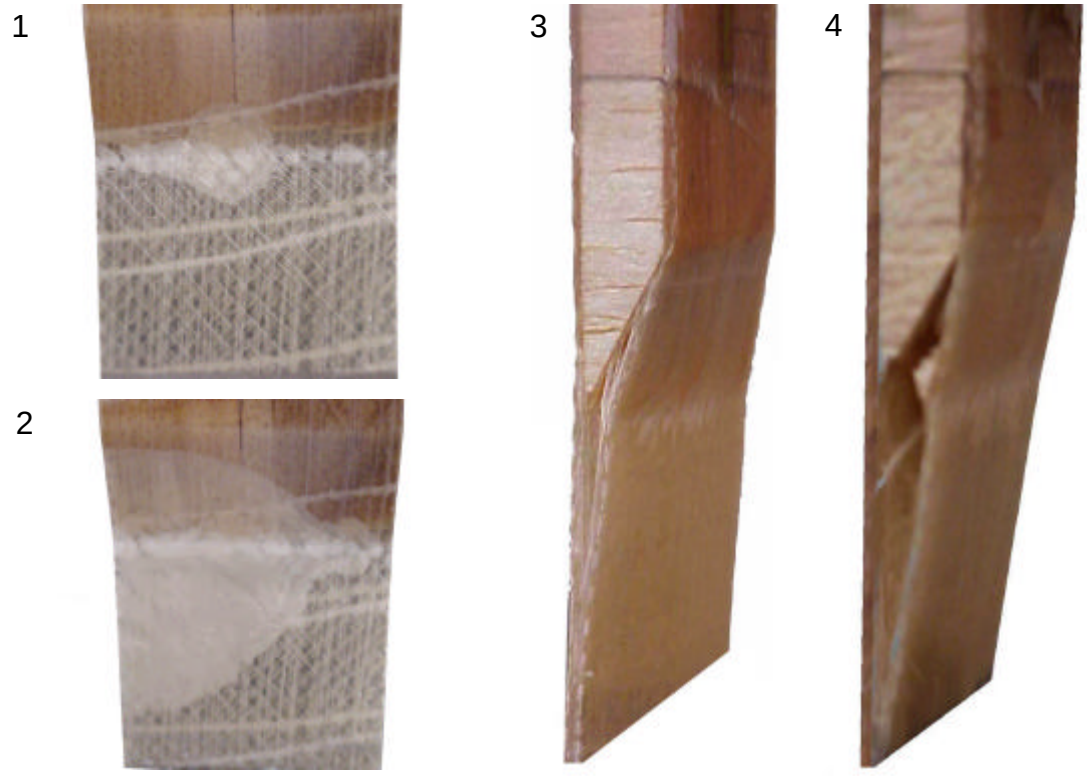

Figure 5.11 Steps during delamination of Fillet Normal specimen (front and side views).

sample in less than a second. The delaminations did not appear to be simple fillet to facesheet bond failures, because there were typically a few fibers left on the surfaces of the fillet, indicating that the fillet to facesheet bond was stronger than the fiber to matrix bond.

Delamination for the Fillet Normal asymmetrric tests occurred at an average stress of 95 MPa, 25 percent of the Facesheet Control failure stress of 383 MPa. The stress was calculated using the thickness of 1.92 mm as discussed earlier. The delamination stresses for the three specimens that were tested had a coefficient of variation of 4.13 percent. This was a very tight group considering that the failure mechanism has so many variables in the fillet region. The delamination strain reported as results is actually a calculated strain. Both facesheet strain gage values are averaged to get the approximate far-field strain. This was used after reviewing the strain mapping plots displayed earlier and seeing that the average of facesheet strains is equal to the far-field strain. This allowed a far-field strain gage to be omitted from all experiments. The COV of the strain measurements are not as small as the COV of stress measurements. This may be because of the method in which far-field strain was calculated; averaging the two strains may soften the variation from test to test. These results are tabulated in Table 5.6.

The delamination rate along the length of the specimen was different from specimen to specimen. As the delamination moved across the width, it would always move up to the edge of the fillet where the nominal sandwich panel began. In some specimens delamination into the thin laminate would

Table 5.6 Delamination and ultimate failure of all fillet and baseline materials

		Delamination				Ultimate Failure			
Experiment		Strain	COV	Stress	COV	Strain	COV	Stress	COV
	# of Spec.	%	%	MPa	%	%	%	MPa	%
Baseline Specimens									
Facesheet	3	na	na	na	na	2.69	3.30	383	2.51
Sand. Panel	3	na	na	na	na	2.64	1.45	409	1.80
Fillet Specimens (asymmetric)									
FN(30 deg)	3	0.44	4.63	95	4.13	1.17	9.45	222	8.06
FR(30 deg)	3	0.56	18.06	99	19.99	1.36	8.07	222	3.83
F 20 deg	3	0.79	14.99	142	14.55	1.48	19.69	242	18.72
F 10 deg	3	1.27	0.23	246	17.57	1.78	6.71	276	16.15
F 5 deg	3	2.31	2.21	359	2.93	2.33	5.27	364	3.59
Fillet Specimens (symmetric)									
FN(30 deg)	3	0.62	1.24	124	13.87	1.31	2.20	256	0.81
FR(30 deg)	3	0.46	7.81	87	1.22	1.11	13.27	242	8.13
F 20 deg	3	0.58	8.40	90	13.5	1.23	12.43	286	7.70
F 10 deg	3	1.39	5.94	242	6.23	1.84	6.97	311	5.46
F 5 deg	3	2.29	5.42	360	4.98	2.29	5.42	360	4.98

self-arrest before reaching the grip and then grow slowly, taking several seconds to delaminate to the grip. On most specimens, the delamination would grow quickly until it hit the grip, where delamination was halted by high grip pressures.

Failure can be defined in a few ways during these tests. Delamination may be a failure especially if the part is a primary structure where it is carrying high loads. If the delamination can be arrested by some external means, the part is still capable of carrying high tensile loads. For this reason the tests were conducted past the point of delamination to see what effects the delamination and fiber reorientation had on ultimate strengths.

Ultimate failure always occurs in the straight facesheet first because it is the shorter of the two facesheets. After delamination, the fillet facesheet is

straightened out (Figure 5.11) but still has a lower strain because its initial length was larger due to the angled section, which goes out of plane. The straight facesheet is typically covered with matrix cracks in the ±45 layer prior to any delamination; this puts most of the load in the zero degree layer. At delamination, more load is transferred to the straight facesheet because shear transfer is eliminated where delamination has occurred. Fiber failure in the straight facesheet occurs in each specimen within 25 mm of the fillet.

The area of damage on the straight side of the specimen, defined mainly as delamination, encompasses the entire thin laminate and typically goes less than 60 mm from the fillet tip into the sandwich panel. The damage in the fillet facesheet is considerably greater, but is primarily due to the energy released at fiber failure. This damage was not used as a means of comparison because of the catastrophic nature of all fiber failures. The fiber failures in the straight facesheet were followed by large out of plane displacements which usually delaminated and finally broke the fillet facesheets.

Secondary fiber failure in the fillet facesheet happens immediately after the elastic energy released, from the straight facesheet failure, is transferred to the fillet facesheet. Ultimate stress is simply reported as the highest stress calculated using the normalized thickness. The ultimate strain was calculated by averaging the strains in each facesheet just as the delamination strain. The ultimate stresses and strains are reported in Table 5.6 along with coefficients of variation.

If fiber failure is used as a failure criterion, then the Fillet Normal test performed to only 58 percent of the facesheet material ultimate stress. This is a huge reduction in static strength, which must be taken seriously when designing parts containing this detail.

Fillet Rigid Asymmetric Tests

The Fillet Rigid tests were conducted to try to increase shear transfer at the fillet by using a stiffer fillet material as discussed earlier. The Fillet Rigid tests had nearly identical results to the Fillet Normal tests. Two of the three specimens tested delaminated all at once to the grips while the third delaminated in a stable fashion over a period of a several seconds. The delamination stresses, calculated as before, averaged 99 MPa, only slightly above the 95 MPa delamination stress for the Fillet Normal test. The COV was the poorest of all tests performed at 19.99 percent.

It was apparent that the stiff fillet material did little for delamination resistance in the fillet region. The bond of the fillet to the facesheet was polyester matrix in both cases (Fillet Normal and Fillet Rigid), and this may be the similarity that caused failure at such close stresses. The stress-strain plots of the Fillet Rigid and Fillet Normal specimens have no notable differences. The facesheets of the Fillet Rigid tests have the same strain difference as the Fillet Normal tests, showing no increase in shear transfer. This may be due to the short length of the rigid material used. As mentioned in the test development

section, the length was chosen to be close to the balsa fillet in order to reduce manufacturing changes.

The fiber failure in the Fillet Rigid test was expected to be the same as for the Fillet Normal test because once the fillet was delaminated, the specimens should have all had had the same residual strength. The average ultimate stress was 222 MPa, the same as for the Fillet Normal tests. While a close value was expected, the exact same average was not. The COV was actually small for fiber failure, at 3.83 percent, compared to the Fillet Normal value of 8.06 percent. The strain values are included in Table 5.6, and were slightly different between Fillet Normal and Rigid tests. The length of damage in the straight facesheet was in the range of 60 to 75 mm, only a small increase from the Fillet Normal test.

The Fillet Rigid specimen had no advantage over the Fillet Normal specimens, with a disadvantage of more weight added by the 9 layer laminate fillet compared to the balsa fillet.

Fillet 20 Degree Asymmetric Tests

A fillet of a shallower angle was tested as a possible improvement over the Fillet Normal tests. The Fillet 20 tests performed a little better than the 30 degree fillets. These tests were very similar to the Fillet Normal tests described earlier. Specimens tested were either stable or unstable at initial delamination, as were the Fillet Normal tests.

The difference in the strains of each facesheet is decreased a small amount compared to the Fillet Normal tests. This can be seen from typical stress-strain plots in Figure 5.12. Part of the difference in the strain may be due to the varying location of the strain gages in each type of test. The position of the strain gages relative to the tip of the balsa fillet had to change for each geometry. To correct for this, a location was chosen for each angle that would nearly capture the peak strain in each specimen just beyond the fillet. This allowed comparison of strains but did not add confusion of having strain gages on the angle section of the specimen. It is interesting to note from Figure 5.12, that the strain convergence is due more to an increase in the fillet facesheet strain than a decrease in the straight facesheet strain.

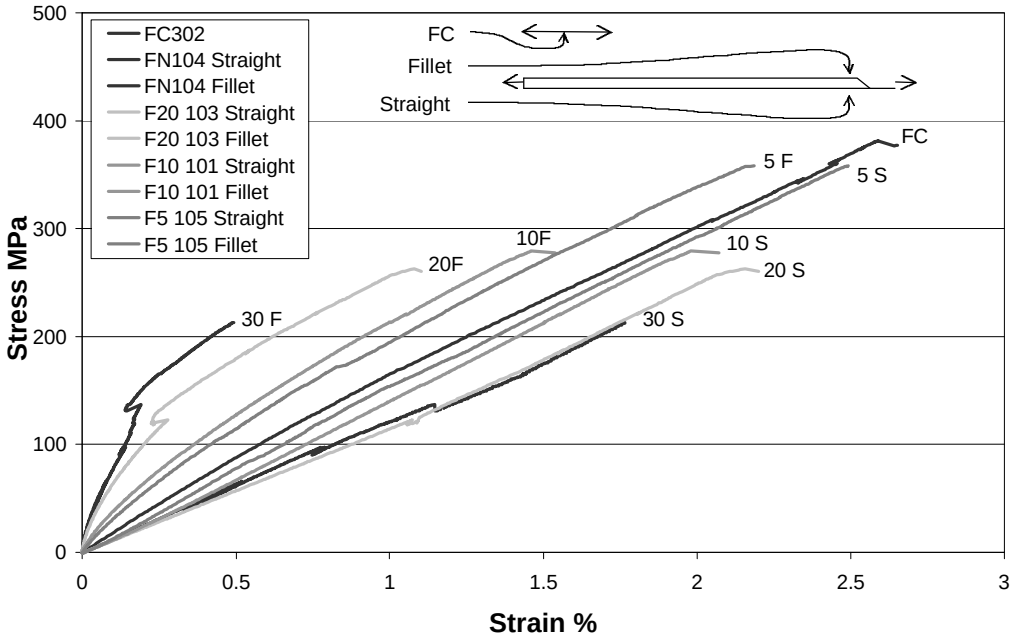

Figure 5.12 Stress-strain plots of each facesheet for asymmetric specimens containing different fillet angles.

The delamination stress is above the Fillet Normal results by 49 percent but is still a meager 37 percent of the facesheet ultimate strength. Ultimate failure of the specimen was increased only 9 percent above the Fillet Normal geometry. This was 73 percent of the baseline facesheet material failure stress. The damage zone on the straight side, characterized by delamination, was increased (compared to previously discussed tests) to a length between 50 and 70 mm.

Fillet 10 Degree Asymmetric Tests

The 10 degree fillet results showed better performance than the 20 degree fillet. The Fillet 10 specimens delaminated at different speeds, as did specimens in the other tests. Two delaminated in a stable manner, while the third was unstable, delaminating to the grip.

The sequences of failure were still very similar to those of the Fillet Normal tests. The delamination stress was increased to 246 MPa, 36 percent below the Facesheet Control failure. The delamination strength of this laminate surpasses the ultimate stress of the Fillet Normal specimens.

The fiber failure in the Fillet 10 specimens happened in the straight facesheet as before, but only one specimen broke in the thin laminate, while the others broke near the thick end of the balsa fillet. The fiber failure occurred at 276 MPa, 28 percent below the baseline value. This value was getting into the realm of acceptable knockdown factors as far as static strengths of design details are concerned. The damage region in the straight fillet extended from 75 to 250

mm into the sandwich from the balsa tip. This was a considerable increase from other tests. This is probably due to the increased amount of energy in the specimen at failure.

Fillet 5 Degree Asymmetric Tests

The fillet tested asymmetrically with the 5 degree balsa fillet failed with outstanding strength. The 5 degree fillet was so strong that there was difficulty in getting the fillet end of the specimen to break. Success finally prevailed on three of the final four tests. One test was performed using the final specimen design, but still failed away from the fillet, so this specimen was dropped. The strains in each facesheet were closer than in any other test as shown in Figure 5.12. The plot in Figure 5.12 also shows that as the fillet angle is decreased, the strains in each facesheet are converging on the Facesheet Conrtrol values. As mentioned earlier, more change in the fillet facesheet strain seems to be present with each increment that the angle is reduced.

The delamination of these specimens did not happen much before fiber failure. Delamination did not reach the grips before fiber failure in any of hte specimens. The delamination and failure stress were nearly the same at 359 and 364 MPa respectively, a mere 6 and 5 percent below the Facesheet Control failure stress. The damage encompassed the entire specimen. The balsa core completely delaminated from both facesheets on one specimen, leaving only the facesheets. Failure in every 5 degree fillet specimen was overwhelmingly catastrophic causing a lot of global damage.

Asymmetric Fillet Overview

A plot of all average stress and strain values at failure is included in Figure 5.13 and Figure 5.14 respectively. The plot including strain values has a line for each specimen tested, with shaded bars indicating the average of each of these tests. The lines of each specimen indicate how much scatter there was in each of the test types. All strains listed on the plot are for the average of that test.

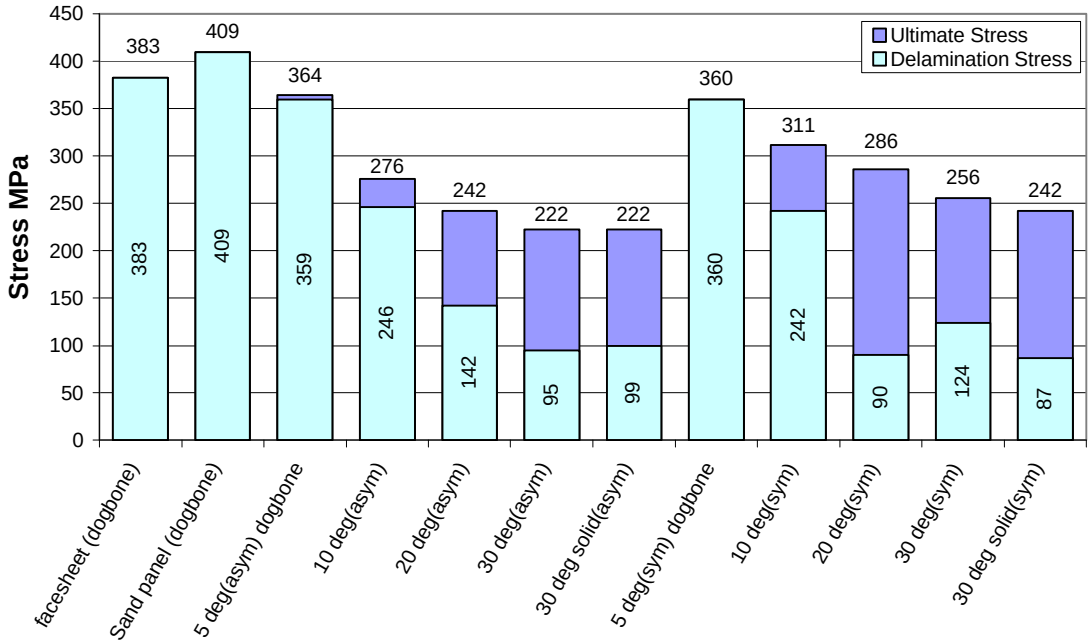

Figure 5.13 Stress values for each type of fillet test, at full width delamination and fiber failure.

There was a 76 percent reduction in strength due to the presence of the Baltek fillet strip when comparing a delamination failure of the Fillet Normal test to the Sandwich Panel baseline test. This improves to only 74 percent when compared to the Facesheet Control baseline test. If fiber failure is used, there is still a reduction of 42 percent when comparing to the Facesheet Control test.

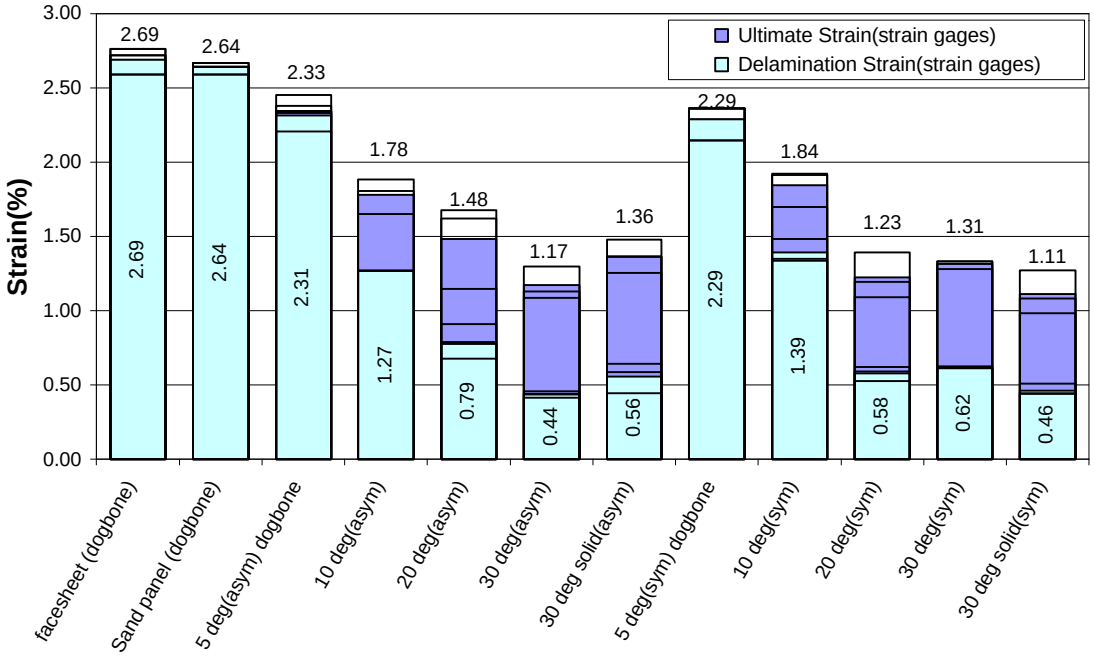

Figure 5.14 Strain values for each type of fillet test, at full width delamination and fiber failure.

A stiffer fillet insert does not increase strength at all. Reducing the angle of the fillet has a dramatic effect on fillet performance, especially when it is reduced to a small angle. A five degree fillet can improve the performance in an asymmetrically loaded application to only 5 or 6 percent below the baseline materials whether using delamination or fiber failure as a failure criterion.

Symmetric Fillet Experiments

Symmetric tests were important to this research because of the closed, curved shell design in the blade discussed earlier. The symmetric and asymmetric results provide two bounds for any range of bending constraints provided by curvature. The symmetric tests had characteristics similar to the

asymmetric tests. Delaminations formed in both a stable and unstable fashion within each specimen type. Symmetric results can be found in Table 5.6.

Fillet Normal Symmetric Tests

The symmetric Fillet Normal specimens outperformed the asymmetric tests. Delaminations happened at a value 31 percent above the asymmetric tests. The fiber failures were in the straight facesheet either at the fillet or in the thin laminate section of the specimen. The damage area after failure was less than 75 mm past the balsa tip. Fiber failure occurred at a stress 15 percent above the asymmetric tests, but failure was still 33 percent below the Facesheet Control test.

The stress-strain plot for a typical symmetric Fillet Normal specimen is included in Figure 5.10. The strains follow each other pretty close until delamination when the strains rapidly diverge to nearly the same strains as in the asymmetric specimen. It is interesting to see that the initial moduli match the Sandwich Panel test so closely. This indicates that the fillet is doing an excellent job of transferring shear when loads are below the delamination load.

Fillet Rigid Symmetric Tests

Once again, these tests closely followed the Fillet Normal tests. Two surprises appeared with this test. The delamination strengths of the symmetric specimens are below those of the asymmetric specimens, which was unexpected since there was no bending present. The large COV in the asymmetric delamination strengths may indicate that more tests need to be performed before

accurate comparisons can be made between the asymmetric and symmetric tests. The second unexpected result was that the Fillet Rigid (symmetric) specimen performance fell below that of the Fillet Normal specimens. A poor bond between the pre-laminated fillet and the facesheets offers one possible reason for the second unexpected reduction in strength.

The specimens all had fiber failures at the fillet tip with small damage regions, extending between 50 and 75 mm from the fillet tip. This small damage region may be attributed to the small amount of energy in the sample at failure because they failed at such low stress levels.

.

Fillet 20 Degree Symmetric Tests

. The 20 degree samples also raised some interesting questions with their disappointing performance. The delamination stresses were 40 percent less than the same specimens tested asymmetrically. Bending in the asymmetric tests may allow some relief in the fillet area by allowing the straight facesheet to move out of plane slightly, and in doing so, reduces the load in it by transferring some of it to the fillet facesheet. The bending may also relieve some transverse stress at the fillet tip where delamination initiates.

Fiber failure occurred in the straight facesheet at the balsa tip in two samples and 5 mm from the thin laminate into the balsa fillet in the third specimen. The damage region was about the same as for the asymmetric test at about 75 mm from the fillet's end. Fiber failure was increased over that for the asymmetric tests by 18 percent to a mean stress value of 286 MPa.

Fillet 10 Degree Symmetric Tests

Delamination stress of these symmetric specimens fell below that for the asymmetric tests once again. Values of stress at delamination were 2 percent below the corresponding asymmetric tests, but strains at delamination were actually improved in the symmetric tests by 9 percent.

In one specimen, FA201, fiber failure occurred in the straight facesheet where the constant thickness core began, just as in the asymmetric test. This was at an ultimate stress of 292 MPa. The other specimens did not fail at the fillet, but at the other end, near the balsa to solid core transition. Although these were not true fillet failures, they represent lower stress limits for fillet fiber failure. Since these failed at a stress above the fillet failure of FA201, the values were used to calculate an approximate failure stress. This resulted in an average, conservative, fillet failure stress of 311 MPa, 13 percent higher than the Fillet 10 asymmetric test. The damage area in these specimens was large, encompassing the entire sample.

Fillet 5 Degree Symmetric Tests

These tests were difficult to perform as mentioned in the test development section. However, even with all of the difficulties, good failures were produced in all specimens, with interesting results. Just as in the asymmetric tests, delamination and fiber failure happened nearly concurrently. Delamination never reached across the entire width of any specimen.

Specimen FB211 failed in the fibers before any delamination was visible. The fibers failed in the fillet facesheet first at the start of the thick cross section. This type of failure had not been observed before. The other two specimens failed in the straight facesheet with delaminations across only a portion of the width. One failed at the tip of the fillet, while the other failed at the thick end of the balsa fillet.

The average ultimate stress for the tests was 360 MPa, similar to the asymmetric tests. At only 6 percent below the Facesheet Control failure, these tests performed very well. The range of failure modes among the specimens indicates that the 5 degree fillet is efficient in transferring loads with minimal stress concentrations.

Symmetric Fillet Overview

The symmetric tests including fillets did not perform too well on the whole. The standard Baltek fillet produced results 72 percent below the facesheet for a delamination failure and 33 percent below the Facesheet Control for fiber failure. Each decrease in fillet angle did improve performance up to a reduction in strength of only 6 percent in the 5 degree fillet.

Asymmetric and Symmetric Fillet Comparison

Several observations can be made between the asymmetric and symmetric tests. All of these results are displayed in Figure 5.14 for easy comparison. The delamination strengths did not improve for the symmetric tests. Two of the five fillet tests delaminated at lower stresses with symmetric

specimens than with asymmetric specimens. One had a significant increase in delamination initiation stress with the asymmetric specimens, while two other tests had little change between the specimen types. A trend correlating delamination, fillet angle, and symmetry was not found. The higher strength in the asymmetric tests may be attributed to the free straight surface, which can bend out of plane, allowing a small amount of the longitudinal stress to be transferred to the fillet facesheet. This transfer would decrease the amount of transverse stress at the fillet tip as mentioned earlier.

The fiber or ultimate strength of the specimens did increase when tested in a symmetric specimen. Four of the five tests showed an increase over the asymmetric tests of 8 to 15 percent. The 5 degree test showed a decrease, but only by 1 percent, nearly negligible when the test has a COV of 5 percent.

The poor performance of the 30 degree fillet came as a slight surprise. In Table 5.7, delamination and ultimate strengths of each specimen type are expressed as a percentage of the Facesheet Control results. It is fortunate that

Table 5.7 Delamination and ultimate strengths of each specimen type expressed as a percentage of the Facesheet Control results.

	Asymmetric Delamination	Symmetric Delamination	Asymmetric Ultimate	Symmetric Ultimate
Experiment	%	%	%	%
FC(baseline)	100	100	100	100
FN(30 deg)	24.7	32.4	58.1	66.8
FR(30 deg)	25.9	23	58.1	63.1
F20 deg	37.1	23	63.2	74.6
F10 deg	64.1	63	72.1	81.3
F5 deg	93.7	93.9	95.0	93.9

the fillet strength can be increased to nearly nominal strengths, if a shallower angle of 5 degrees is used. This is applicable to both flat and curved panels, as bounded by the symmetric and asymmetric tests.

Sandwich to Thick Laminate Transition

Three types of tests were performed to evaluate the performance of a sandwich panel termination into a thick laminate. These specimens were described in detail in earlier sections.

Sandwich Termination-90 Degree Tests

Two batches of these specimens, from two different panels, were tested. The first batch had one specimen with a very low strength and the delamination stresses were not recorded. For these two reasons, mainly the second, three other specimens were made and tested. In the second batch of tests, one specimen performed well below the others. This simply shows variation in manufacturing even within the one panel from which all specimens were cut. The COV's included with results in Table 5.8 are large due to these variations.

Table 5.8 Delamination and ultimate failure of all sandwich terminations and baseline material.

		Delamination				Ultimate			
Experiment		Strain	COV	Stress	COV	Strain	COV	Stress	COV
	# of Spec.	%	%	MPa	%	%	%	MPa	%
SP(baseline)	3	na	na	na	na	2.64	1.45	409	1.80
ST(90 deg)	3	1.00	35.7	176	32.17	1.31	39.23	230	28.19
S10 deg	3	1.46	10.00	256	8.93	2.01	7.70	335	4.63
S5 deg	3	2.11	6.59	314	3.82	2.11	6.59	314	3.82

The sandwich termination tests were compared to the Sandwich Panel test results because they were the weakest sub component of the part. It no longer made sense to compare their performance to the Facesheet Control material when it was not included in the specimen. As before, the stress values are reported using the normalized thickness of 1.92 mm and the specimen width, to allow direct comparison of failure loads per unit width.

It was suspected that there would be a small reduction in strength due to the abrupt modulus change at the transition, but large reductions were not expected. The test results proved otherwise, with delamination at the transition happening at 186 MPa. The delamination stress was 57 percent below that of the Sandwich Panel tests. One apparent reason for delamination was a slight thickness change at the start of the balsa core. The thick laminate shrinks more than the balsa sandwich panel, so an offset and thickness reduction of 0.3 mm is present on one facesheet. This caused a small amount of transverse stress where the fibers go out of plane for a small distance. Another reason delamination might be so low, is the presence of a matrix region nearly 5 mm in length extending from the end of the balsa core, this is shown in Figure 5.15.

Figure 5.15 Detail of resin rich region in Sandwich Termination specimen.

Even though special attention was taken to keep the fibers close to the balsa core, the fibers still moved away from the balsa a small amount.

Fiber failure came a little closer to the Sandwich Panel results, at 230 MPa or 44 percent below the baseline value. The damage zone in the parts was relatively small, on the order of 50 mm in length. The small damage zone is probably due to the low failure stresses because most of the material in the specimen was well below its material ultimate stress at the time of specimen failure.

Sandwich 10 Degree Termination Tests

The Sandwich 10 degree tests were conducted using two strain gages to capture any strain differences between the top and bottom facesheets. The gages registered strains differing by only 0.07 percent, which is minimal. Strains from each gage were averaged at delamination and failure, to get the strain results. The Sandwich 10 degree specimens had no resin rich regions or thickness changes like the Sandwich Termination specimens did, so delamination was expected to improve. The 10 degree taper increased delamination resistance as expected, to a value 37 percent below the sandwich panel failure.

Fiber failure did improve, to a value only 18 percent lower than the Sandwich Panel tests. This was a significant improvement, but the early delamination is still undesirable, especially in reversed loading situations. There was also a large damage zone present at failure, between 200 and 300 mm.

Sandwich 5 Degree Termination Tests

The 5 degree sandwich terminations had much better delamination resistance. Again, there were no thickness changes, and no resin rich region. Delamination was never detected until fiber failure at 314 MPa, only 23 percent below the Sandwich Panel tests, which was a lower stress than the 10 degree termination.

Two of the specimens failed at the thick end of balsa fillet used to taper the transition, the same as all Sandwich Acute tests. The other test however, failed in the center of the gage section, 100 mm from each end of the constant thickness balsa core. The Sandwich 5 degree tests also had large damage zones between 100 and 300 mm.

Sandwich Transition into Thick Laminate Summary

These tests proved to be a lot weaker than originally thought. Values comparing each test's performance to the Sandwich Panel results are included in Table 5.9. With strengths as low as 55 percent below the baseline, Sandwich Panel tests, this must receive special attention if it is present in a design. For

Table 5.9 Strength of sandwich terminations into thick laminates expressed as a percentage of the Sandwich Panel strength.

	Delamination	Ultimate
Experiment	%	%
Sand. Panel(baseline)	100	100
Sand Term.(90 deg)	43.0	56.2
Sand. 10 deg	62.6	81.9
Sand. 5 deg	76.8	76.8

critical applications, a tapered transition should be used, reducing the strength by a noticeable, but more tolerable 23 percent.

Fatigue Performance

The fatigue tests on the baseline materials, facesheets and sandwich panels, were conducted using specimens identical to the static specimens. On the other hand, the fillet fatigue tests were performed on shorter specimens than the static tests, as described earlier. These specimens were tested statically to ensure that static strength would not vary with the decreased length.

Fillet Fatigue Static Performance

The strain mapping results in Figure 5.9 were reviewed to see changes in the strain field with shorter gage sections. Both short and long specimens have nearly identical strain profiles along each facesheet. These tests were not conducted on the Fillet Fatigue specimen, but the Fillet Single specimen, which has about the same length of the sandwich panel. This was used to validate the shorter length of the Fillet Fatigue specimen relative to the Fillet Normal specimens which had a longer sandwich panel section. Static tests, like the Fillet Normal tests, provided more validation.

As expected, the Fillet Fatigue static tests followed the same patterns as the Fillet Normal tests. Damage zones in each type of test were about the same size when compared to the respective symmetric and asymmetric tests. A comparison of the Fillet Normal and Fillet Fatigue static tensile test results is

included in Table 5.10. When comparing the stress values of the asymmetric tests, delamination was 17 percent higher and fiber failure was only 7 percent higher in Fillet Fatigue specimens than the Fillet Normal specimens. The similar static results gave confidence that the Fillet Fatigue specimens could provide valuable fatigue information with a lot less testing time and machine wear.

Table 5.10 Static tensile delamination and ultimate failure of Fillet Fatigue (FF) and Fillet Normal (FN) specimens.

		Delamination				Ultimate			
Experiment		Strain	COV	Stress	COV	Strain	COV	Stress	COV
	# of Spec.	%	%	MPa	%	%	%	MPa	%
FN(asym)	3	0.44	18.06	99	4.13	1.17	9.45	222	8.06
FF(asym)	3	0.63	13.22	116	12.53	1.45	4.79	238	5.11
FN(sym)	3	0.62	1.24	124	13.87	1.31	2.20	256	0.81
FF(sym)	3	0.52	21.75	101	16.51	1.64	2.83	256	4.17

Fatigue Performance of Facesheet Control

The Facesheet Control material performed very well when fatigued. Figure 5.16 has all of the fatigue data taken for this material. The slope of the fitted curve is relatively shallow, at 0.083 per decade. Typically, the best fiberglass/polyester laminates would have a slope no less than 0.10 per decade. The slope of 0.08 is merely a preliminary result, simply because there is such a small number of samples. The slope would be much steeper if it was not forced to fit the static results.

The failures of nearly all specimens were preceded by side splits at all four corners of the gage section as in the static tests. The fibers failed a distance of 20 mm away from the grips in most cases. The fiber failure did not typically

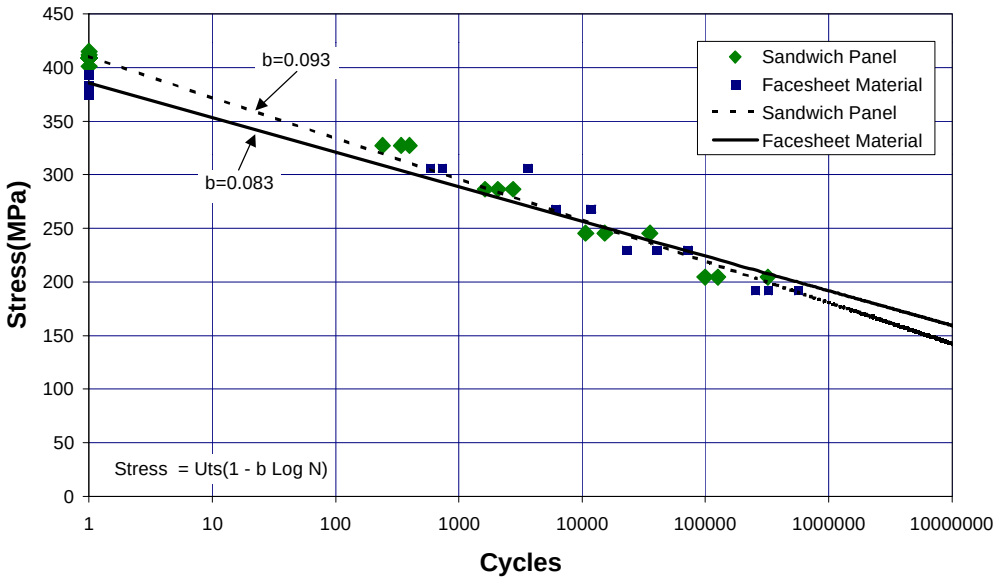

Figure 5.16 S-N plot for tensile failure of Facesheet Control and Sandwich Panel specimens tested in fatigue at R=0.1.

happen in a linear fashion across the specimen width, but over a long length of 100 mm as shown in Figure 5.17.Many specimens failed in areas of wider cross section away from the center of the gage section. This may be due to the

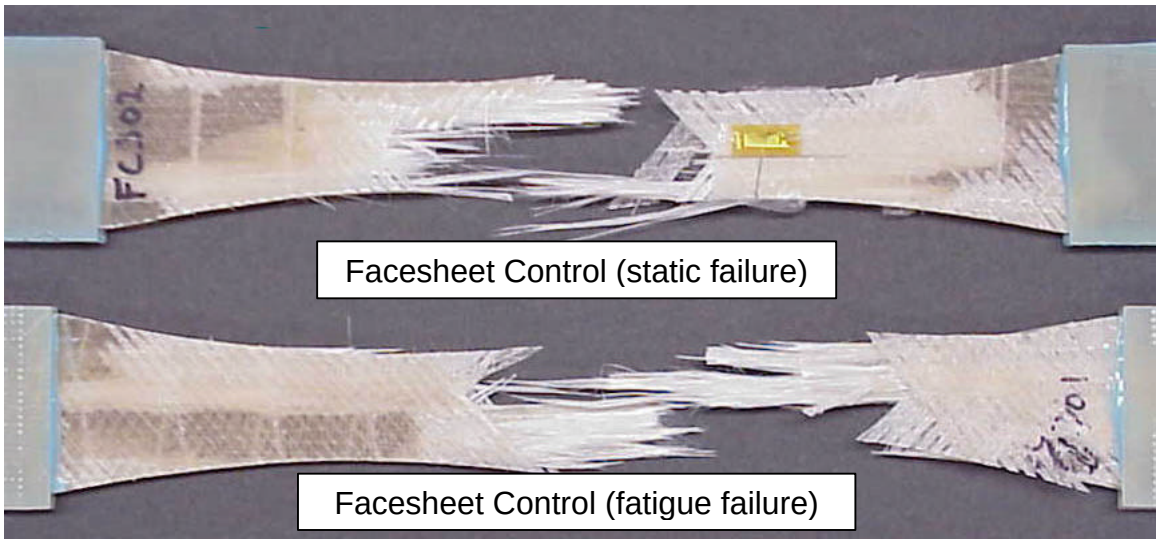

Figure 5.17 Failed Fillet Control specimens--failed in a static test and fatigue tests (Fatigue specimen has longer distance over which fiber failure occurred).

ineffectiveness of the increased width after the side splits are present, which do not allow any load sharing because all shear transfer is eliminated.

Sandwich Panel Fatigue Tests

The sandwich panels had good fatigue performance, just as the thin Facesheet Control material. Figure 5.16 includes the Sandwich Panel data with a fitted line having a slope of 0.093 per decade. This is still above a high performing laminate, which is surprising, considering there is balsa present in the laminate. It was suspected that the balsa with the score marks may reduce the laminate fatigue performance. It did lower performance, but only slightly.

When the sandwich panels were tested, side splits were nearly always present at all four corners on the front and back facesheets, but not nearly to the degree that the Facesheet Control specimens were side splitting. Fiber failure typically happened in one facesheet and then in the next facesheet immediately, because the load was doubled as the other facesheet failed. Fibers that failed in the first facesheet were the most important because they broke at the intended stress level with a pure axial load. The second facesheet had high stress in the last cycle and was subjected to bending and other stresses since the other facesheet was not functional. Fibers tended to fail at stitches, but usually at two or three locations near the center of the gage section, making the fiber failure length about 30 mm, a lot smaller than was typical in the Facesheet Control tests. The second facesheet to fail usually looked similar to the Facesheet Control material, with a long length of failure not local to stitches.

The balsa core did not ever delaminate from the facesheets prior to failure, except locally, near the side splits. The balsa did, however, develop several discrete cracks along the length of the sample. These cracks were in the grain direction through the thickness, and could be seen opening and closing with each cycle.

Fillet Fatigue Tests

With the addition of the fillet detail, many more subtleties were observed and recorded with these specimens. Delamination was the first thing that was recorded. Several stages of delamination were recorded to establish some knowledge of damage tolerance. A plot containing all delamination data points is included in Figure 5.18. Delamination information was difficult to obtain,

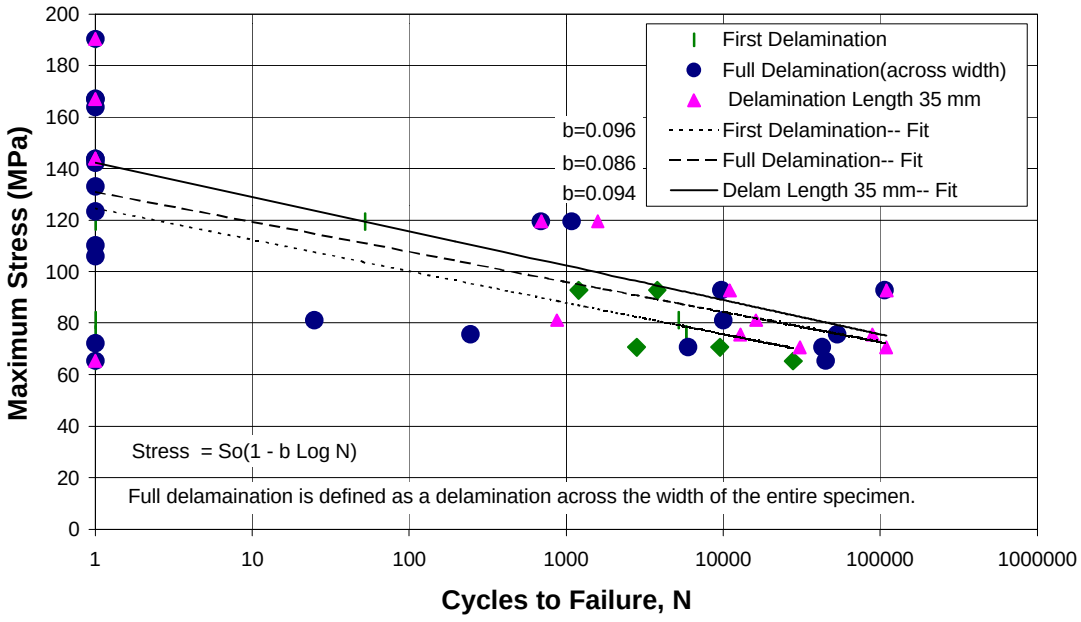

Figure 5.18 S-N plot of delamination initiation, delamination across width of specimen, and delamination of thin laminate section for a distance of 35 mm in Fillet Fatigue (asymmetric) specimens tested in fatigue at R=0.1.

especially in high cycle tests, because the tests had to be watched the entire time.

The initiation of delamination was the first item recorded. This was done when any delamination between the zero degree plies was noticed. Before zero delaminations in some tests, a delamination between the individual tows of the DB120 fabric was noted. This was caused by the out of plane forces on the surface ply of the fillet facesheet. These were very local, on the order of 3 mm in each dimension and not as opaque as the zero ply delaminations. A photo of this type of delamination is shown in Figure 5.19. This type of delamination is notably different than the first delamination in Figure 5.11.

Figure 5.19 Close-up view of fillet region showing local delaminations of tows in the DB120 fabric during a fatigue test of a Fillet Fatigue specimen

The delamination initiated at different spots in each specimen. In some specimens, delamination was initiated in the center of the specimen, away from the edges. This gave more confidence in the fact that edge effects were negligible. Sometimes two separate delaminations would form independently from one another and eventually coalesce. This supported the fact that the

sample was not being loaded eccentrically, causing moments that would concentrate delamination initiation in one spot or direction. In other specimens, delamination would begin from one side and propagate to the other side.

The number of cycles was recorded as soon as the delamination reached across the width of the specimen. Then, it began propagating through the thin laminate. The number of cycles was recorded when any part of the delamination hit the grip, 35 mm from the fillet tip.

The data in Figure 5.18 is useful in analyzing damage tolerance. The distance between the initial delamination and the 35 mm delamination fit lines is about one decade. This allows the delamination to grow for an entire decade of cycles before a large delamination is formed. A decade of cycles should be used to establish maximum inspection intervals allowing delaminations to be detected before they grow too large. The boundaries of the delamination were recorded at several times during it propagation. This gives an idea how the delamination is moving in the specimen. A plot of delamination fronts for each side of a specimen is included Figure 5.20. These show how delamination moved up and down on the specimen, but were bounded on the fillet facesheet at the start of the constant cross section. The straight facesheet, however, did not arrest delamination so it typically moved a distance, sometimes 150 mm, into the nominal sandwich panel section.

Cycles recorded at fiber failure as well as full width delamination are plotted in Figure 5.21. Delamination values have significantly more scatter than any of the fiber failure data. A line fitted to the fiber failure data has a slope of

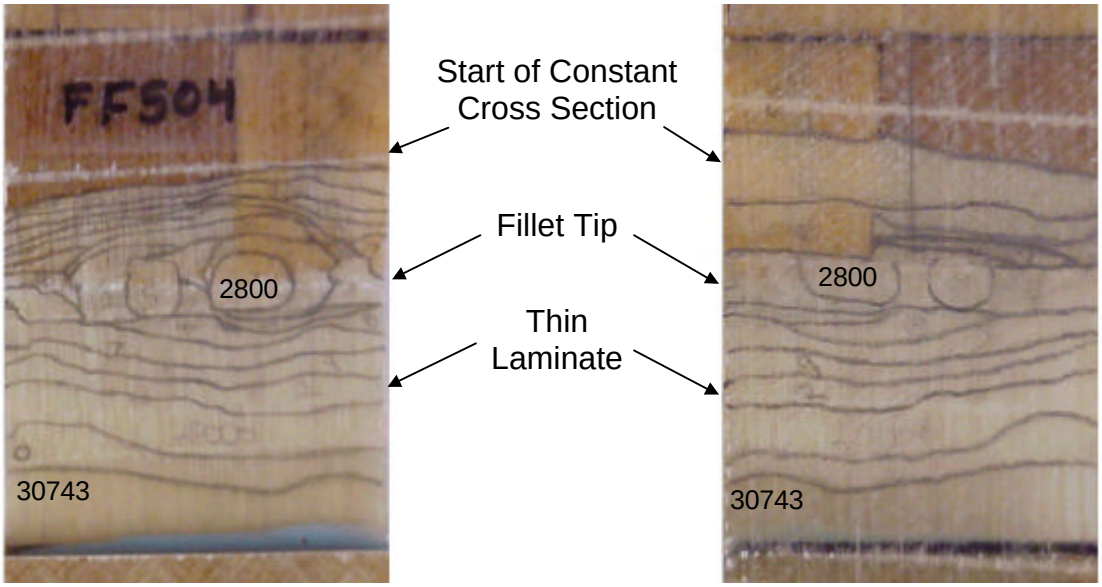

Figure 5.20 Delamination boundaries at various numbers of cycles during fatigue of Fillet Fatigue specimen.

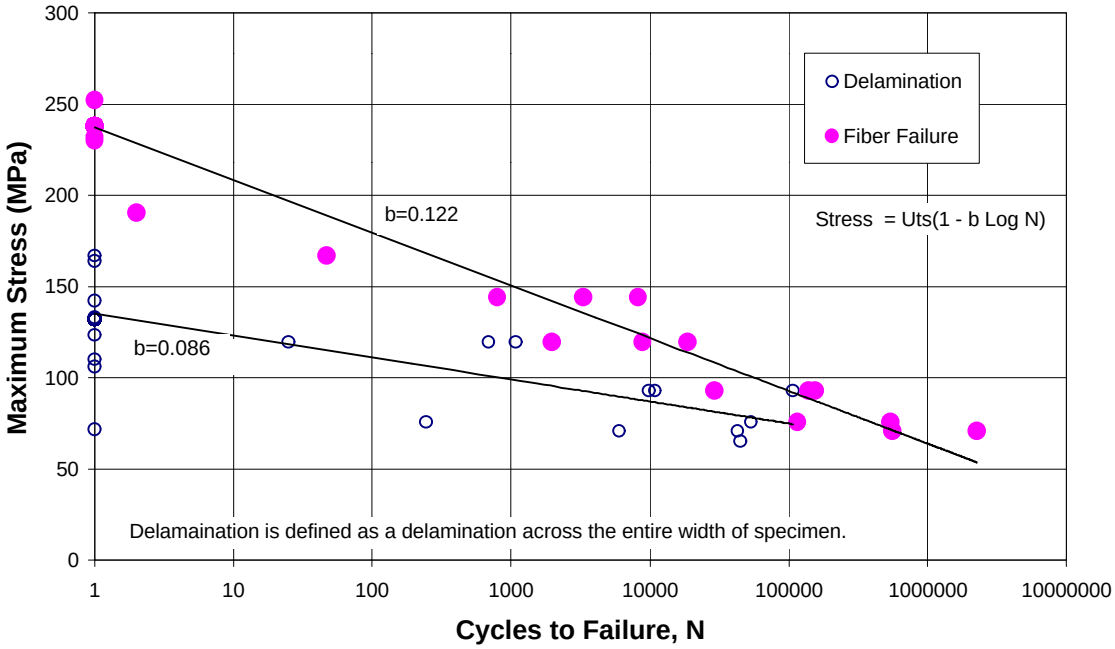

Figure 5.21 S-N plot for delamination and tensile failure of Fillet Fatigue specimen tested in fatigue at R=0.1.

0.122 per decade. This is poor compared to the baseline material fatigue performance. However, it does fit in the range of typical fiberglass fatigue slopes between 0.1 and 0.14, so its fatigue performance is not unusually bad. The two curve fits indicate that at low stresses and high cycles, delamination and fiber failure may happen simultaneously.

Side splits could be seen in a few specimens where the fabric had a small amount of fiber misalignment. This is one defect discussed on the background section. The misalignment of fibers makes some fibers exit the composite at the specimen edges. This doesn't allow the fiber's full potential to be used, especially when the fibers debond by shear, creating a side split. These were only present in a few specimens, and their performance was not below typical scatter.

Fiber failure happened in the straight facesheet first, as in the static tests. Fiber failure almost always followed a stitch or the fillet tip, making very linear failures across the width of the sample. A typical failure is shown in Figure 5.22.

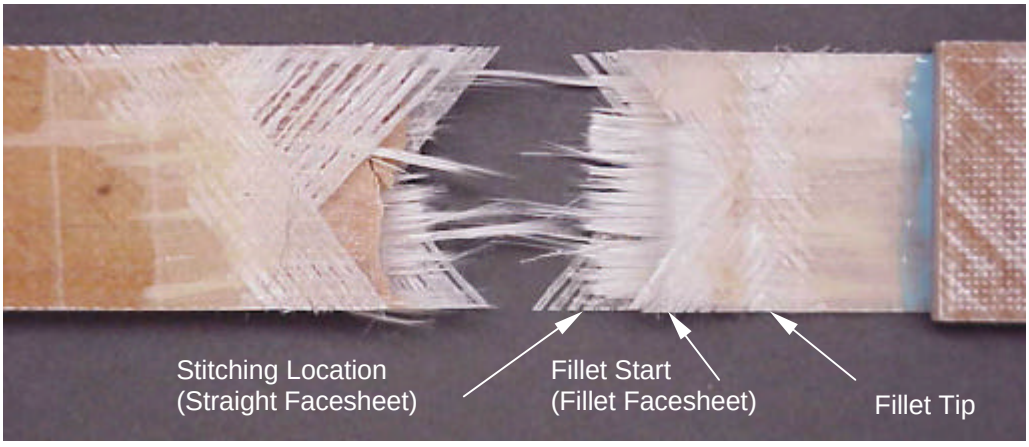

Figure 5.22 Detail of typical fatigue failure of Fillet Fatigue specimen.

All Fatigue Results

All of the fatigue tests conducted provided valuable information on material and detail performance. Static strength comparisons cannot provide all of the data important to designers. Sandwich panels were found to have only marginally lower fatigue performance than their facesheets tested alone. These results can be seen along with the Fillet Fatigue results in Figure 5.23.

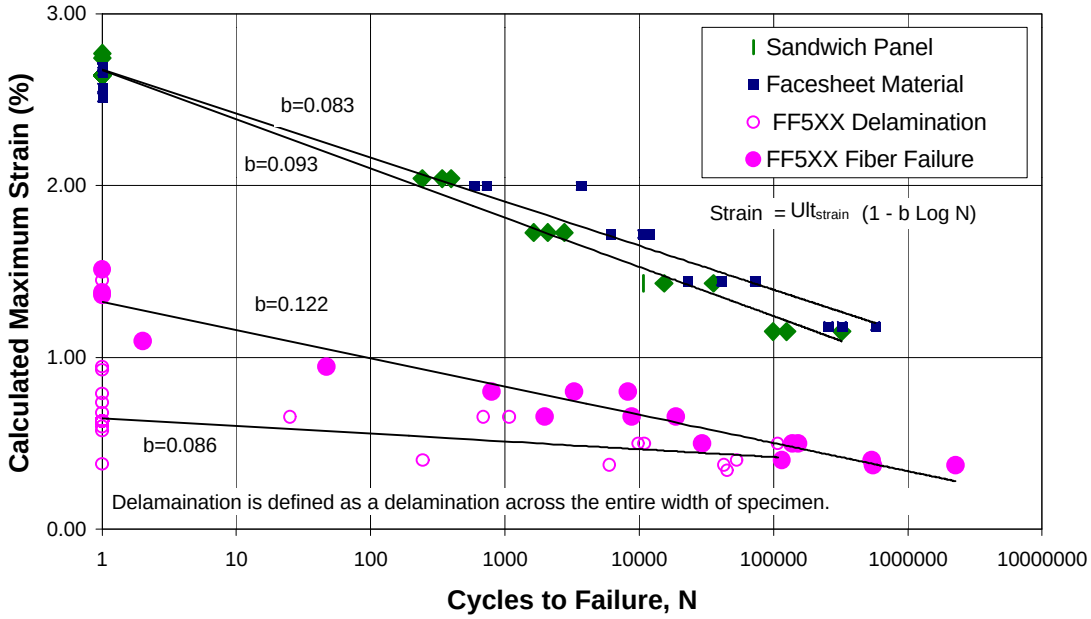

Figure 5.23 S-N Plot of Fillet Fatigue (FF5XX), Sandwich Panel, and Facesheet Control tested in fatigue at R=0.1.

All data are presented in terms of maximum strain of the fatigue waveform. This is useful to the designer looking for strains to failure. These strains were calculated by doing second order polynomial curve fits to a typical static test corresponding to each fatigue specimen. These equations were used to calculate the maximum strains corresponding to the maximum stresses

present in each specimen. The Fillet Fatigue strain was found by curve fitting the average of the straight and fillet facesheet strains recorded. This represents an approximate far-field strain as described before.

Relative strains to failure and fatigue performance can be seen easily in Figure 5.23. The delamination and fiber failure of the fillet specimens appear to meet the baseline materials, but not until very high cycles where fatigue behavior may no longer be linear. The plot also shows relative scatter in each test. The two baseline materials have much less scatter than the fillet data.

The graph included in Figure 2.24 contains all fatigue data normalized with respect to each specimen's static strength. This is helpful in seeing the slopes of each data set. The slope of the fillet delamination is roughly the same as the

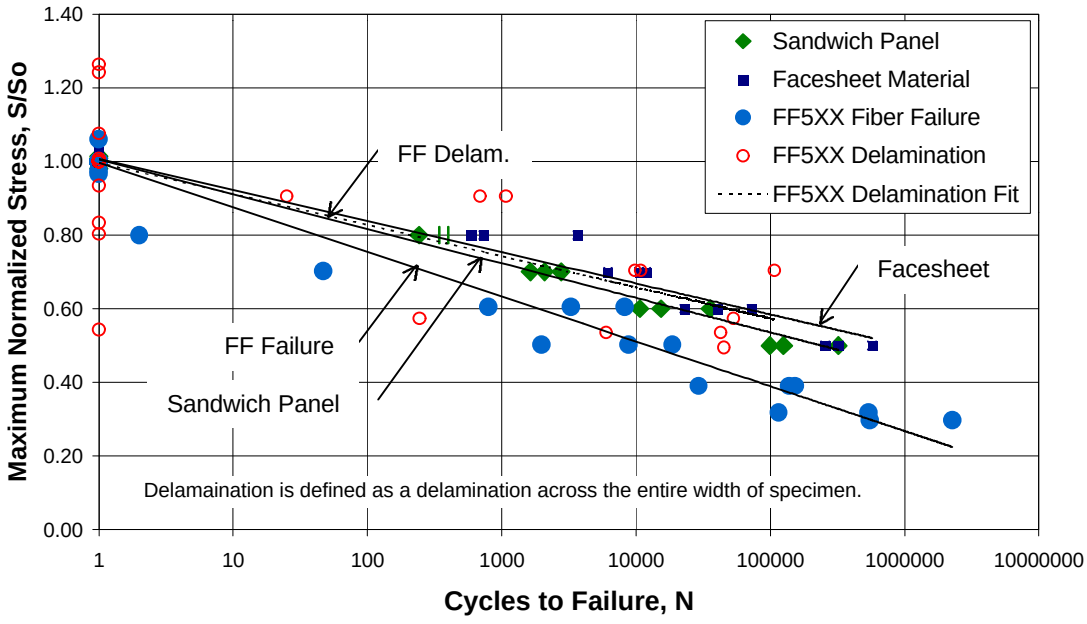

Figure 5.24 Normalized S-N Plot of Fillet Fatigue (FF5XX), Sandwich Panel, and Facesheet Control tested in fatigue at R=0.1.

Sandwich Panel and Facesheet Control slopes, while the fillet fiber failure slope is steeper. Figure 5.25 includes tensile fatigue knock-down factors similar to Figure 2.3 shown in the background section. Again the factors are calculated at a lifetime of one million cycles for the detail and a simple coupon. The factor of 3.4 for the 30 degree fillet delamination is probably the most important, the fiber failure factor of 3, can only be used if a significant amount of delamination is allowed in the application.

Detail	Sketch		F
Simple Coupon (Two Facesheets)	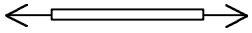		1.0
Sandwich Panel (Balsa Core)			1.1
Sandwich To Thin Laminate(Balsa Core) 30 Deg. Fillet (Asym.)	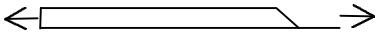	Delamination	3.4
		Fiber Failure	3.0

$$F = \frac{10^6 \text{ Cycle Stress (Coupon)}}{10^6 \text{ Cycle Stress}}$$

Figure 5.25 Preliminary Tensile fatigue knock-down factors for selected structural details relative to simple coupon (±45, 0, 0, ±45).

Fatigue is an important consideration when using fillets in designs. If delamination is used as a failure criterion for high cycles, the fatigue knock-down is a considerable improvement at 3.4, compared to the static strength knock-down of 4.3. When fiber failure is critical, fatigue values are important too. Static fiber failure of the 30 degree fillet has a static strength knock-down of 1.7 while

the fatigue knock-down is more detrimental at 3. These preliminary results will give designers insight to the problems associated with cyclic loading of sandwich panel transitions.

CHAPTER 6

NUMERICAL RESULTS

This chapter presents the results of finite element models for several of the cases studied experimentally. The finite element predictions are compared with experimental results to validate the methodologies used to predict stress distributions and failures. A strength of materials basis was used for all failure predictions. Element solutions were used exclusively, because they are not presented as average values, in contrast to nodal solution results.

Baseline Materials

The baseline materials were modeled to ensure that appropriate material properties were used. These models were only used to validate the material properties; they were not used to correct the material properties so numerical results would match experimental results more closely.

The Facesheet Control material was modeled using Plane 13 elements. It should be understood that the macro for this model was actually created from the Fillet Normal macro, as discussed earlier. The dogbone experimental results were used to compare to the model. By comparing the same geometry in each case, the effect of the balsa could be identified.

A stress-strain plot of the experimental and numerical results follows in Figure 6.1. The fiber failure was predicted using a maximum stress criterion and

is indicated in Figure 6.1. All of the experimental tests are included in the plot so the experimental scatter as well as the experimental/numerical correlation can be seen.

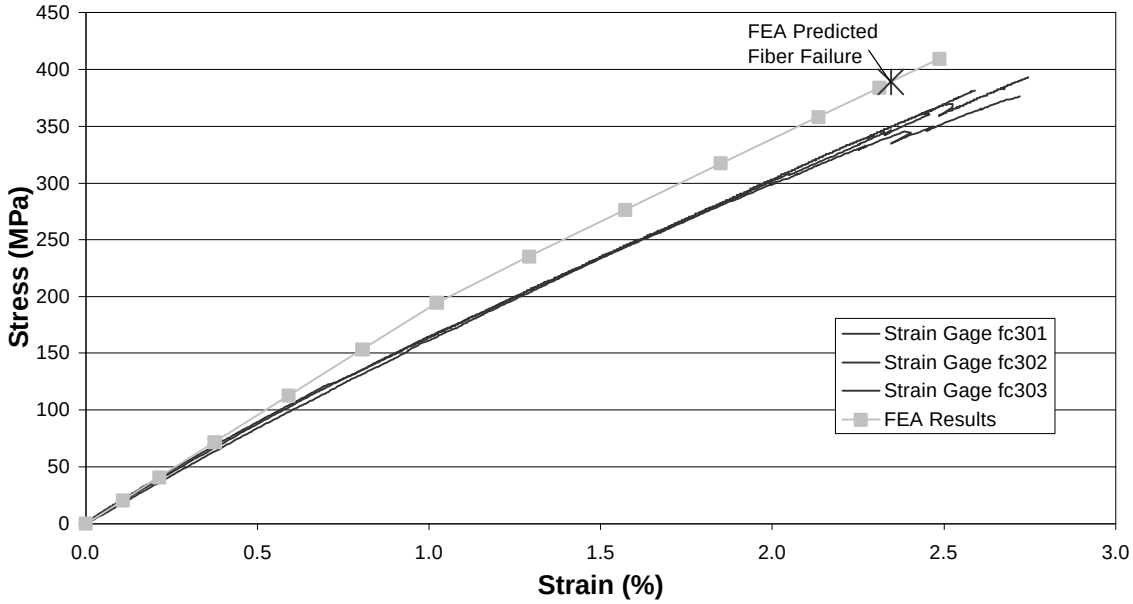

Figure 6.1 Stress-strain plot for dogboned Facesheet Control tests including all experimental plots and Finite Element Analysis (FEA) results.

Values for both experimental and numerical tests are summarized in Table 6.1. The values are very close in the initial stages of the tests, when comparing the initial modulus, indicating that the initial stiffness of the material is modeled accurately. The secant modulus, taken at failure, does not match as well. Presumably, this is because the bilinear stress-strain behavior used to model the damage in the DB120 fabric is too simplified, so that, as the ±45 degree layers are damaged, the model does not capture all experimental damage. The DB120 failure stress would have to be reduced to 20 percent of its calculated strength to

match the modulus of the experiment. This was not done because there is no knowledge, excluding the modulus difference, to do so. The ultimate failure was predicted using a maximum stress criterion in the fibers at 1.6 percent above experimental failure.

Table 6.1 Experimental and finite element results for baseline materials.

	Experimental Results			**FEA Results***		
	Elastic Modulus (GPa)		Strength (MPa)	Elastic Modulus (GPa)		Strength (MPa)
Model	Initial	Secant-Ult.	Ultimate	Initial	Secant-Ult.	Ultimate
Facesheet Control	18.09	14.2	383	19.1 (5.6)	16.6 (16.9)	389 (1.6)
Sandwich Panel	21.13	13.9	409	19.4 (-8.2)	16.9 (21.6)	395 (-3.4)
	Load Deflection Slope (N/mm)		Strength (N)	Load Deflection Slope (N/mm)		Strength (N)
Sandwich Flexural	195	213	2013	277 (42.1)	271 (27.2)	2224 (10.5)

*Numbers in parentheses are percent difference between experimental and FEA results.

The Sandwich Panel results are similar to the Facesheet Control results, which was expected since the inclusion of the core is the only difference. The stress-strain plot included in Figure 6.2 matches better than the Facesheet Control results. However, when comparing the results in Table 6.1, the Sandwich Panel has slightly larger differences, which is not too surprising because the balsa has variable properties which are difficult to model, making error more likely. It is important to note that both the initial modulus and ultimate

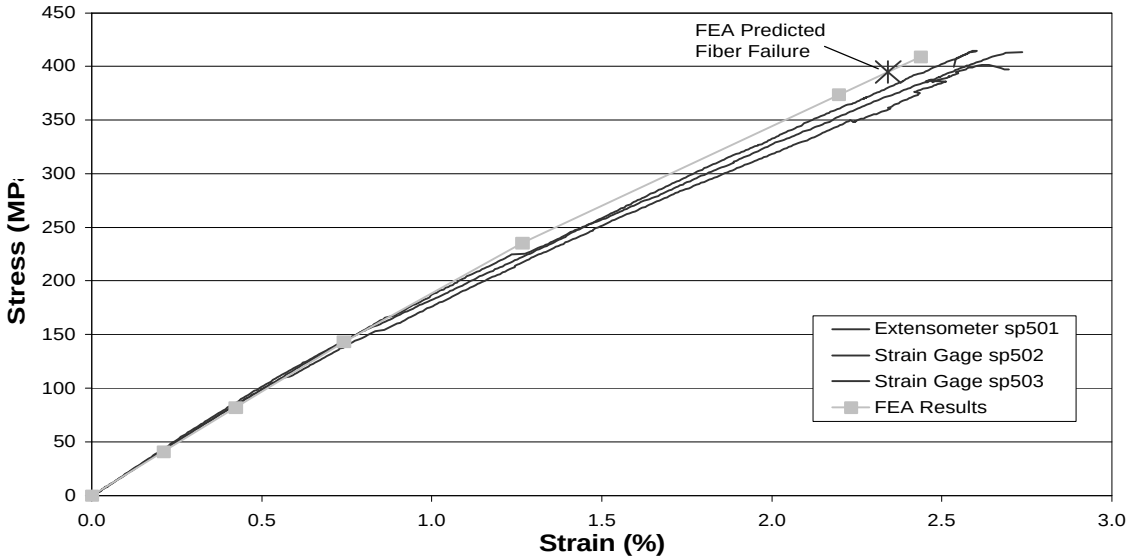

Figure 6.2 Stress-strain plot for dogboned Sandwich Panel tests including all experimental plots and FEA results.

strength increased in the sandwich panel with the addition of balsa in both experimental and numerical tests.

The Sandwich Flexural model was modeled with less success due to the complications noted previously in the Sandwich Flexural section of Chapter 5. The load-deflection plot is displayed in Figure 6.3. Two failures are indicated on the FEA line. The first failure predicted is a compressive fiber failure. The allowable, taken from the MSU Database, was found by doing compression tests on thin laminates that were not supported on the surfaces to alleviate laminate buckling. Therefore, the allowable has a small amount of buckling, which reduces compressive strength, but is typically found in most compressive applications.

The sandwich panel, on the other hand, supports the laminate, through the core to facesheet bond in the flexural test. The loading apparatus in the test

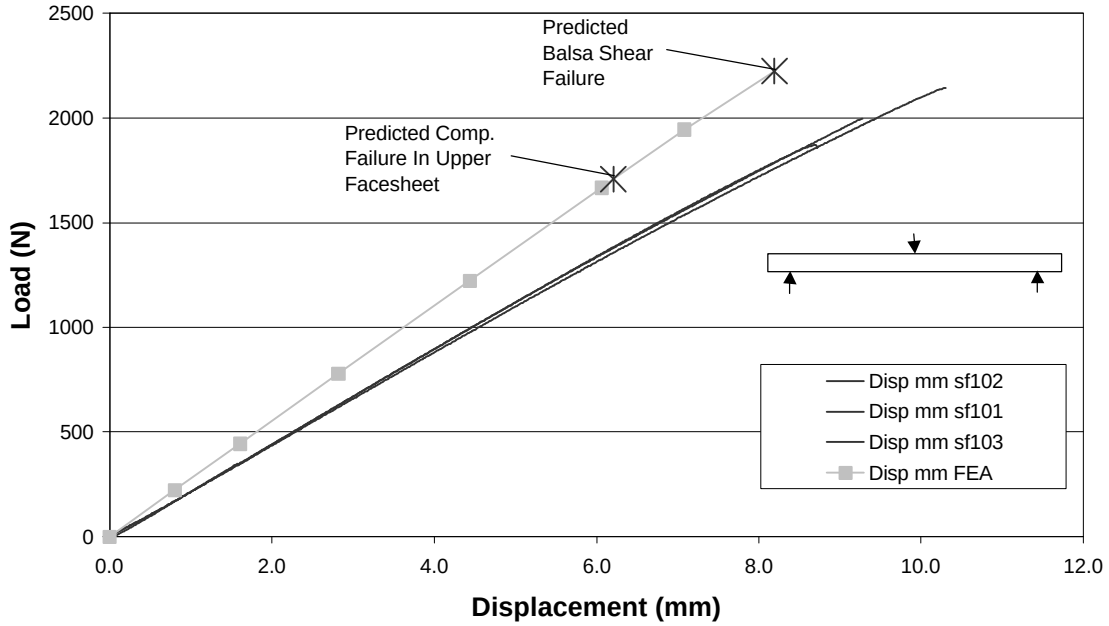

Figure 6.3 Load-displacement plot for Sandwich Flexural tests including all experimental plots and Finite Element Analysis (FEA) results.

also prevents buckling by forcing the laminate to stay planar under its tip. Both of these factors are expected to increase the allowable compressive strength of the zero degree ply in the upper facesheet, making predictions of this type of failure difficult. No compression failures happened during the experimental tests, so it is supposed that the compressive allowable is actually above other failure modes.

A balsa shear failure is noted as the next and final failure, after assuming that the fibers did not fail in compression. The specimens all had balsa core failures when they broke. The failure load predicted by the numerical model is only 10.5 percent above experimental test failure loads (Table 6.1). A prediction 10 percent from experimental is good considering the variability in balsa wood and the problems with balsa properties presented in literature.

The slopes of the load-deflection plots, given in Table 6.1, were used to check the stiffness of the numerical model with the experiments. Rather large errors were encountered when comparing slopes of the model with the tests. The thickness of the facesheets may be one reason for the difference in stiffness. The thickness of the specimens was smaller than that of the model. The model was constructed to match the thickness of several specimens, but due to manufacturing variances, the thickness of the Sandwich Flexural specimens were slightly different than the model. Fiber contents were calculated and ply properties were all derived using the model dimensions, so changing the model thickness would not be the only change. The thickness difference could have decreased the moment of inertia by a considerable amount, especially because the thickness of the panel is cubed when calculating the moment of inertia. The balsa core properties are also variable with changing density, so there could be a small error in averaging these properties for the nominal density. However, the difference in the bending stiffness was not of great concern because there was little bending in the fillet experiments.

Numerical Models Containing Sandwich To Thin Laminate Transition

The Fillet Normal model was constructed and run with the length corresponding to the Fillet Long specimens. This was used to compare the strain and displacement mapping discussed earlier to the numerical model.

The strain mapping included in Figure 6.4 shows excellent correlation between experimental and numerical results. The peak stress and bending

stresses in the thin laminate are the only areas with notable differences. The

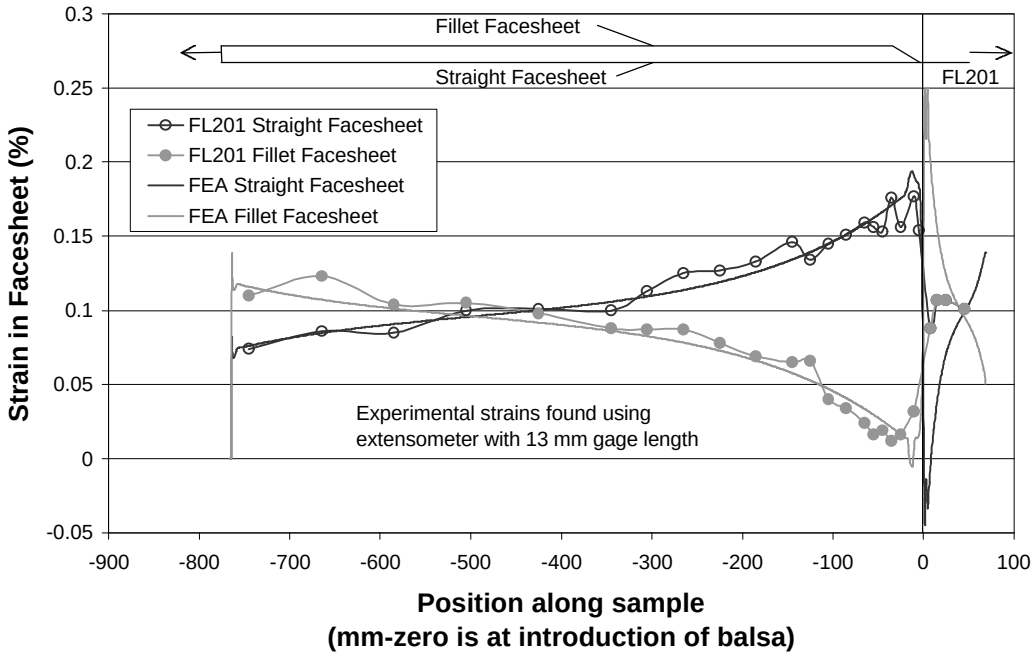

Figure 6.4 Strain mapping of Fillet Long specimen tested experimentally and modeled with finite elements.

experimental strain was found using an extensometer; consequently, the strain was measured over a distance of 13 mm so the peak strain is impossible to capture. The extensometer is also limited in capturing bending, so there is some deviation from the numerical results in the thin laminate section.

The Fillet Long specimen was loaded and out of plane displacement was measured and compared to the model. Figure 6.5 has the results of both tests, numerical and experimental, at two loads. There is a slight difference in the displacements for each load. The model predicts a slightly stiffer specimen with 15 percent less deflection. The Sandwich Flexure model also predicted a stiffer

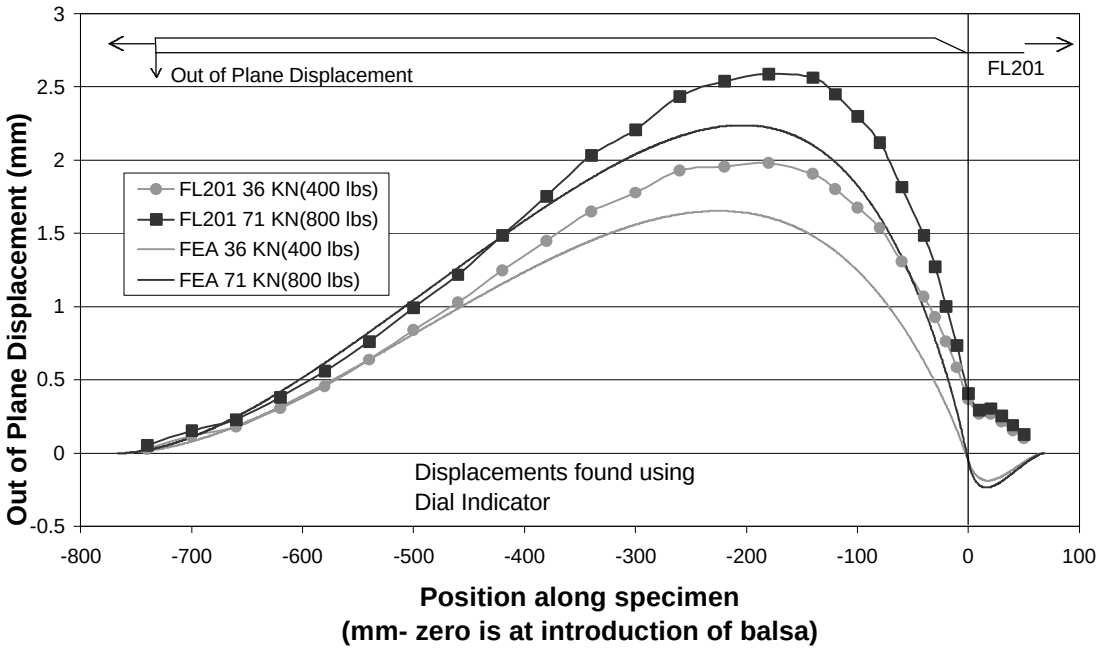

Figure 6.5 Out-of-plane displacement due to bending caused by eccentric loading in Fillet Long specimen tested experimentally and modeled with finite elements.

specimen with deflection 21 percent less than the experimental results. Once again this may be due to the facesheet thickness because the Fillet long specimen had a smaller thickness than the model. These two experiments helped validate and give confidence to the modeling methodology.

Fillet Normal (30 degree) Model

The Fillet Normal model was analyzed the most because it included the readily available Baltek fillet strip. As with other models, the stress-strain plot was used as a comparison to the experimental tests. The plot, included in Figure 6.6, shows both numerical and experimental results. There are two FEA results presented. The first FEA results correspond to the Fillet Normal model, which

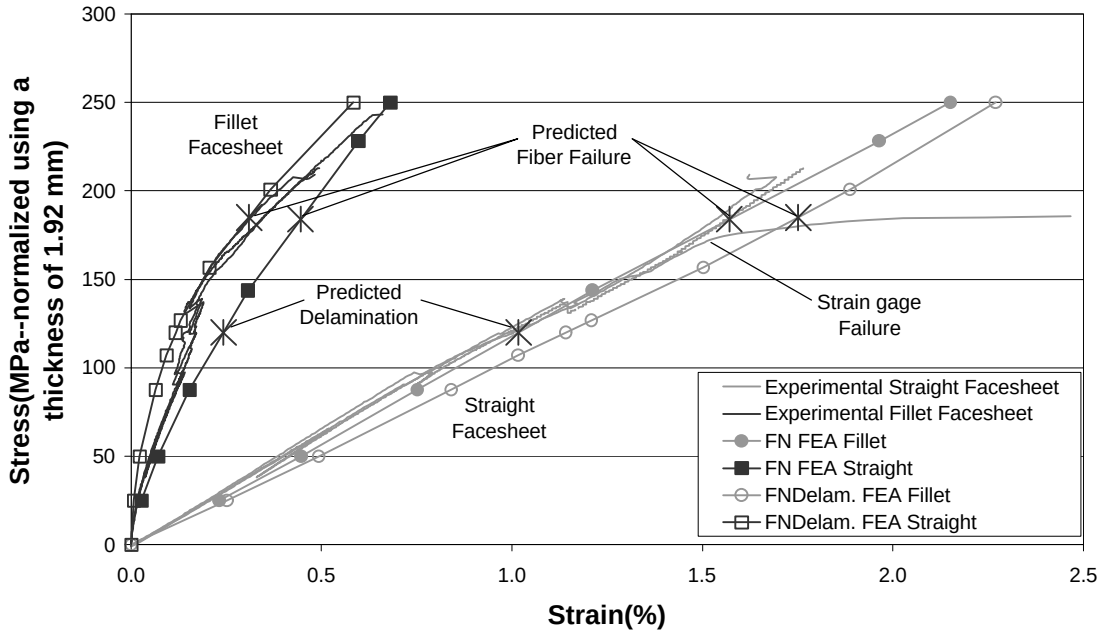

Figure 6.6 Fillet Normal experimental data with FEA results for model with and without delamination modeled.

did not include discrete delaminations. The FNDelam model contains the delaminations caused from resin failures. Each plot includes strain values for the fillet and straight facesheet at a location 35 mm from the balsa tip.

It was suspected that the FN model would follow the experiment until delamination and then the FNDelam model would follow the experiment in its later stages. The fillet facesheet did exhibit this, except for a small initial modulus difference. The straight facesheet did not follow suit. The FN model matched the experiment even after delamination. Plots of the surface strains at the experimental ultimate strength for each model, FN and FNDelam, are presented in Figure 6.7.

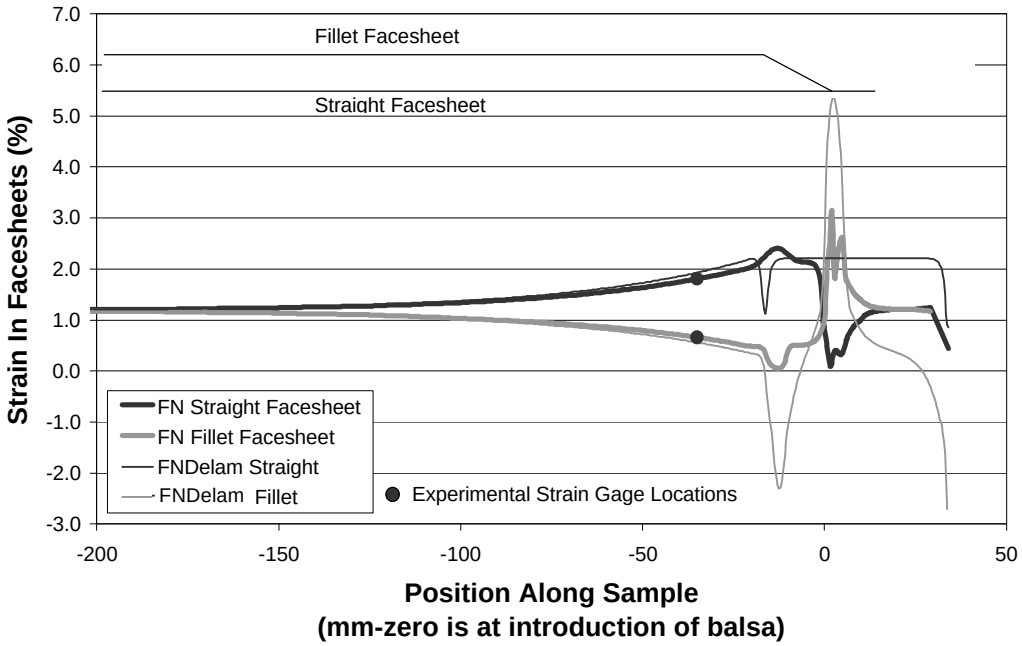

Figure 6.7 Surface strain mapping from FN and FNDelam models at a stress of 222 MPa (30 degree fiber failure stress).

The plot represents the experimental fiber failure stress, but all of the same trends are present at the lower delamination stress. It is easily seen that nearly the same strains are present in each model at fiber failure in all but the thin laminate section. Much of the difference between the facesheet strains is due to bending, except the increase and decrease at –20 mm, which are due to the fillet.

The fiber failure prediction for each model was within 1.6 percent, allowing the FN model to be used for fiber failure as well as delamination predictions. With all of these results, it was apparent that modeling the delamination was not necessary to capture the behavior after delamination. The fillet facesheet has little stress whether or not the delamination is present. Figure 6.8 contains a

longitudinal strain contour plot of the A130 fabrics in the area of the fillet at the experimental delamination stress. The strain in the straight facesheet is 7 times that in the fillet facesheet in the constant core section included in Figure 6.8.

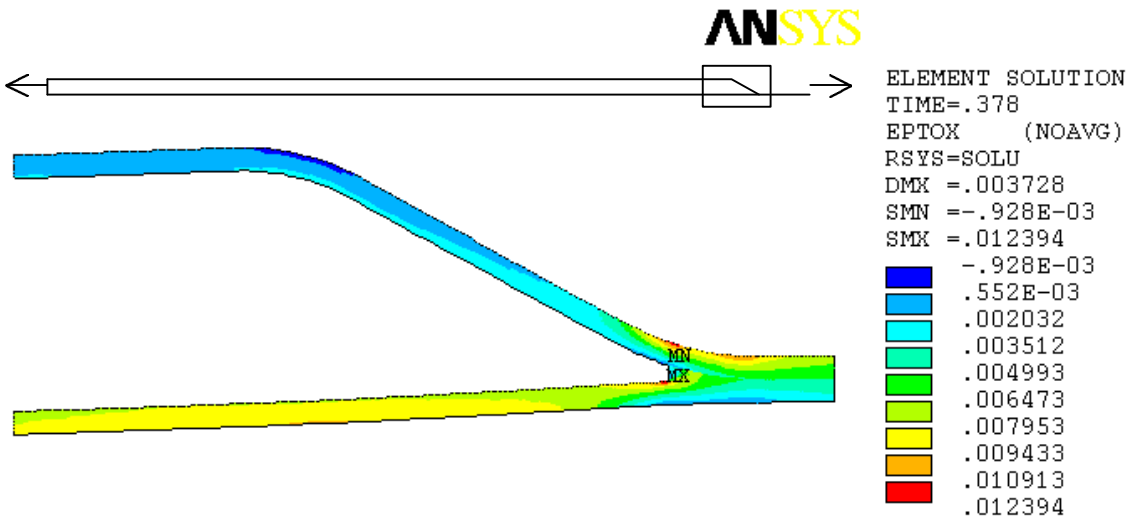

Figure 6.8 Longitudinal strain at fillet in A130 layers of Fillet Normal model at 95 MPa (experimental delamination stress).

As the model was loaded, two areas exceeded their allowables given in Table 4.1. The resin region failed at a global stress of 47 MPa using a Von Mises strain failure criterion at its lower right corner (location where resin meets balsa and A130 fabric) as pictured in Figure 4.2. The high strain area was very local, on the order of one millimeter. The balsa failed at a slightly lower global stress by shear failure at the same location, also locally, in a region 0.6 to 2.33 mm thick by 3 millimeters long. Each of these failures was dismissed as a false stress concentration caused by the modeling.

The three materials at the intersection described above have a wide range of elastic moduli. The model simply has the resin region, shown as the white region in Figure 4.4, terminating at a right angle. The resin region actually has a radius at its termination as shown in Figure 4.2. This radius is too small to practically model in a specimen this size, which led to the geometry of the Fillet Normal model. The A130 fabric is not uniform, and has a resin rich area at the surface, so the actual stress concentration is reduced when compared to the model at this interface.

The modulus and strength of the balsa near the resin region is higher, raising the allowables. As explained earlier, the fillet is not coated, as the core is, so it absorbs a small amount of resin during fabrication. The addition of the resin to the balsa stiffens it by creating a small composite structure. The small thickness of the balsa in the fillet tip will also make the balsa stronger in shear [Kilbourn (2000)], which will raise the local shear strength allowable.

After dismissing the stress concentration, delamination was initiated in the resin region on the upper curved surface, at about the midpoint along the length, calculated using a Von Mises strain failure criterion. This was the same location that experimental delamination initiated. This failure had much smoother strain contours than the stress concentration area discussed earlier. The distance from the point of maximum strain to where it was half of that, was between 0.7 and 1.8 mm compared to a local 0.1 and 0.6 mm found in the first stress concentration discussed. The numerical predictions of delamination and failure stresses are tabulated, along with their experimental counterparts in Table 6.2. The

delamination found with the FN model was one of the few cases in all models where a nonconservative strength resulted from the FE model.

Table 6.2 Experimental and numerical values for asymmetric fillet specimens.

	Delamination				Ultimate			
	Experiment		Model		Experiment		Model	
	Stress	COV	Stress	Error	Stress	COV	Stress	Error
Specimen	MPa	%	MPa	%	MPa	%	MPa	%
FN(30 deg)	95	4.13	120	26.98	222	8.06	184	-17.24
FR(30 deg)	99	19.99	109	9.73	222	3.83	193	-13.19
F20 deg	142	14.55	123	-13.38	242	18.72	219	-9.50
F10 deg	246	17.57	204	-16.90	276	16.15	274	-0.72
F5 deg	359	2.93	250	-30.36	364	3.59	308	-15.38

*Negative errors are conservative.

The shear transfer in the balsa is not as great as was expected. Figure 6.9 is a detailed plot of shear transfer in the balsa fillet region loaded to the experimental delamination stress. The high stresses at the balsa tip, discussed earlier, are easily identified as any stress above 3 MPa, the balsa shear allowable.

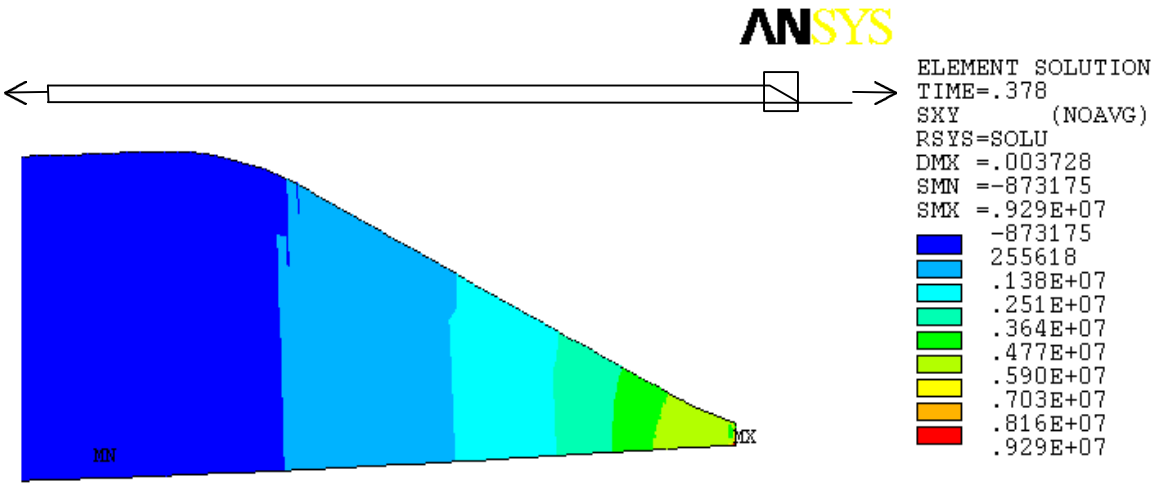

Figure 6.9 Shear stress in balsa fillet of Fillet Normal model at 95 MPa (experimental delamination stress)

Figure 6.10 includes a stress contour plot of balsa in the constant cross section with a small part of the fillet. The part of the core that has been omitted has a shear stress near zero. It is noted that there is little shear transfer in the core after the fillet region.

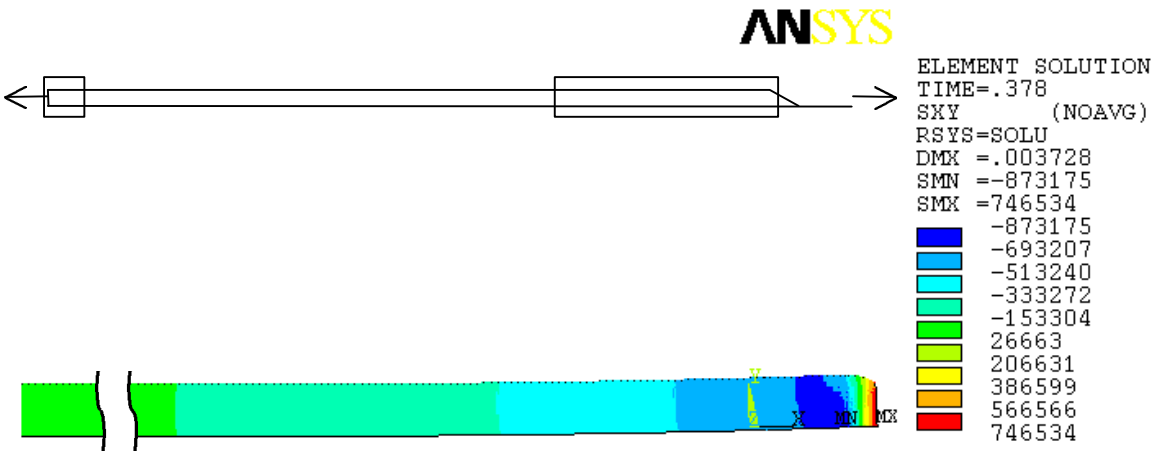

Figure 6.10 Shear stress in balsa core of Fillet Normal model at 95 MPa (experimental delamination stress).

The small shear stresses in the core are even more surprising when looking at surface strain mapping found from the FN model in Figure 6.11. Only a portion of the length of the specimen is included in Figure 6.11 to give more detail near the fillet. There are two sets of data, one set at the surface of the specimen in the DB120 fabric, and one set at the outer surface of the A130 layer fabric in each facesheet. The DB120 strains were used primarily in this study because they were available in experimental tests and allowed direct comparisons of numerical and experimental data.

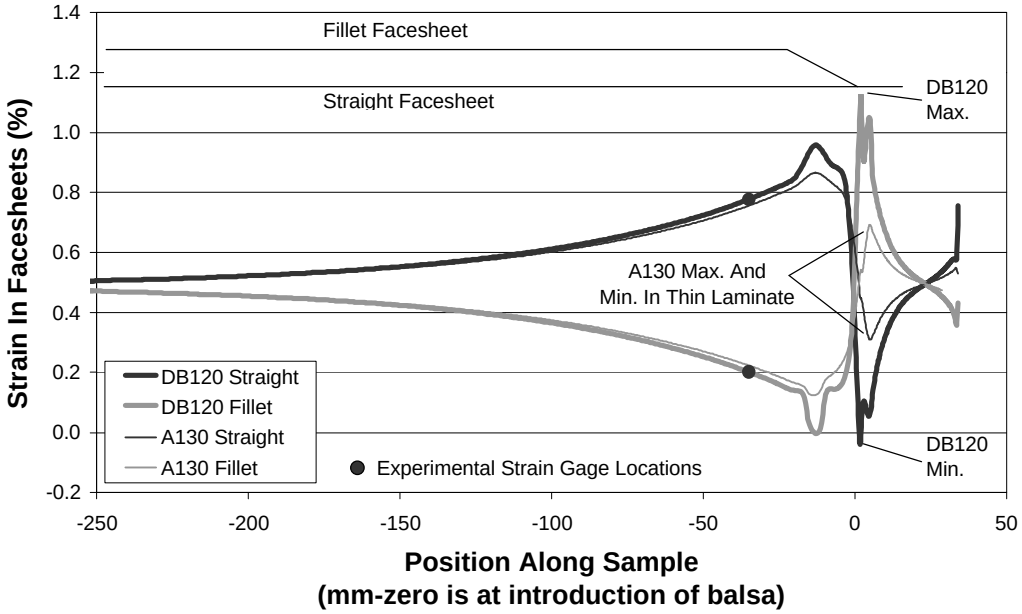

Figure 6.11 Strains in each layer of the Fillet Normal model at a stress of 95 MPa (30 degree experimental delamination stress).

In the plot, A130 data are included to show that the maximum and minimum strains in the DB120 layers of the thin laminate are not representative of the strains to which the A130 layers are subjected. The A130 layers are closer to the neutral axis so there is naturally less strain caused by the bending in the thin laminate. On the other hand, in the fillet region the A130 fabric is subjected to nearly the same strains as the DB120 fabric. Although the DB120 strains were used for all mapped strains, it is important to remember that the strains in the thin laminate are not the strains that will be found in the main, load carrying, A130 fibers.

Fillet Rigid (30 degree) Model

The Fillet Rigid model predicted stress-strain performance as shown in Figure 6.12. The initial moduli matched very well and the secant modulus of the model at failure is the same as one of the experimental specimens. The delamination was predicted when the resin in the resin rich region failed at the upper surface midway along its length, just as for the Fillet Normal model. The stress concentration that created problems in the Fillet Normal model was eliminated with the rigid fillet.

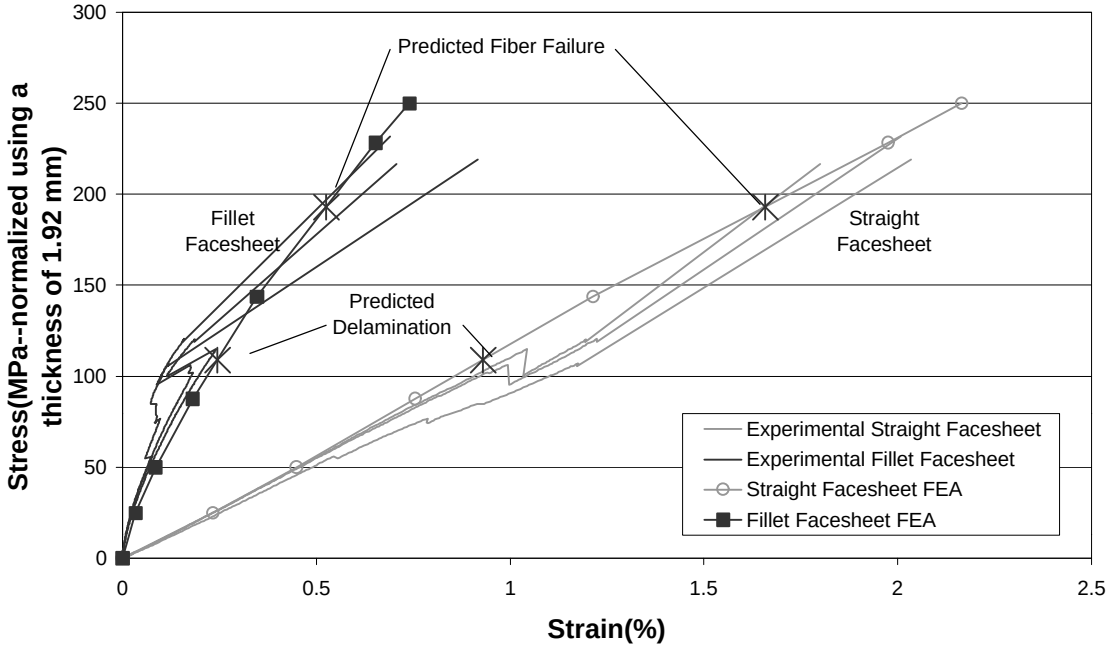

Figure 6.12 Fillet Rigid experimental data with FEA results.

The performance of the model in terms of predicting failures was fair as shown in Table 6.2. The delamination prediction was only 9.7 percent off of the

experiment but in a nonconservative direction. An error of this magnitude is not bad, especially when it falls within the experimental COV.

The fiber failure prediction is 13 percent lower than the experimental value; not bad considering that the delamination was not modeled. The error was conservative, although it did not fall within the COV.

The rigid fillet was not extremely successful in transferring load to the fillet facesheet. The contour plot in Figure 6.13 includes the A130 layers and the rigid fillet loaded to the experimental delamination stress. The strain in the straight facesheet is still 4 times the strain in the fillet facesheet, only slightly better than the factor of 7 for the balsa fillet. When comparing the strains in the A130 layers, in Fillet Normal and Fillet Rigid models, the A130's have strains 12 percent higher in the Fillet Rigid model which is unfavorable, considering that the goal of the rigid fillet was to reduce the strain in the A130 fibers.

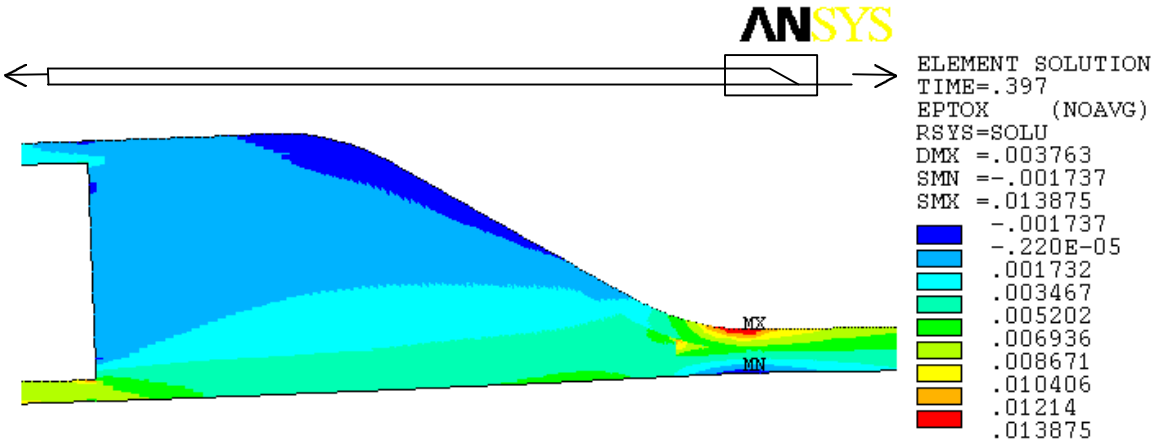

Figure 6.13 Longitudinal strain at fillet in A130 layers and DB400 fillet of Fillet Rigid model at 99 MPa (experimental delamination stress)

The 12 percent rise in strain may be discounted to 7 percent because the load in the Fillet Rigid model was slightly higher than the load in the Fillet Normal model due to their differences in experimental delamination stresses. Even so, a 7 percent increase in A130 fiber strain shows that the rigid fillet has a negative impact.

The presence of the rigid fillet can be compared to the balsa fillet of the Fillet Normal model in Figure 6.14. The surface strains in thin laminates are for the DB120 as explained earlier, but are helpful in comparing different fillet materials. The thin laminate produces higher strains in the rigid fillet as discussed earlier. The shear transfer in the fillet reduces the maximum strain near the fillet, but the strain is still high due to the bending stresses present.

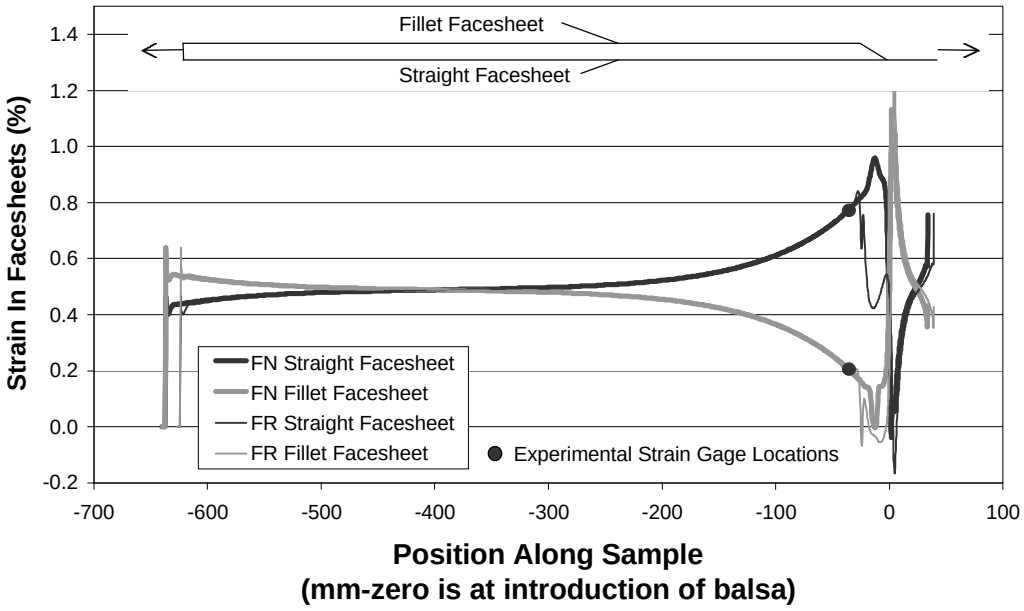

Figure 6.14 Surface strain mapping from FN and FR models at a stress of 95 MPa (30 degree experimental delamination stress)

Fillet 20 Degree Model

The Fillet 20 model performed well in terms of predicting strengths; both delamination and fiber failure were predicted within the experimental COV's. Additionally, both predictions erred on the conservative side. The stress-strain plots including experimental and numerical results are included in Figure 5.15.

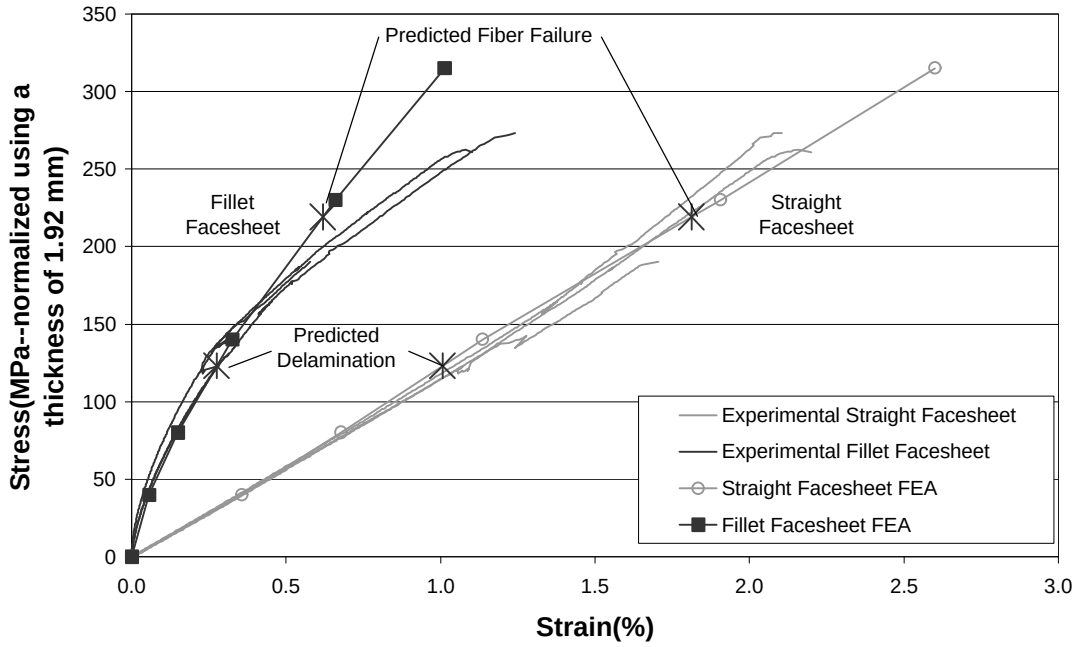

Figure 6.15 Fillet 20 degree experimental data with FEA results.

The straight facesheet strains are identical for numerical and experimental data, but the fillet facesheet has some difference at higher stresses. Damage modeling of the DB120 fabric, or the lack of delamination modeling, or both may cause the difference. The damage in the Fillet Control model did not follow the experiment at high stresses, so it would seem reasonable that it may diverge

slightly in this model as well. In the model, delamination is omitted as discussed in the Fillet Normal model section. Without the delamination in place, the model will behave slightly stiffer, as the stress-strain plot indicates with lower fillet facesheet strains.

The stress concentration in the resin region was encountered once again and disregarded for the same reasons as before. Putting that aside, delamination was initiated by resin failure once again at the same location as other specimens. The predicted fiber failure was in the straight facesheet at the resin region at a stress only 10 percent below the experimental failure stress and well within the COV of 19 percent.

Fillet 10 Degree Model

The stress-strain plot for the 10 degree fillet is shown in Figure 5.16 with a good correlation between numerical and experimental results. There is a slight dissimilarity in the moduli of the experiment and FEA model. This is probably due to the reasons mentioned for the previous model. One of the strain gages in the experiment failed during the test and is noted on the plot.

The delamination was predicted at the same location as in the other tests after discrediting the high stress concentration as before. The fiber failure was also predicted at the same location as for other models, near the balsa tip, in the straight facesheet. The errors for both predictions were within the COV's for the experiment and were on the conservative side.

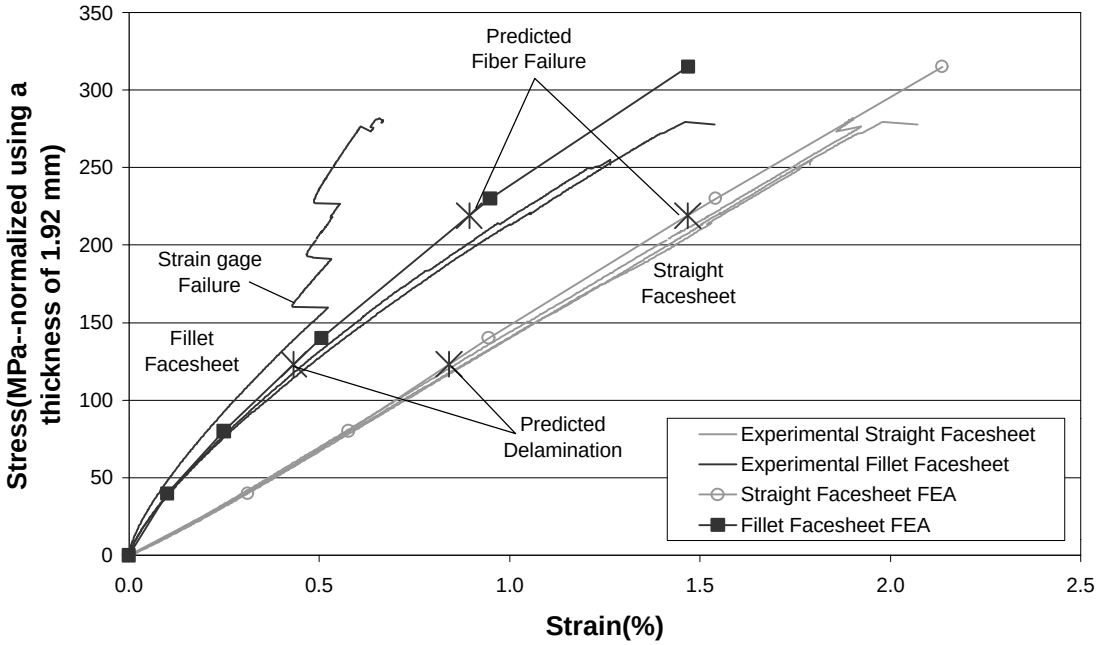

Figure 6.16 Fillet 10 degree experimental data with FEA results.

Fillet 5 Degree Model

The 5 degree fillet model was investigated in more detail than the two previous models since it was the shallowest angle tested and modeled. The stress-strain plot in Figure 6.17 shows good correlation with a little divergence in the fillet facesheet at higher stresses.

The prediction for delamination was found, ignoring the stress concentration as for the other models, in the upper surface of the resin region as in other models. The predicted delamination stress was 30 percent lower than the experimental value. The fiber failure prediction was also low, by 15 percent. Both of these errors are larger than the COV's, which were around 3 percent.

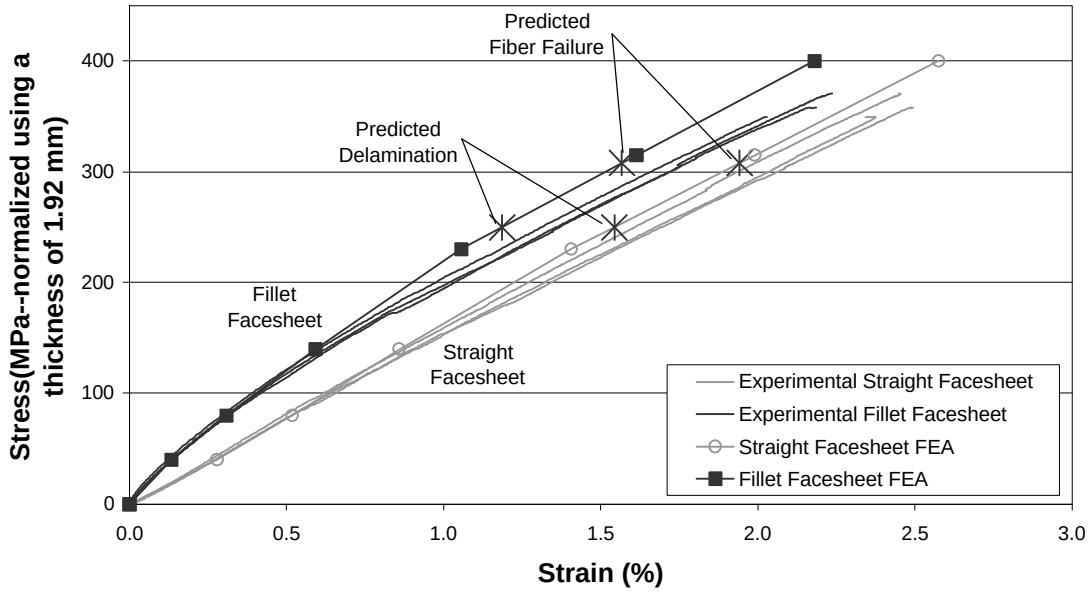

Figure 6.17 Fillet 5 degree experimental data with FEA results.

The length of the Fillet 5 specimen was more difficult to model than the other specimens due to the reduced cross-section. Initially, a model was run using the length of only the narrow section. Then, a model was run using the entire balsa length. Both models predicted delamination and fiber failure at the same respective stresses.

To investigate the convergence of the model, a different mesh was created and used. All mesh dimensions were roughly doubled, creating a mesh with a fourth of the elements. This model was run and delamination failure was predicted at a stress 0.8 percent lower than the original model. Results this close indicate that the solution was not mesh dependent.

A strain contour plot is included in Figure 5.18 with the A130 layers loaded to the Fillet 5 experimental delamination stress of 359. The contours reveal that

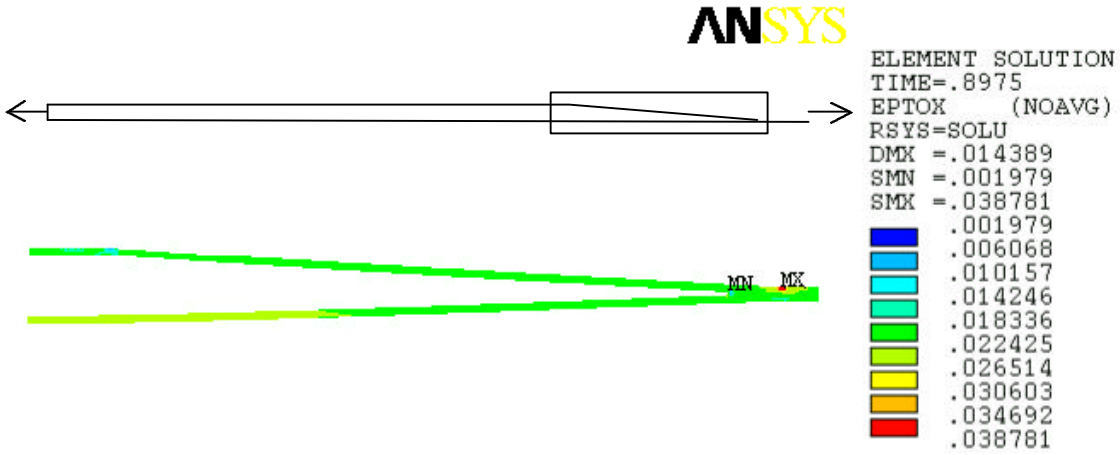

Figure 6.18 Longitudinal strain at fillet in A130 layers of Fillet 5 degree model at 359 MPa (experimental delamination stress).

the straight facesheet carries a stress only 1.2 times that in the fillet facesheet, far from the factor of 7 for the Fillet Normal specimen. This shows that the 5 degree fillet is efficient in transferring the load to the fillet facesheet.

All Fillet Models

Each model was loaded to its experimental delamination stress and the maximum Von Mises strain was found in the resin region at the area of the stress concentration. The maximum strains were averaged, producing a value of 4.07 percent with a standard deviation of .32 percent. This is well above the allowable and is certainly the result of the stress concentration created in the models, which does not exist in the experiments as explained earlier. If these maximums are disregarded and the maximum is found once again, a value of 2.23 percent is calculated with a standard deviation of .54 percent. The allowable maximum strain presented by Orozco (1999) was 2 percent with a standard deviation of .37

percent. The 2.23 value from the numerical models falls easily within one standard deviation of the resin allowable.

Surface strains from each of the angles modeled at a load of 95 MPa (Fillet Normal experimental delamination stress) are included in Figure 6.19. The location of strain gages is indicated on the plot as an additional reference. The plots all match each other in the farfield regions due to the bending in the samples. It is noticeable that the strain in the straight facesheet is not as high due to bending in the shallower models because the fillet loses flexural rigidity and helps reduce load eccentricity. The jump in strains at the fillet in the straight facesheet is decreased as the fillet angle becomes shallower.

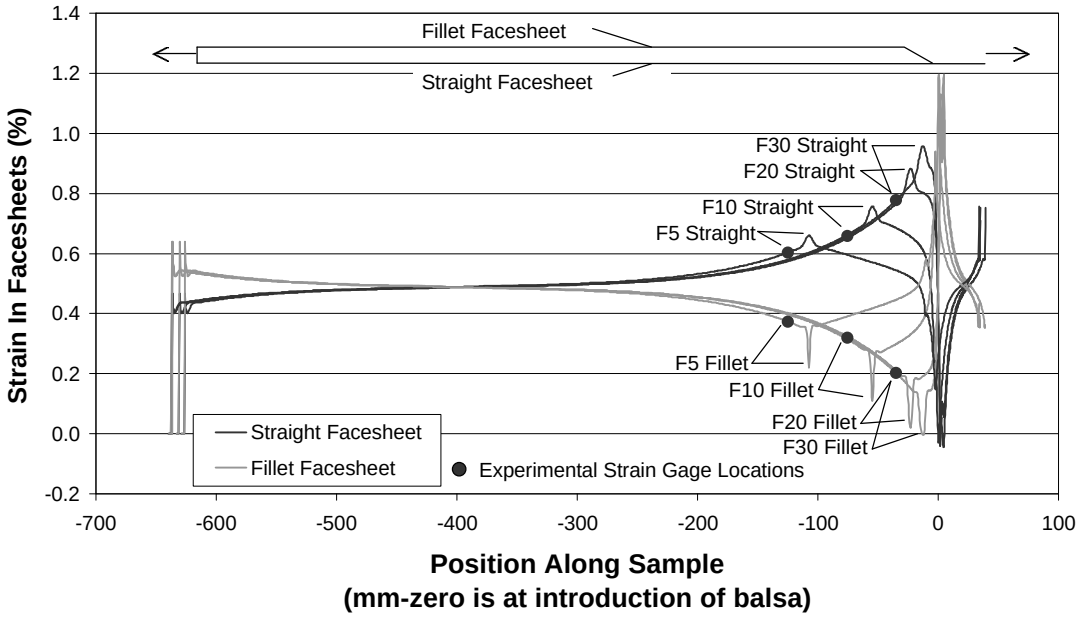

Figure 6.19 Strains in each facesheet of fillet specimens at a stress of 95 MPa (30 degree experimental delamination stress)

The group of fillet models matches experimental results closely in terms of stress-strain plots, especially before delamination. The models continued to follow the experiments fairly closely after delamination even without the delaminations modeled. The divergence that is present in most models is due to the lack of sufficient damage modeling in the DB120 fabric.

Fiber failure predictions are low in every model. This may indicate that a point stress criterion is not adequate to define failure. Instead an approach which requires stress in a predefined volume to be above the allowable might be more accurate. However, the point stress failure criterion was conservative in every model whereas another criterion might not be as conservative.

CHAPTER 7

CONCLUSIONS AND FUTURE WORK

Summary of Research

Baseline Material Results

The facesheet material failure strain was 2.69 percent. The straight specimens actually had higher strains to failure than the dogboned specimens. The model of the facesheet material predicted fiber failure accurately using a maximum stress criterion, but was slightly stiffer than the experimental specimens. The increased stiffness of the model is a result of not incorporating enough damage in the DB120 fabric.

The sandwich panel tests revealed that the addition of balsa core produces a small increase in strength with a failure stress 7 percent above that of the facesheets alone. The balsa adds some longitudinal stiffness, causing it to fail at a slightly lower strain of 2.64 percent. Once again, the model predicts failure accurately, but the secant modulus at failure is slightly off. The bending stiffness of the sandwich panel is also slightly off, due to the lack of damage modeled in the DB120 fabric and a small variation in thickness. However, the bending strength of the sandwich panel was predicted accurately, initiated by balsa shear failure.

Sandwich Transition into Thin Laminates

The 30 degree fillet specimens failed at stresses and strains well below the facesheet and sandwich panel values. Delamination in the fillet was initiated at 26 percent of the facesheet failure stress while fiber failure occurred at 58 percent of the facesheet failure. The 30 degree fillets delaminated at a strain of 0.44 percent, and failed at 1.17 percent.

Symmetry did not improve results; it helped with some fillet angles, but reduced the strength in others. On the average, symmetric parts had 4 percent lower delamination stresses and 11 percent higher fiber failure stresses. This necessitates the testing of both symmetric and asymmetric geometries.

Strength increased incrementally as the fillet angle decreased, but dramatically improved with the 5 degree fillet. The 5 degree fillet delaminated at nearly the same strain as that which produced fiber failure. Delamination happened at a strain of 2.31 percent, while fiber failure happened at 2.33 percent. The stress at delamination was only 6 percent below that for facesheet failure.

The models of the terminations had excellent correlation to experimental data, regarding the surface strains along the length of the specimen, and the out-of-plane displacement. Delamination was predicted in all models within 30 percent, but not all models were conservative in their errors. If the stress concentration at the resin corner was used, delaminations would have been predicted conservatively, but not nearly as accurately. Fiber failure was

predicted within 17 percent of the experimental results, on the conservative side for every model.

A model consisting of three linear elements through the thickness of the fabric and aspect ratios not exceeding 2 and 3 in critical and farfield areas respectively, provided accurate, converged results. Smooth contours were found throughout each individual material for all of the models. Damage modeling of the DB120 fabric with a bilinear modulus may not incorporate all damage accumulated in experimental specimens.

Sandwich Termination into Thick Laminates

These specimens did not perform well, with delamination at 1.00 percent and failure at 1.31 percent in the 90 degree tests. Unlike the thin laminate transitions, the 5 degree did not come nearly as close to the baseline strength. The 5 degree termination failed without delaminating at 2.11 percent, below the sandwich panel result of 2.64 percent. There was very little bending present in any of these specimens, which is helpful in design when out-of-plane displacements are a problem.

Fatigue Results

The facesheets had good fatigue properties, with a drop in strength of only 8.3 percent per decade of cycles. The sandwich panel material dropped in strength by 9.3 percent per decade of cycles, only slightly poorer than the facesheets alone. A knock-down factor at one million cycles was calculated as 1.1 for the sandwich panel compared to the facesheet material.

The 30 degree termination into thin laminate did not perform well in fatigue. Delamination data had a lot of scatter, with a drop in strength of 8.6 percent per decade. This was not too steep, but with such low static strengths, it pales in comparison to the facesheet performance. Delaminations moved slowly in these tests, taking a decade of cycles to move 35 mm allowing a sizable interval for damage detection. Fiber failure in the 30 degree specimens had the steepest fatigue curve of all, losing strength at the rate of 12.2 percent per decade. Once again, this steep slope is compounded by the low static strengths.

Knock-down factors were calculated at one million cycles for delamination and fiber failure as 3.4 and 3, respectively. This design detail demands attention, whether it is included in a static or cyclical application.

Design and Manufacturing Recommendations

Steps can be taken to ensure a successful design when a sandwich termination, to thick or thin laminate, must be used. After an initial design, a model can be built following the guidelines in this paper. The model will be helpful in determining stresses in each ply which may be used to determine the global failure stresses. Delamination may be predicted, using caution around any changes in materials. These will show up as false stress concentrations. Checking the distance to where the stress is cut in half will indicate how local, and how admissible the stress concentration is.

A modeling should be done with elements with aspect ratios better than two and three in local and far-field areas respectively. If linear elements are used the element density should not be changed through the thickness of the ply.

Once models are built and a preliminary design is selected using the model as a design tool, an experimental test should be done on the final design. If the boundary conditions of the application are not entirely known, both asymmetric and symmetric tests should be done. If these tests perform as the model predicted, the design can be finalized. Otherwise, changes may be made using the model once again, reducing any shortcomings the finite model may have had from the information gained in the first experiment.

Thin Laminates

When laying up thin laminates, make sure that the fabric is not distorted as it was received, or as the resin is being worked into the fabric. Both of these problems can cause free edge effects among other problems. If the absence of twist coupling is critical, the laminate should be a true $(\pm 45, 0)_s$ by rotating one of the ± 45 plies; otherwise a laminate of $(\pm 45, 0, 0, \pm 45)$ will be produced. The asymmetry will add a twist component to the laminate. The use of an upper caul plate will dramatically improve part surface finish and uniformity in any laminate laid-up by hand.

Sandwich Panel

Sandwich panel construction is not much more difficult than manufacturing thin laminates. Care should be taken when positioning the core so there are no

voids between adjacent pieces of core. These voids will create resin rich regions which are detrimental to strength as portrayed by the performance of the 90 degree thick terminations. It is also important to ensure that all balsa is wetted out with resin, to enable good facesheet adhesion.

Sandwich Termination into Thin or Thick Laminates

In each type of termination, shallow angles will be stronger. The terminations to thin laminates will have nearly nominal strength if a 5 degree taper is used, and there is not much difference between symmetric and asymmetric results. The use of a caul plate is probably not necessary in the shallow angles, but will improve performance. With larger fillet angles the fabric will not lay down on the fillet without a caul plate in place.

In some designs, catastrophic failure is to be avoided at all costs, even at ultimate strength. Using a 10 degree fillet in the termination to a thin laminate will fail first, as a delamination, still carrying tensile loads. This will allow the delamination to be found during inspections and prevent disastrous fiber failure. A reduction in strength must be traded for a progressive failure in the 10 degree fillet as opposed to the catastrophic 5 degree failure with higher strength. The 10 degree fillets are easier to handle, because at 5 degrees, the fillet becomes long and has a delicate leading edge which can be damaged.

In thick laminate transitions, the same can be said about delamination with the 10 degree fillet and a one step fiber failure in the 5 degree fillet. As before, the smaller the fillet angle used, the stronger the sandwich to thick laminate

transition will be. Unfortunately, the 5 degree angle in the thick termination is not small enough to approach the nominal strength of the sandwich panel. A fillet smaller than 5 degrees must be used if a strength better than 77 percent of nominal is desired.

In any of the thick transitions, care should be taken to avoid a large resin rich region at the end of the balsa core, as it severely lowered the delamination and ultimate strength in the experiments.

Future Work

The results of this research answered some questions about sandwich panel terminations, but there is still more work that can be done in this area. The following discussion includes both experiments and numerical modeling details that may add to the information gained in this research.

There was a problem modeling the DB120 fabric because there is limited stress-strain data on the fabric. Experiments including this could improve damage modeling. Experiments and models including other facesheet layups and resin systems could be done to see if the transitions can be increased in strength. Additionally, experiments could be done with 0 degree fabric added locally near the fillet in the straight facesheet.

Experiments exploring the effects of tough resin systems would be helpful. Additionally, tests of the fillet compressive strength would be beneficial because of the compressive loads in wind turbine blades.

Fatigue of shallower angles could be done to see if the increased static strengths are synonymous with better fatigue performance.

Shear properties of balsa infused with resin may be investigated to achieve better fillet properties. Furthermore, very thin balsa on the order of a millimeter or two could be tested to see if local shear strength at the fillet tip is increased. Resin material properties should be investigated in-situ rather than using neat resin tests, which may not represent resin rich regions accurately.

Numerical models with symmetric boundary conditions could be done to compare with experiments included in this research. Discrete crack modeling incorporating fracture mechanics could be investigated for delamination modeling. A local-global modeling approach could be taken to model the fillet area with more detail, while imposing boundary conditions found using a global model. A fiber failure criterion incorporating a failure volume rather than a point stress failure might also be examined.

REFERENCES CITED

Allen, H. (1969), Analysis and Design of Structural Sandwich Panels, Pergamon Press, Oxford, UK.

Ansys (Revision 5.5 and 5.6) Engineering Analysis System, Houston, PA.

ASTM (1997), “C 273-94: Standard Test Method for Shear Properties of Sandwich Core Materials,” 1997 Annual Book of ASTM Standards; Section 15; Volume 15.03, West Conshohocken, PA.

ASTM (1997), “C 393-94: Standard Test Method for Flexural Properties of Sandwich Core Materials,” 1997 Annual Book of ASTM Standards; Section 15; Volume 15.03, West Conshohocken, PA.

Baltek Corporation (1999), Baltek Corporation Product Data, Northvale, NJ.

Cheremisinoff, N., (1978), Fundamentals of Wind Energy, Ann Arbor Science Publishers Inc., Ann Arbor, MI.

Dostal, C. (1989), Composites(Engineered Materials Handbook, Vol. 1), Metals Park, Ohio.

Easterling, K., Harrysson, R., Gibson, L., Ashby, M., (1982) On the mechanics of balsa and other woods, University of Lulea, Sweden, and University of Cambridge, U. K.

Fiechtinger, K. (1986), Properties of End-Grain Balsa Core Material as a Function of Density, March, 1986.

Forest Products Laboratory (1987) Wood Handbook: Wood as an Engineering Material, Handbook 72, U. S. Department of Agriculture, Washington, DC.

Forest Products Laboratory (1944) Strength and Related Properties of Balsa and Quippo Woods, No. 1511, U. S. Department of Agriculture, Washington, DC.

Gere, J., Timoshenko, S. (1990), Mechanics of Materials-Fourth Ed., PWS-KENT Publishing Co., Boston, MA.

Gin-Boay, C, Leong_Keey, S, Lee-Soon, C, (1999), “Stress Distribution in Sandwich Beams Under Tension,” Composite Structures 45, 195-204.

Gipe, P., (1995), Wind Energy Comes of Age, John Wiley & Sons, Inc., New York, NY.

Haugen, D (1998), Fracture of Skin-Stiffener Intersections in Composite Wind Turbine Blade Structures, Master's Thesis in Department of Mechanical Engineering, Montana State University, Bozeman, MT.

Hedley, C. (1998), Headwaters Composites Owner.

Kilbourn, C. (2000), "Balsa Wood Core Material Design Values," 1331-1340, Procedings of the 45th International SAMPE Syposium and Exhibition, Covina, CA.

Mandell, J., Samborsky, D., (1997), DOE, MSU composite material fatigue database: Test methods, material, and analysis (Contractor Report No. SAND97-3002). Albuquerque, NM: Sandia National Laboratories.

Mandell, J., Samborsky, D., Scott, M., Cairns, D. (1998), "Effects Of Structural Details On Delamination And Fatigue Life Of Fiberglass Laminates," 1998 ASME Wind Energy Syposium, American Institute of Aeronautics and Astronautics, Inc.

McKittrick, L., Cairns, D., Mandell, J., Combs, D., Rabern, D., VanLuchene, R. (1999) Design of a Composite Blade for the AOC 15/50 Wind Turbine using a Finite Element Model, (Interim Report), Sandia National Laboratories, Albuquerque, NM.

Mil-Handbook-23A (1968) Structural Sandwich Composites, U. S. Department of Defense.

Morehead, R, (2000), Fatigue of Skin-Stiffener Intersections in Composite Wind Turbine Blade Structures, Master's Thesis in Department of Mechanical Engineering, Montana State University, Bozeman, MT.

Orozco, R, (1999), Effects of Toughened Matrix Resins on Composite Materials for Wind Turbine Blades, Master's Thesis in Department of Chemical Engineering, Montana State University, Bozeman, MT.

Rossell, S, (2000), Fluid Flow Modeling of Resin Transfer Molding for Composite Material Wind Turbine Blade Structure, Master's Thesis in Department of Chemical Engineering, Montana State University, Bozeman, MT.

Samborsky D., Mandell, J., and Cairns, D. (1999), "Selection of Reinforcing Fabrics for Wind Turbine Blades," AIAA, New York, NY.

Sears, A, (1999), Experimental Validation of Finite Element Techniques for Buckling and and Post buckling of Composite Sandwich Shells, Master's Thesis in Department of Mechanical Engineering, Montana State University, Bozeman, MT.

Tsoumis, G. (1991) Science and Technology of Wood-Structure, Properties, Utilization, Van Nostrand Reinhold, New York, NY.

Wienhold, P., Lennon, A., Roberts, J., Rooney, M., Kercher, A., Nagle, D., Sorathia, U. (2000), "Characterization of Carbonized Wood Core for Use in FRP Sandwich Ship Structures," 1700-1712, Procedings of the 45th International SAMPE Syposium and Exhibition, Covina, CA.

APPENDICES

APPENDIX A

STATIC TEST DATA

Test data for Balsa Extensional Modulus tests.

Specimen	Thick	Width	Length	Load	Stress	Modulus	Mass	Density	Mod/Density	Strength/Density
	mm	mm	mm	N	MPa	MPa	g	kg/m3	MPa m3 /kg	Pa m3 /kg
BE101	9.08	50.02	49.85	551.55	1.21	85.30	3.95	21.56	3.96	6.96
BE102	9.00	49.13	50.05	209.06	0.47	42.15	2.02	22.75	1.85	5.18
BE103	9.07	49.36	49.63	422.56	0.94	49.41	3.29	22.19	2.23	6.37
BE201	9.10	50.22	50.31	266.88	0.58	49.31	2.90	21.30	2.32	4.63
BE202	9.10	50.04	48.48	315.81	0.69	47.80	2.79	21.45	2.23	5.49
BE203	9.07	50.11	48.50	209.06	0.46	42.76	2.13	21.53	1.99	4.76
BE100 Avg.	9.05	49.50	49.84	394.39	0.88	58.95	3.09	22.17	2.68	6.17
BE200 Avg.	9.09	50.12	49.10	263.91	0.58	46.62	2.61	21.43	2.18	4.96
BE Avg.	**9.07**	**49.81**	**49.47**	**329.15**	**0.73**	**52.79**	**2.85**	**21.80**	**2.43**	**5.57**

Test data for Balsa Shear modulus tests.

Specimen	Density	Length:	Width:	Minor Th:	Max load:	Max load DAQ:	Shear Mod	Ult Shear
	kg/m3(spec.)	mm	mm	mm	kN	kN	MPa	MPa
BS201	150	151.03	50.45	9.33	19.95	19.89	160	2.62
BS202	150	151.38	50.93	9.33	23.73	23.66	231	3.08
BS203	150	151.23	50.36	9.33	23.48	23.41	234	3.08
BS ave.	**150**	**151.21**	**50.58**	**9.33**	**22.38**	**22.32**	**208.35**	**2.93**

Data from static Sandwich Flexural tests.

Specimen	Shear Stress	Max Disp	Secant Slope	Initial Slope	Length:	Width:	Right Th:	Center Th:	Left Th:	Max load:
	MPa (Balsa)				mm	mm	mm	mm	mm	N
SF101	1.95	9.28	215.30	198.00	203	47.80	11.36	11.98	10.82	1928.21
SF102	2.13	10.31	207.76	195.00	203	48.01	10.78	11.05	11.43	2074.10
SF103	1.88	8.71	214.58	191.00	203	48.15	11.35	10.97	10.78	1828.13
SF104	2.02				203	48.01	10.88	10.90	11.46	1970.02
Average	**2.00**	**9.43**	**212.55**	**194.67**	**203**	**47.99**	**11.09**	**11.23**	**11.12**	**1950.11**
COV	**5.34**	**8.60**	**1.96**	**1.80**	**0**	**0.30**	**2.76**	**4.52**	**3.35**	**5.22**

Static test information for all baseline and fillet specimens.

Initial Delamination					Ultimate Failure									
Spec.	**Strian 1**	**Strain2**	**Ave 1&2**	**Stress**	**Strian 1**	**Strain2**	**Ave 1&2**	**Stress**	**length:**	**Width:**	**Minor Th:**	**Major Th:**	**Max load:**	**Max loadDAQ:**
	%	**%**	**%**	**MPa**	**%**	**%**	**%**	**MPa**	**mm**	**mm**	**mm**	**mm**	**kN**	**kN**
fc301					2.76		2.76	393.0	127	22.18	1.53		16.77	16.75
fc302					2.59		2.59	381.0	127	22.26	1.53		16.33	16.30
fc303					2.72		2.72	374.0	127	21.72	1.58		15.73	15.70
Avg.					2.69		**2.69**	**382.7**						
COV%					3.30		**3.30**	**2.5**						
fc201					2.84		2.84	386.0	74	24.93	1.51		18.53	18.50
fc202					2.65		2.65	397.0	74	25.30	1.51		19.33	19.29
fc203					2.90		2.90	398.0	74	25.20	1.49		19.26	19.24
Avg.					2.80		**2.80**	**393.7**						
COV%					4.67		**4.67**	**1.7**						
sp501					2.64		2.64	401.0	333	21.63		10.80	16.76	16.67
sp502					2.59		2.59	415.0	333	21.91		10.74	17.53	17.45
sp503					2.69		2.69	412.0	333	21.58		10.75	17.19	17.11
Avg.					2.64		**2.64**	**409.3**						
COV%					1.89		**1.89**	**1.8**						
fn101	0.74	0.14	0.44	96.5	1.93	0.66	1.30	243.0	677	49.68	2.06	11.87	23.29	23.20
fn103	0.71	0.12	0.42	90.0	1.72	0.45	1.09	211.0	677	49.90	2.34	12.14	20.13	20.04
fn104	0.77	0.14	0.46	97.0	1.77	0.49	1.13	213.0	677	49.84	2.34	12.14	20.46	20.37
Avg.	0.74	0.13	**0.44**	**94.5**	1.81	0.53	**1.17**	**222.3**						
COV%	4.05	8.66	**4.63**	**4.1**	6.07	20.91	**9.45**	**8.1**						
fn202	0.77	0.45	0.61	105.0	1.33	1.33	1.33	254.0	675	49.47	4.04	23.60	48.79	48.75
fn203	0.68	0.56	0.62	131.5	1.33	1.33	1.33	258.0	675	49.78	4.48	24.08	49.33	49.24
fn204	0.66	0.59	0.63	137.5	1.74	0.82	1.28	255.0	675	49.68	5.88	25.52	48.71	48.61
Avg.	0.70	0.53	**0.62**	**124.7**	1.47	1.16	**1.31**	**255.7**						
COV%	8.33	13.82	**1.24**	**13.9**	16.14	25.38	**2.20**	**0.8**						
fr101	1.04	0.24	0.64	115.0	1.80	0.71	1.26	216.0	666	49.38	1.28	10.95	11.42	11.40
fr102	0.99	0.18	0.59	106.0	2.01	0.71	1.36	232.0	666	49.59	1.36	10.98	11.50	11.47
fr103	0.79	0.10	0.45	77.0	2.04	0.91	1.48	219.0	666	49.85	1.53	11.13	10.16	10.24
Avg.	0.94	0.17	**0.56**	**99.3**	1.95	0.78	**1.36**	**222.3**						
COV%	14.07	40.52	**18.06**	**20.0**	6.71	14.87	**8.07**	**3.8**						

Initial Delamination					Ultimate Failure									
Spec.	**Strian 1**	**Strain2**	**Ave 1&2**	**Stress**	**Strian 1**	**Strain2**	**Ave 1&2**	**Stress**	**length:**	**Width:**	**Minor Th:**	**Major Th:**	**Max load:**	**Max loadDAQ:**
	%	**%**	**%**	**MPa**	**%**	**%**	**%**	**MPa**	**mm**	**mm**	**mm**	**mm**	**kN**	**kN**
fr201	0.52	0.49	0.51		1.06	1.10	1.08	252.0	666	49.70	2.97	22.25	21.91	1.29
fr202	0.46	0.43	0.45	88.0	0.96	1.00	0.98	254.0	666	49.73	2.91	22.35	18.61	17.30
fr203	0.46	0.42	0.44	86.5	1.27	1.27	1.27	219.0	666	49.67	2.93	22.41	41.92	41.86
Avg.	0.48	0.45	**0.46**	**87.3**	1.10	1.12	**1.11**	**241.7**						
COV%	7.22	8.48	**7.81**	**1.2**	14.43	12.15	**13.27**	**8.1**						
fi101	1.37	0.45	0.91	164.0	2.11	1.24	1.68	273.0	668	50.33	1.60	11.12	17.17	17.14
fi102	1.28	0.27	0.78	139.0	1.71	0.58	1.15	190.0	668	49.94	1.44	10.97	0.00	14.50
fi103	1.07	0.28	0.68	123.0	2.16	1.08	1.62	263.0	668	50.14	1.55	11.11	11.89	11.82
Avg.	1.24	0.33	**0.79**	**142.0**	1.99	0.97	**1.48**	**242.0**						
COV%	12.42	30.35	**14.99**	**14.6**	12.37	35.62	**19.69**	**18.7**						
fi201	0.61	0.57	0.59	81.8	0.78	1.40	1.09	264.0	668	49.86	3.04	22.17	50.53	50.50
fi202	0.58	0.47	0.53	99.0	0.82	1.57	1.20	285.0	668	50.14	3.19	22.48	31.06	31.03
fi203	0.65	0.59	0.62		1.14	1.64	1.39	308.0	668	50.27	3.19	22.48	25.80	1.62
Avg.	0.61	0.54	**0.58**	**90.4**	0.91	1.54	**1.23**	**285.7**						
COV%	5.73	11.83	**8.40**	**13.5**	21.60	8.03	**12.43**	**7.7**						
fa101	1.52	1.02	1.27		2.07	1.54	1.81	279.0	668	50.07	1.78	11.19	26.89	26.85
fa102	1.54	0.99	1.27	215.0	2.09	1.68	1.89	319.0	668	50.17	1.83	11.15	24.61	24.58
fa103	1.92	0.61	1.27	276.0	1.62	1.68	1.65	230.0	668	49.91	1.72	11.05	27.03	27.00
Avg.	1.66	0.87	**1.27**	**245.5**	1.93	1.63	**1.78**	**276.0**						
COV%	13.58	26.17	**0.23**	**17.6**	13.79	4.95	**6.71**	**16.2**						
fa201	1.52	1.45	1.49	258.5	1.72	1.67	1.70	292.0	668	49.91	3.05	22.02	56.18	56.12
fa202	1.35	1.35	1.35	237.0	1.96	1.88	1.92	318.0	668	49.96	3.46	22.41	61.07	61.06
fa203	1.36	1.31	1.34	229.5	2.03	1.80	1.92	324.0	668	50.02	3.77	22.41	53.69	53.65
Avg.	1.41	1.37	**1.39**	**241.7**	1.90	1.78	**1.84**	**311.3**						
COV%	6.77	5.26	**5.94**	**6.2**	8.54	5.94	**6.97**	**5.5**						
fb104	2.45	2.24	2.35	370.0	2.45	2.24	2.35	370.0	417	30.79	1.59	11.12	21.98	21.90
fb105	2.49	2.17	2.33	358.0	2.61	2.29	2.45	373.0	417	30.50	1.75	11.24	22.16	21.81
fb111	2.38	2.12	2.25	349.0	2.38	2.03	2.21	349.0	417	34.73	1.29	10.72	23.33	23.31
Avg.	2.44	2.18	**2.31**	**359.0**	2.48	2.19	**2.33**	**364.0**						
COV%	2.28	2.77	**2.21**	**2.9**	4.75	6.31	**5.27**	**3.6**						

Initial Delamination					Ultimate Failure									
Spec.	**Strian 1**	**Strain2**	**Ave 1&2**	**Stress**	**Strian 1**	**Strain2**	**Ave 1&2**	**Stress**	**length:**	**Width:**	**Minor Th:**	**Major Th:**	**Max load:**	**Max loadDAQ:**
	%	**%**	**%**	**MPa**	**%**	**%**	**%**	**MPa**	**mm**	**mm**	**mm**	**mm**	**kN**	**kN**
fb211	2.40	2.32	2.36	371.0	2.40	2.32	2.36	371.0	417	34.85	2.63	21.55	49.64	33.86
fb212	2.18	2.11	2.15	339.0	2.18	2.11	2.15	339.0	417	34.98	2.56	21.48	45.68	45.64
fb213	2.40	2.32	2.36	369.0	2.40	2.32	2.36	369.0	417	34.75	2.61	21.58	49.28	49.25
Avg.	2.33	2.25	**2.29**	**359.7**	2.33	2.25	**2.29**	**359.7**						
COV%	5.46	5.39	**5.42**	**5.0**	5.46	5.39	**5.42**	**5.0**						
ff106	1.18	0.26	0.72	133.0	2.14	0.67	1.41	232.0	222	50.14	1.42	10.96	22.40	22.31
ff107	0.96	0.18	0.57	106.0	2.09	0.74	1.42	230.0	222	50.29	1.27	10.85	22.40	22.30
ff108	1.02	0.15	0.59	110.0	2.42	0.64	1.53	252.0	222	50.30	1.34	10.89	24.67	24.57
Avg.	1.05	0.20	**0.63**	**116.3**	2.22	0.68	**1.45**	**238.0**						
COV%	10.80	28.91	**13.22**	**12.5**	8.02	7.51	**4.79**	**5.1**						
ff201	0.66	0.61	0.64	116.0	2.27	1.12	1.70	247.0	307	50.31	2.48	21.53	47.95	47.80
ff202	0.44	0.38	0.41	83.0	2.12	1.10	1.61	254.0	307	50.36	2.89	22.00	49.19	49.03
ff203	0.53	0.49	0.51	103.0	2.19	1.05	1.62	268.0	307	50.23	2.97	22.15	51.95	51.79
Avg.	0.54	0.49	**0.52**	**100.7**	2.19	1.09	**1.64**	**256.3**						
COV%	20.36	23.32	**21.75**	**16.5**	3.42	3.31	**2.83**	**4.2**						
st104	1.19		1.19	205.0	1.76	1.76	1.76	288.0	333	50.56		10.75	28.08	27.94
st105	1.23		1.23	213.0	1.42	1.42	1.42	242.0	333	50.55		10.73	23.60	23.50
st106	0.59		0.59	111.0	0.75	0.75	0.75	160.0	333	50.35		10.72	17.53	17.44
Avg.	1.00		**1.00**	**176.3**	1.31	1.31	**1.31**	**230.0**						
COV%	35.73		**35.73**	**32.2**	39.23	39.23	**39.23**	**28.2**						
sa101	1.53	1.55	1.54	265.0	2.21	2.15	2.18	350.0	333	50.35		10.65	33.91	33.80
sa102	1.50	1.59	1.55	273.0	1.90	1.85	1.88	319.0	333	50.17		10.68	30.84	30.74
sa103	1.24	1.34	1.29	230.0	1.97	1.99	1.98	336.0	333	50.43		10.70	32.64	32.51
Avg.	1.42	1.49	**1.46**	**256.0**	2.03	2.00	**2.01**	**335.0**						
COV%	11.20	8.99	**10.00**	**8.9**	8.02	7.52	**7.70**	**4.6**						
sb101					2.02	2.15	2.09	314.0	430	50.75	10.29	10.56	30.66	30.58
sb102					2.24	2.27	2.26	326.0	430	50.92	10.28	10.51	31.95	31.88
sb103					1.90	2.06	1.98	302.0	430	50.86	10.32	10.51	29.54	29.47
Avg.					2.05	2.16	**2.11**	**314.0**						
COV%					8.40	4.88	**6.59**	**3.8**						

APPENDIX B

FATIGUE TEST DATA

Test data for fatigue of Facesheet Control specimens*.

Specimen	Width	Thickness	S/So	Max Stress	Avg Load	Half Amp	Max Load	Cyc. Fail	Max Strain
	mm	mm		MPa	N	N	N	#	%
FC701	21.87	1.58	0.80	306	7076	5790	12866	591	2.00
FC702	22.23	1.54	0.70	268	6294	5149	11443	6161	1.72
FC703	21.86	1.63	0.60	230	5305	4340	9645	72140	1.45
FC704	21.93	1.66	0.50	192	4435	3628	8063	570725	1.18
FC705	22.26	1.56	0.50	192	4502	3683	8185	255565	1.18
FC706	21.87	1.65	0.80	306	7076	5790	12866	3649	2.00
FC707	21.83	1.65	0.70	268	6180	5057	11237	11944	1.72
FC708	21.67	1.58	0.60	230	5259	4303	9561	40629	1.45
FC709	22.25	1.53	0.50	192	4499	3681	8181	322482	1.18
FC710	21.81	1.61	0.60	230	5293	4330	9623	22982	1.45
FC711	22.24	1.56	0.70	268	6296	5152	11448	11689	1.72
FC712	22.24	1.54	0.80	306	7196	5888	13084	733	2.00

Test data for fatigue of Sandwich Panel specimens*.

Specimen	Width	Thickness	S/So	Max Stress	Avg Load	Half Amp	Max Load	Cyc. Fail	Max Strain
	mm	mm		MPa	N	N	N	#	%
SP701	21.69	10.79	0.80	327	7494	6132	13626	241	2.04
SP702	21.60	10.85	0.70	286	6530	5343	11873	2757	1.73
SP703	21.60	10.68	0.60	245	5597	4580	10177	10677	1.43
SP704	21.56	10.85	0.50	205	4656	3809	8465	99054	1.15
SP705	21.68	10.90	0.50	205	4682	3831	8512	125391	1.15
SP706	21.58	10.88	0.80	327	7456	6101	13557	341	2.04
SP707	21.57	10.63	0.70	286	6521	5336	11857	2075	1.73
SP708	21.75	10.76	0.60	245	5636	4612	10248	35513	1.43
SP709	21.62	10.85	0.50	205	4669	3820	8489	322431	1.15
SP710	21.55	10.72	0.60	245	5585	4569	10154	15326	1.43
SP711	21.31	10.44	0.70	286	6443	5271	11714	1634	1.73
SP712	21.35	10.57	0.80	327	7377	6036	13413	398	2.04

* R=0.1 for all specimens

Test data for delamination progression during fatigue of Fillet Fatigue specimens.

Specimen	Max Stress	S/So	Cycles at			
	MPa		First Delam	Full Delam	35mm Delam	Fiber Fail
FF501*	65	27	27900	45000		
FF502	65	27	1	1	1	795
FF503	76	32	1	245	12848	539379
FF504	71	30	2800	5983	30743	554263
FF505**	76	32	5800	53250	89151	115629
FF506	71	30	9500	42881	109171	2264645
FF507	81	34	5200	10000	16205	29236
FF508	81	34	1	25	875	18641
FF509	119	50	52	692	692	1976
FF510	190	80	1	1	1	2
FF511	167	70	1	1	1	47
FF512	119	50	1	1080	1590	8859
FF513	93	39	3800	9810	11000	138606
FF514	144	60	1	1	1	3293
FF515	93	39	1200	107450	109650	153312
FF516	144	60	1	1	1	8228

*not full delam

**had static spike load just after delam to grip

Test data for fatigue of Fillet Fatigue specimens.

Specimen	Width	Maj. Thick.	Min. Thick.	Max Stress	Avg Load	Half Amp	Max Load	Cyc. Delam	Cyc. Fail	S/So	D/Do	Max Strain
	mm	mm	mm	Mpa	N	N	N	#	#			%
FF501*	50.86	11.08	1.48	65	3504	2867	28342	45000		0.27	0.49	0.34
FF502	50.25	11.10	1.52	144	7633	6245	61728		795	0.60	1.09	0.80
FF503	50.07	11.19	1.64	76	4002	3274	32365	245	539379	0.32	0.57	0.40
FF504	50.35	10.96	1.41	71	3756	3073	30377	5983	554263	0.30	0.54	0.37
FF505**	51.21	10.79	1.23	76	4093	3349	33102	53250	115629	0.32	0.57	0.40
FF506	50.61	10.98	1.36	71	3776	3089	30534	42881	2264645	0.30	0.54	0.37
FF507	50.64	10.85	1.25	93	4963	4060	40134	10900	29236	0.39	0.70	0.50
FF508	50.48	10.96	1.34	119	6369	5211	51509	25	18641	0.50	0.91	0.65
FF509	51.11	10.87	1.26	119	6449	5276	52152	692	1976	0.50	0.91	0.65
FF510	50.71	10.95	1.33	190	10187	8335	82388		2	0.80	1.44	1.10
FF511	50.76	10.90	1.28	167	8954	7326	72412		47	0.70	1.27	0.95
FF512	50.86	11.00	1.40	119	6417	5250	51896	1080	8859	0.50	0.91	0.65
FF513	50.74	11.00	1.39	93	4972	4068	40213	9810	138606	0.39	0.70	0.50
FF514	50.88	10.97	1.37	144	7728	6323	62502		3293	0.60	1.09	0.80
FF515	50.72	10.93	1.34	93	4970	4067	40197	107450	153312	0.39	0.70	0.50
FF516	50.76	10.98	1.37	144	7710	6308	62354		8228	0.60	1.09	0.80

*not full delam

**had static spike load just after delam to grip

*** R=0.1 for all specimens

First cycle delaminations(Static values)					
Specimen	Width	Maj. Thick.	Min. Thick.	Load	Stress
	mm	mm	mm	N	MPa
FF510	50.71	10.95	1.33	70969	164
FF511	50.76	10.90	1.28	72286	167
FF514	50.76	10.90	1.28	53429	123
FF516	50.76	10.90	1.28	61575	142
FF502	50.76	10.90	1.28	31062	72
Average				**57864**	**134**
COV (%)				**29.07**	**29.08**

Number of cycles when traces were drawn.

FF503	FF504	FF505	FF506	FF507	FF513	FF515
1	2800	5800	9500	5200	3800	82850
115	3700	12500	11000	5650	5400	87600
245	4210	20500	14482	5740	7350	87900
2600	5000	30000	19520	6800	8600	91700
4505	5150	39000	21786	10000	9810	93700
7099	5225	44000	27682	10450	9839	107450
8160	5983	52500	32130	11130	10200	108350
11000	6250	53250	39930	12755	10420	108760
12848	7503		41532	14475	11000	109650
	9800		42881	15000	11200	
	12002		46478	15200		
	28509		55000	15772		
	30743		57985	16205		
	420500		65500			
			75250			
			84000			
			92224			
			95500			
			101874			
			109171			

Traces of delamination progression.

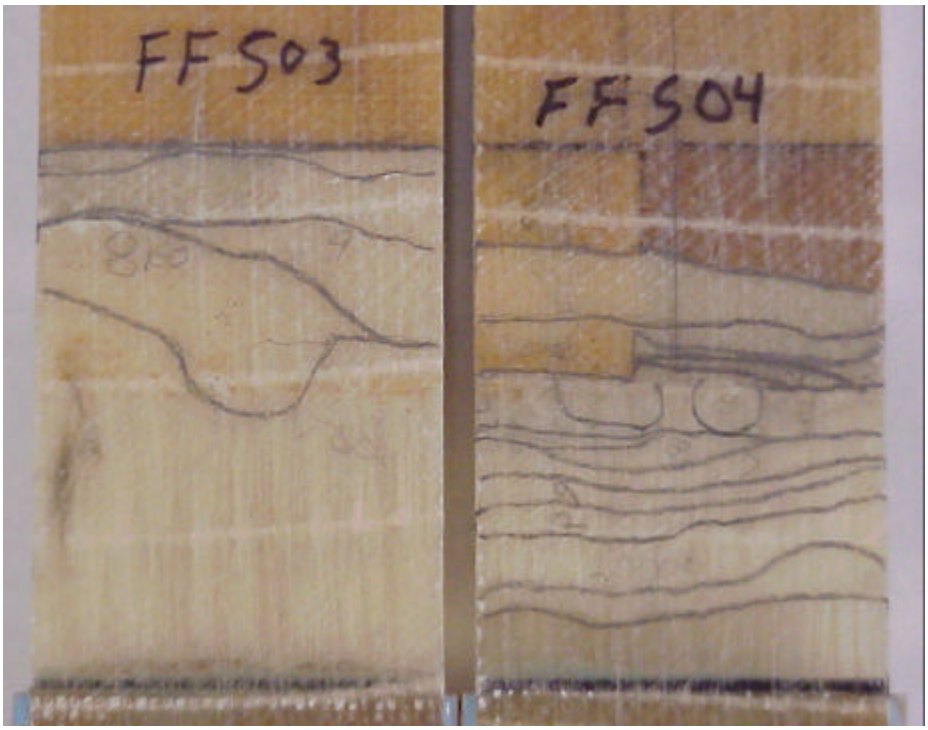

Fillet Surface (top view), Straight Surface (lower view)

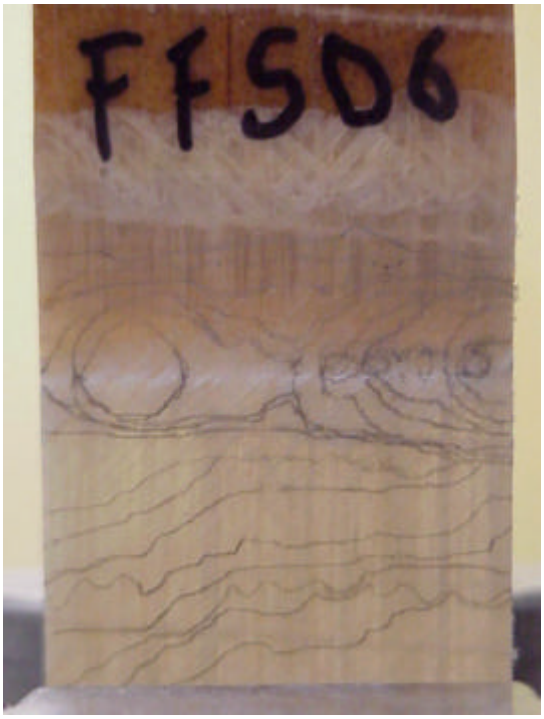

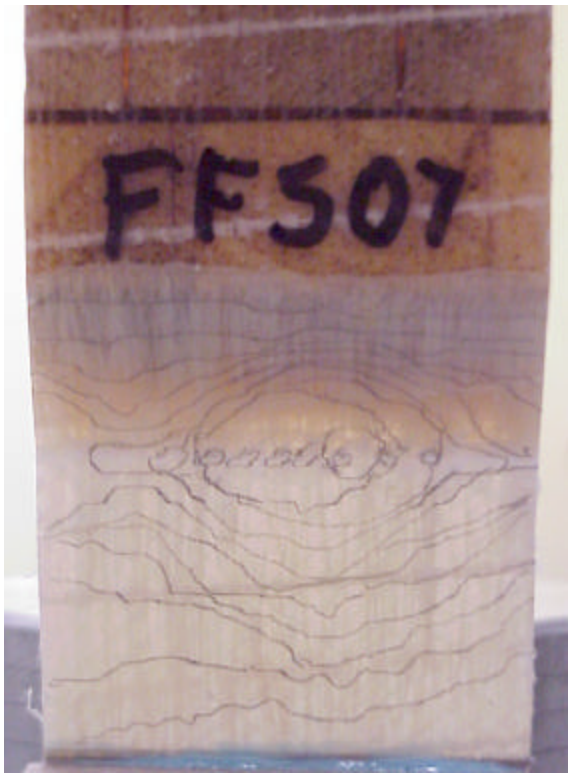

All Views-Fillet Surfaces

All Views-Fillet Surfaces

APPENDIX C

FILLET NORMAL MACRO

Macro written for Ansys modeling Fillet Normal specimen in tension.

```
/prep7
!fillmacr
!fillet model made to match fn101
!dimensions from mt-1-13
!element type--plane13
et,1,plane13
keyopt,1,1,3  !ux,uy degrees of freedom
keyopt,1,2,1      !do not include extra shapes

keyopt,1,3,2      !plane stress 2

keyopt,1,4,1      !follow ij side of ele

width=.049769  !width in m


load=250*1e6*.00192    !newtons equals lbs x 4.448n / width(m)
                       !newtons equals Mpa x 1e6 x .00192
                       !used only if a force loading condition is used

disp=0.002        !meters of displacement to thin end
                  !used only if a displacement loading condition is used

endb=-609e-3   !end of Balsa endb must be actual length of balsa-31 mm
!endb=-6e-3
endl=65e-3        !end of laminate, length from balsa end plus 31 mm


!material prop for a130's
mp,ex,1,29.9617e9
mp,ey,1,7.0980e9
mp,ez,1,7.4339e9
mp,gxy,1,2.4281e9
mp,gxz,1,2.8594e9
mp,gyz,1,1.6481e9
mp,prxy,1,0.3493
mp,prxz,1,0.3326
mp,pryz,1,0.4420

!material prop for db120's
mp,ex,2,8.346e9
mp,ey,2,5.96e9
mp,ez,2,8.346e9
mp,gxy,2,1.986e9
mp,gxz,2,5.025e9
mp,gyz,2,5.025e9
mp,prxy,2,0.372
mp,prxz,2,0.444
mp,pryz,2,0.2657
```

```
tb,aniso,2        !initialize table for bilinear mat prop
tbdata,1,88e6     !tensile yield stress x,y,z
tbdata,2,88e6
tbdata,3,88e6
tbdata,4,10       !tens tangent moduli x,y,z
tbdata,5,1e9
tbdata,6,1e9
tbdata,7,88e6     !compressive yield stress x,y,z
tbdata,8,88e6
tbdata,9,88e6
tbdata,10,1000  !comp tangent moduli x,y,z
tbdata,11,1000
tbdata,12,1000
tbdata,13,44e6  !Shear yeild stress in the material xy,yz,xz
tbdata,14,44e6
tbdata,15,44e6
tbdata,16,1.985e9         !shear tangent moduli
tbdata,17,5.024e9
tbdata,18,5.024e9


!material prop for db120's softened once
mp,ex,5,2.076e9
mp,ey,5,1.386e9
mp,ez,5,2.076e9
mp,gxy,5,.3972e9
mp,gxz,5,4.618e9
mp,gyz,5,4.618e9
mp,prxy,5,.126
mp,prxz,5,.796
mp,pryz,5,.0481


!material prop for db120's totally damaged
mp,ex,6,2.26
mp,ey,6,2.26
mp,ez,6,1.55
mp,gxy,6,2.091e9
mp,gxz,6,.511e9
mp,gyz,6,5.13e9
mp,prxy,6,.799
mp,prxz,6,.127
mp,pryz,6,.127


!material prop for Balsa
mp,ex,3,.0528e9          !1.015  .183
mp,ey,3,2.513e9
mp,ez,3,.0528e9                    !1.015  .183
mp,gxy,3,.159e9
mp,gxz,3,.159e9
mp,gyz,3,.159e9
mp,prxy,3,.112
```

```
mp,prxz,3,.338
mp,pryz,3,.3585


!material prop for resin area
mp,ex,4,3.18e9
mp,ey,4,3.18e9
mp,ez,4,3.18e9
mp,gxy,4,1.1778e9
mp,gxz,4,1.1778e9
mp,gyz,4,1.1778e9
mp,prxy,4,.35
mp,prxz,4,.35
mp,pryz,4,.35


!create keypoints for area corners
!points are duplicated with a 100 series
k,1,0,0,0
k,2,0,.48e-3,0
k,3,0,.96e-3,0
k,101,0,0,0
k,102,0,.48e-3,0
k,103,0,.96e-3,0
k,4,0,10.64e-3,0
k,5,0,11.12e-3,0
k,6,0,11.60e-3,0
k,104,0,10.64e-3,0
k,105,0,11.12e-3,0
k,106,0,11.60e-3,0
k,7,endl,0,0  !thin end
k,8,endl,.48e-3,0  !thin end
k,9,endl,.96e-3,0   !thin end
k,10,endl,1.44e-3,0   !thin end
k,11,endl,1.92e-3,0   !thin end
k,107,endl,0,0  !thin end
k,108,endl,.48e-3,0  !thin end
k,109,endl,.96e-3,0   !thin end
k,110,endl,1.44e-3,0   !thin end
k,111,endl,1.92e-3,0   !thin end
k,12,15.10e-3,10.64e-3,0
k,13,15.1e-3,11.12e-3,0
k,14,15.1e-3,11.60e-3,0
k,112,15.10e-3,10.64e-3,0
k,113,15.1e-3,11.12e-3,0
k,114,15.1e-3,11.60e-3,0
k,15,19.9e-3,9.27e-3,0
k,16,20.15e-3,9.67e-3,0
k,17,20.4e-3,10.08e-3,0
k,115,19.9e-3,9.27e-3,0
k,116,20.15e-3,9.67e-3,0
k,117,20.4e-3,10.08e-3,0
k,18,30.52e-3,2.68e-3,0
k,19,30.78e-3,3.03e-3,0
```

```
k,20,31.03e-3,3.44e-3,0
k,118,30.52e-3,2.68e-3,0
k,119,30.78e-3,3.03e-3,0
k,120,31.03e-3,3.44e-3,0
k,21,36.33e-3,.96e-3,0
k,22,36.33e-3,1.44e-3,0
k,23,36.33e-3,1.92e-3,0
k,121,36.33e-3,.96e-3,0
k,122,36.33e-3,1.44e-3,0
k,123,36.33e-3,1.92e-3,0
k,24,15.1e-3,1.6e-3,0
k,25,36.33e-3,11.92e-3,0    !Zero at end of fillet
k,26,30.52e-3,0,0
k,27,30.52e-3,.48e-3,0
k,28,30.52e-3,.96e-3,0
k,126,30.52e-3,0,0
k,127,30.52e-3,.48e-3,0
k,128,30.52e-3,.96e-3,0
k,29,36.33e-3,0,0
k,30,36.33e-3,.48e-3,0
k,129,36.33e-3,0,0
k,130,36.33e-3,.48e-3,0
k,31,41.33e-3,9.27e-3,0
k,32,17e-3,1.6e-3,0
k,33,15.1e-3,.96e-3,0
k,34,15.1e-3,.48e-3,0
k,35,15.1e-3,0,0
k,133,15.1e-3,.96e-3,0
k,134,15.1e-3,.48e-3,0
k,135,15.1e-3,0,0
k,36,19.9e-3,0,0
k,37,19.9e-3,.48e-3,0
k,38,19.9e-3,.96e-3,0
k,136,19.9e-3,0,0
k,137,19.9e-3,.48e-3,0
k,138,19.9e-3,.96e-3,0
k,39,endb,0,0
k,40,endb,.48e-3,0
k,41,endb,.96e-3,0
k,139,endb,0,0
k,140,endb,.48e-3,0
k,141,endb,.96e-3,0
k,42,endb,10.64e-3,0
k,43,endb,11.12e-3,0
k,44,endb,11.60e-3,0
k,142,endb,10.64e-3,0
k,143,endb,11.12e-3,0
k,144,endb,11.60e-3,0
!keypoints to make balsa tip smaller

k,51,32.66e-3,0,0
k,52,32.66e-3,.48e-3,0
k,53,32.66e-3,.96e-3,0
k,54,32.66e-3,1.62e-3,0
```

```
k,55,32.82e-3,2.04e-3,0
k,56,32.98e-3,2.50e-3,0
k,151,32.66e-3,0,0
k,152,32.66e-3,.48e-3,0
k,153,32.66e-3,.96e-3,0
k,154,32.66e-3,1.62e-3,0
k,155,32.82e-3,2.04e-3,0

!create polar coords
cskp,11,1,24,12,32 !upper rad

!Create coord for angled section
cskp,12,0,15,17,18

!create polar coords
cskp,13,1,25,20,31 !lower rad

!local coords for cart
cskp,14,0,1,26,2


!create rectangular areas
!The bottom of the areas will have 100 series
a,39,1,2,40       !A1
a,1,35,34,2       !A2
a,35,36,37,34     !A3
a,36,26,27,37     !A4
a,126,151,52,27           !A5
a,29,7,8,30       !A6
a,140,102,3,41    !A7
a,102,134,33,3    !A8
a,134,137,38,33           !A9
a,137,127,28,38           !A10
a,127,152,53,28           !A11
a,130,108,9,21    !A12
a,142,104,5,43    !A13
a,104,112,13,5    !A14
csys,11
a,112,115,16,13           !A15
csys,12
a,115,118,19,16           !A16
csys,13
l,55,19             !curved line for area 23
l,119,155           !curved line for area 17
l,18,54         !curved line for area 29
l,54,121!curved line for area 29
l,118,154           !curved line for area 17
a,118,154,55,19           !A17
csys,0
a,121,109,10,22           !A18
a,143,105,6,44    !A19
a,105,113,14,6    !A20
csys,11
a,113,116,17,14           !A21
```

```
csys,12
a,116,119,20,17          !A22
csys,13
a,119,155,56,20          !A23
csys,0
a,122,110,11,23          !A24
a,141,103,4,42  !A25
a,103,133,12,4  !A26
csys,11
l,12,15             !curved line for area 27
csys,0
a,133,138,15,12          !A27
a,138,128,18,15          !A28
csys,13
csys,0
a,128,153,54,18          !A29
csys,13
 l,22,55             !curved line for area 23
l,155,122           !curved line for area 17
l,54,121!curved line for area 29
l,154,121           !curved line for area 17


csys,13
a,155,122,23,56          !A30
a,154,121,22,55          !A31
csys,0
a,153,121,54     !A32
a,152,130,21,53          !A33
a,151,129,30,52          !A34


/pnum,line,1      !turns on line number if option 1 or off if 0
/pnum,area,1


layerdiv=3
slaydiv=3

  ! line division by size
csys,0
lesize,68,,,slaydiv                    ! vert lines associated with balsa end
lesize,45,,,slaydiv
lesize,87,,,10
lesize,25,,,slaydiv
lesize,4,,,slaydiv

var1=.4e-3
lesize,67,var1,,,!hor lines of major sandwich section
lesize,44,var1,,,
lesize,65,var1,,,
lesize,42,var1,,,
lesize,86,var1,,,
lesize,24,var1,,,
```

```
lesize,84,var1,,,
lesize,3,var1,,,
lesize,22,var1,,,
lesize,1,var1,,,

lesize,66,,,slaydiv         ! vert lines just left of start of thick cross section
lesize,43,,,slaydiv
lesize,85,,,10
lesize,23,,,slaydiv
lesize,2,,,slaydiv

var2=.4e-3
lesize,71,var2,,, !hor lines of small sandwich section
lesize,48,var2,,,
lesize,69,var2,,,
lesize,46,var2,,,
lesize,90,var2,,,
lesize,28,var2,,,
lesize,88,var2,,,
lesize,7,var2,,,
lesize,26,var2,,,
lesize,5,var2,,,

lesize,70,,,layerdiv                ! vert lines associated with
lesize,47,,,layerdiv                !start of thick cross section
lesize,89,,,10
lesize,27,,,layerdiv
lesize,6,,,layerdiv

var3=13
lesize,74,,,var3            ! hor lines at upper fillet location
lesize,51,,,var3
lesize,72,,,var3
lesize,49,,,var3
lesize,91,,,var3
lesize,31,,,var3
lesize,92,,,var3
lesize,10,,,var3
lesize,29,,,var3
lesize,8,,,var3

lesize,73,,,layerdiv                ! vert lines right of upper fillet
lesize,50,,,layerdiv
lesize,93,,,10
lesize,30,,,layerdiv
lesize,9,,,layerdiv

var4=45
lesize,77,,,var4,2                  ! hor lines at angled section
lesize,54,,,var4,2
lesize,75,,,var4,.5
lesize,52,,,var4,.5
lesize,96,,,var4,2
lesize,34,,,var4,2
```

```
lesize,94,,,var4,.5
lesize,13,,,var4,2
lesize,32,,,var4,.5
lesize,11,,,var4,.5


lesize,76,,,layerdiv                ! vert lines right of angled section
lesize,53,,,layerdiv
lesize,95,,,10
lesize,33,,,layerdiv
lesize,12,,,layerdiv

var5=15
lesize,79,,,var5+2          ! hor lines at lower fillet location
lesize,55,,,var5+2
lesize,56,,,var5+2
lesize,57,,,var5+2
lesize,59,,,var5+2
lesize,37,,,var5
lesize,97,,,var5
lesize,16,,,var5
lesize,35,,,var5
lesize,14,,,var5

lesize,78,,,layerdiv                ! vert lines center of lower fillet
lesize,60,,,layerdiv
lesize,98,,,6
lesize,36,,,layerdiv
lesize,15,,,layerdiv

var5=27
lesize,102,,,var5+5,.7575757575                 ! hor lines at rt lower fillet location
lesize,99,,,var5+5,.7575757575
lesize,100,,,var5+5,1.32
lesize,58,,,var5+5,1.32
lesize,101,,,var5+5,1.32
lesize,103,,,var5
lesize,105,,,var5
lesize,104,,,var5
lesize,108,,,var5
lesize,106,,,var5

lesize,83,,,layerdiv                ! vert lines right of lower fillet
lesize,64,,,layerdiv
lesize,41,,,layerdiv
lesize,21,,,layerdiv
lesize,107,,,layerdiv


var6=.16e-3
lesize,82,var6,,,!hor lines in thin end
lesize,63,var6,,,!
lesize,80,var6,,,!
lesize,40,var6,,,!
```

```
lesize,61,var6,,,!
lesize,20,var6,,,!
lesize,38,var6,,,!
lesize,18,var6,,,!


lesize,81,,,layerdiv                    !vert lines at thin end
lesize,62,,,layerdiv
lesize,39,,,layerdiv
lesize,19,,,layerdiv


!Begin Meshing
!turn on mapped meshing
mshkey,1

!desize,,,,,,,.02e-3
esize,.16e-3
!!Internal element size option.
!mopt,iesz,.12e-3
!mopt,trans,1.001          !each interior element can be n time bigger than adj ele
!mopt,expnd,1.001          !internal elements can be n time larger than surface ele
!areas which are in the long sandwich section are free mapped
! DB120 outer surface
mat,2
mshkey,1
amesh,2
mshkey,1
amesh,1
amesh,3
amesh,4
amesh,5
amesh,6
amesh,34

! DB120 inner surface
mshkey,1
amesh,20
mshkey,1
amesh,19
amesh,21
amesh,22
amesh,23
amesh,24
amesh,30

! A130 outer surface
mat,1
mshkey,1
amesh,8
mshkey,1
amesh,7
amesh,9
amesh,10
```

```
amesh,11
amesh,12
amesh,33

! A130 inner surface
mshkey,1
amesh,14
mshkey,1
amesh,13
amesh,15
amesh,16
amesh,17
amesh,18
amesh,31

! Balsa
esys,14          !element coord follosws global coords
mat,3
mshkey,0
amesh,29

amesh,27

mshkey,1
amesh,26
amesh,25
amesh,28


!turn off mapped meshing
mshkey,0

esys,14

! Resin
mat,4
amesh,32

nummrg,node,1e-6      !merges all nodes within tol
!boundary conditions
csys,0


!thin end

! count all nodes in grip
nsel,s,loc,x,endl-.0001,endl+.0001

*get,numnode,node,,count
! total load divided by num nodes
f,all,fx,load/numnode     !force load
!d,all,ux,disp            !displacement load
cp,1,ux,all
d,all,uy
```

```
!balsa end

nsel,s,loc,x,endb,endb
!cp,1,uy,all
d,all,ux
d,all,uy

allsel

!Create components for output

nsel,s,ext                          !nodes on straight surface
nsel,s,loc,x,endb+.0001,endl-.0001
nsel,s,loc,y,0,.0001
cm,st-nodes,node          !create component
allsel

nsel,s,ext                          !nodes on fillet surface
nsel,r,loc,x,endb+.0001,endl-.0001
nsel,u,loc,y,0,.0001
cm,flt-nodes,node          !create component
allsel
allsel

nsel,r,loc,x,5.84e-3,1.16e-3
nsel,u,loc,y,.14e-3,11.61e-3
esln,s
cm,gage1,elem !create component
allsel


nsel,r,loc,x,5.84e-3,1.16e-3
nsel,u,loc,y,0,11.4e-3
esln,s
cm,gage2,elem !create component
allsel


asel,s,mat,,1,2
nsla,s
nsel,r,loc,x,endb+12e-3,endl-5e-3
esln
cm,face,elem     !create component  facesheets
allsel

asel,s,mat,,1
nsla,s
nsel,r,loc,x,endb+12e-3,endl-5e-3
esln
cm,a130,elem

asel,s,mat,,2
```

```
nsla,s
nsel,r,loc,x,endb+12e-3,endl-5e-3
esln
cm,db120,elem

asel,s,mat,,3
nsla,s
nsel,r,loc,x,endb+12e-3,endl-5e-3
esln
cm,balsa,elem

asel,s,mat,,4
esla,s
cm,resin,elem

        !cmsel,s,name   to select the appropriate components

allsel

!solution
/solu
!large deformation  nonlinear
nlgeom,on

autots,on       !auto time stepping
time,1          !time at end of load step
!deltim,1               !size of time step
antype,static           !Static analysis
outres,all,all          !store all results from all substeps
nsubst,10,20,1
solve

/output
/post1
rsys,solu
/post26
numvar,30

                        !var#,ele #,nod#,el strain,name
gageloc=3.5e-3
esol,11,enearn(node(gageloc,0,0)),(node(gageloc,0,0)),epel,x,g1elas
esol,12,enearn(node(gageloc,0,0)),(node(gageloc,0,0)),eppl,x,g1plas
add,13,11,12,,g1strain
esol,21,enearn(node(gageloc,11.6e-3,0)),(node(gageloc,11.6e-3,0)),epel,x,g2elas
esol,22,enearn(node(gageloc,11.6e-3,0)),(node(gageloc,11.6e-3,0)),eppl,x,g2plas
add,23,21,22,,g2strain
plvar,13,23             !plot time and variables
prvar,13,23
save
```